DOE-EMSP Project Final Report

Project Title: Solvent Effects on Cesium Complexation with Crown Ethers from Liquid to Supercritical Fluids

Grant Number: DE-FG07-98ER14913

P.I.: Chien M. Wai, Department of Chemistry, University of Idaho, Moscow, Idaho 83844

Duration: September 15, 1998 – September 14, 2002

Scientific Personnel Supported by the Project

Graduate students - Anne Rustenholtz, Shaofen Wang, Su-Chen Lee
Undergraduate student – Jamie Herman
Visiting scientists – Richard A. Porter, M.D. Samsonov

Publications Derived from the Project

1. Han-Wen Cheng, Anne Rustenholtz, Richard A. Porter, Xiang R. Ye, Chien M. Wai, "Partition Coefficients and Equilibrium Constants of Crown Ethers Between Water and Organic Solvents Determined by Proton Nuclear Magnetic Resonance", *J. Chem. Eng. Data*, ASAP Web Release Date: March 2, **2004**.

2. Anne Rustenholtz, John L. Fulton, Chien M. Wai, "An FT-IR Study of Crown Ether-Water Complexation in Supercritical CO_2", *J. Phys. Chem. A*, 107, 11239-11244 (2003).

3. Shaofen Wang, Xiang-Rong Ye, Jamie Herman, Qingyong Lang, Chien M. Wai, "Lewis Acid-Base Complex Formation for Dissolution of Acids in Supercritical Carbon Dioxide", *Chem. Comm.*, submitted in March 2004.

4. Yuichi Enokida, Osamu Tomioka, Su-Chen Lee, Anne Rustenholta, Chien M. Wai, "Characterization of Tri-n-butylphosphate-Nitric Acid Complex – A CO_2-Soluble Extractant for Dissolution of UO_2", *Ind. Eng. Chem. Res.*, 42, 5037-5041 (2003).

5. M.D. Samsonov, C.M. Wai, Su-Chen Lee, Yuri Kulyako, N.G. Smart, "Dissolution of Uranium Dioxide in Supercritical Fluid Carbon Dioxide", *Chem. Commun.*, 1868-1869 (2001).

6. Shaofen Wang, M. Koh, C.M. Wai, "Nuclear Laundry Using Supercritical Fluid Solutions", *Ind. Eng. Chem. Res.*, 43, 1580-1585 (2004).

Project Summary

Nuclear magnetic resonance (NMR) techniques were used to study crown ether-water interactions in solvents of low dielectric constants such as chloroform and carbon tetrachloride. Water forms a 1:1 complex with a number of crown ethers including 12-crown-4, 15-crown-5, 18-crown-6, dicyclohexano-18-crown-6, dichclohexano-24-crown 8, and dibenzl-24-crown-8 in chloroform. Among these crown ethers, the 18-crown-6-H_2O complex has the largest equilibrium constant (K=545) and 97% of the crown is complexed to water in chloroform. Addition of carbon tetrachloride to chloroform lowers the equilibrium constants of the crown-water complexes. The partition coefficients of crown ethers (D = crown in water/crown in solvent) between water and organic solvent also vary with solvent composition. At room temperature, the D value for 18-crown-6 is about 0.25 between water and chloroform and the value increases to 48 between water and carbon tetrachloride. NMR studies of cesium-crown ether-water interactions in chloroform in the presence of picric acid turned out to be complicated for spectral analysis. Some results were obtained but with large uncertainties. NMR studies of crown-water interactions in supercritical CO_2 using a capillary tubing technique was also not successful due to experimental difficulties. Instead, Fourier-Transform Infrared (FT-IR) spectroscopy was used to study crown-water interactions in liquid and supercritical CO_2 using a high-pressure view-cell with diamond windows.

FT-IR spectra of 18-crown-6-water and dicyclohexo-18-crown-6-water complexes in liquid and in supercritical CO_2 were studies under various experimental conditions. Water forms a 1:1 complex with 18-crown-6 at low ligand concentrations and a 1:2 sandwich complex at high ligand concentrations. Spectral analysis indicates that the 1:1 complex has two forms, one with both hydrogen atoms of the H_2O molecule bonded to the oxygen atoms of the host cavity and the other with only one hydrogen bonding between water and the cavity oxygen. The equilibrium constant of the single hydrogen bond 18-crown-6-H_2O complex decreases from 21±2 to13±1 L mol^{-1} with an increase in temperature from 25 °C to 60 °C at 200 atm CO_2. The equilibrium constant of the double hydrogen bond complex decreases from 14±2 to 2±1 from 25 °C to 60 °C under the same CO_2 pressure. The enthalpis of the reaction for the single hydrogen bond and the double hydrogen bond complexes were determined to be -12±2 KJ mol^{-1} and -38±3 KJ mol^{-1}, respectively. Density shows little effect on the equilibrium constants of the crown-water complex in supercritical CO_2. The crown-water complex can be regarded as a Lewis acid-base complex with the crown being the electron donor and the water as the electron acceptor. This Lewis acid-base complex formation mechanism may provide a means of introducing insoluble hydrophilic acids into supercritical CO_2 for chemical reactions and separations.

Several techniques were used to characterize complex formation between tri-n-butylphosphate (TBP) and some inorganic acids using NMR and other methods. TBP forms complexes with aqueous acids such as nitric acid and hydrochloric acid through hydrogen bonding of the electron donating P=O group. The Lewis acid-base complex has a general formula of $TBP(acid)_x(H_2O)_y$ with x and y values depending on the relative amounts of TBP and acid used in the preparation. The x and y values can be determined by conventional titration methods. NMR spectra show that the protons of the acid and the water in the complex undergo rapid exchange resulting in a single resonance peak. The solubilities of some complexes such as $TBP(HNO_3)_{0.7}(H_2O)_{0.7}$ and $TBP(HCl)_{0.8}(H_2O)_{2.8}$ are in the range of 1-2 mol% in supercritical CO_2 at 40 °C and around 110 atm. When the TBP-nitric acid complex is added to the supercritical CO_2, an anti-solvent effect of CO_2 causes part of the acid in the complex to

precipitate out forming small droplets in the fluid phase. These small acid droplets may be highly effective for oxidization and dissolution of metals and oxides in supercritical CO_2. Nitric acid and hydrochloric acid are normally not soluble in supercritical CO_2. Using the Lewis acid-base complex formation mechanism with TBP as a carrier, these acids become soluble in supercritical CO_2 because TBP is CO_2-philic. This simple method of introducing acids into supercritical CO_2 may have a wide range of applications for developing potential supercritical fluid processes.

One application of the TBP-nitric acid complex is for dissolution of uranium dioxide in supercritical CO_2. Our study has shown that solid UO_3 and UO_2 powders can be dissolved in supercritical CO_2 using a TBP-nitric acid complex such as $TBP(HNO_3)_{0.7}(H_2O)_{0.7}$. The dissolution of UO_2 with the TBP-nitric acid complex in supercritical CO_2 is particularly interesting because it may lead to the development of a dry and green process for treating UO_2 contaminated wastes. The dissolution of UO_2 probably involves oxidation of UO_2 to uranyl ions $(UO_2)^{2+}$ followed by formation of the $UO_2(NO_3)_2(TBP)_2$ complex which is very soluble in supercritical CO_2. Demonstration of this direct supercritical fluid dissolution process for treatment of uranium dioxide contaminated wastes and for reprocessing of spent nuclear fuels are current being conducted by the Nagoya University in collaboration with Japanese companies including Mitsubishi Heavy Industries, Japan Nuclear Cycle Corp and Kobe Steel.

This project has provided valuable opportunities for research as well as for education at the University of Idaho. Three graduate students, one undergraduate student, and two visiting scientists received financial support from the project for their research at the University of Idaho. The project has produced 6 journal publications plus an equal number of presentations at professional meetings.

Table of Contents

I. Introduction

Utilizing supercritical fluids as solvents for extraction, separation, synthesis, and cleaning has been a very active research area in the past two decades.[1-3] The reasons behind this technology development are mainly due to the changing environmental regulations and increasing costs for disposal of conventional liquid solvents. Carbon dioxide is widely used in supercritical fluid extraction (SFE) applications because of its moderate critical constants (T_c = 31.1 °C, P_c = 72.8 atm, φ_c = 0.471 g/mL), inertness, low cost, and availability in pure form. However, because CO_2 is a linear triatomic molecule (with no dipole moment), it is actually a poor solvent for dissolving polar compounds and ionic species. A method of dissolving metal ions in supercritical CO_2 was developed in the early 1990s' using an *in situ* chelation technique. In this method, a CO_2-soluble chelating agent is used to convert metal ions into soluble metal chelates in the supercritical fluid phase. Quantitative measurements of metal chelate solubilities in supercritical CO_2 were first made by Laintz et al. in 1991 using a high pressure view cell and UV/Vis spectroscopy.[4] In this pioneering study, the authors noted that fluorine substitution in the chelating agent could greatly enhance (by 2-3 orders of magnitude) the solubility of metal chelates in supercritical CO_2. A demonstration of copper ion extraction from solid and liquid materials using supercritical CO_2 containing a fluorinated chelating agent bis(trifluoroethyl)dithiocarbamate was reported in 1992.[5] Since then, a variety of chelating agents including dithiocarbamates, β-diketones, organophosphorus reagents, and macrocyclic ligands have been tested for metal extraction in supercritical fluid CO_2.[6] Highly CO_2-soluble metal complexes involving organophosphorus reagents have been found and reported in the literature.[7] Recently, direct dissolution of metal oxides such as uranium dioxide and lanthanide oxides in supercritical CO_2 using a tri-n-butylphosphate-nitric acid complex as the extractant has also been demonstrated.[8,9] These studies have greatly expanded potential uses of the supercritical fluid extraction technology for metal related applications.

The *in situ* chelation-SFE technique appears attractive for nuclear waste management because it can greatly reduce the secondary waste generation compared with the conventional processes using organic solvents and aqueous solutions. Other advantages of using the SFE technology for nuclear waste management include fast extraction rate, capability of penetration into small pores of solid mataterials, and rapid separation of solutes by depressurization. The tunable solvation strength of supercritical fluid CO_2 also allows potential separation of metal complexes based on their difference in solubility and partition between the fluid phase and the matrix.

This study started with a study of crown ether-water interactions in a water/organic solvent biphasic system. Proton nuclear magnetic resonance (NMR) spectroscopy was used as a probe to evaluate chemical environments and to calculate equilibrium constants of a number of crown ether-water complexes in chloroform (dielectric constant ε = 4.8 at 20 °C) and in mixtures of chloroform and carbon tetrachloride (ε = 2.2 at 20 °C). The partition coefficients of a number of crown ethers between water (ε = 80.4 at 20 °C) and the organic solvents were also determined by the proton NMR technique. The results are given in a paper entitled "Partition Coefficients and Equilibrium Constants of Crown Ethers Between Water and Organic Solvents Determined by Proton Nuclear Magnetic Resonance" published by the *Journal of Chemical and Engineering Data*.[10] NMR studies of cesium-crown ether-water interactions in chloroform in the presence of picric acid turned out to be complicated for spectral analysis. Some results were obtained but with large uncertainties. An approach to use a capillary tubing NMR technique to study crown ether-water interactions in supercritical CO_2 was also not successful because of experimental

difficulties. Finally, a Fourier-Transform Infrared (FT-IR) technique was chosen to study crown ether-water complexes with 18-crown-6 and with dicyclohexo-18-crown-6 as hosts in liquid and in supercritical CO_2. FT-IR spectroscopic evidence shows that water can form 1:1 and 1:2 (sandwich) complexes with 18-crown-6 in supercritical CO_2. In the 1:1 complex, H_2O can be bonded to the crown ether with one hydrogen bond or with both hydrogen atoms bonded to the oxygen atoms of the host cavity. The equilibrium constants of the 18-crown-6-water complex at different temperatures and pressures were measured. Density showed little change of the equilibrium constant. The enthalpies of formation of the crown-water complexes involving a single hydrogen bond and with two hydrogen bonds with the water molecule were also determined. The FT-IR results are published in a *Journal of Physical Chemistry-A* article entitled "An FT-IR Study of Crown Ether-Water Complexation in Supercritical CO_2".[11]

The crown-water complex in supercritical CO_2 can be considered a Lewis acid-base complex with crown ether acting as a Lewis base (electron donor) and water as a Lewis acid (electron acceptor). This Lewis acid-base complex formation mechanism may provide a method of introducing hydrophilic compounds such as water or water soluble acids in supercritical CO_2. An NMR study of some Lewis acid-base complexes of relevance to nuclear waste related problems was conducted. Tri-n-butylphosphate (TBP) was chosen as a Lewis base for this study because it is highly soluble in supercritical CO_2 and is known to form stable complexes with many metal species particularly lanthanides and actinides. TBP forms a 1:1 complex with water through hydrogen bonding with the electron donating P=O group of TBP. TBP also forms Lewis acid-base complexes with other hydrophilic acids such as nitric acid and hydrochloric acid in a general form $(TBP)(acid)_x(H_2O)_y$. These inorganic acids (i.e. aqueous nitric acid and hydrochloric acid) are not soluble in CO_2. Through hydrogen bonding, these acids can be dissolved in supercritical CO_2 using TBP as a carrier with solubilities typically in the order of 1-2 mol% in supercritical CO_2 at 40 °C and 110 atm. Some examples of the Lewis acid-base complex formation method for introducing hydrophilic acids in supercritical CO_2 are given in a paper entitled "Lewis Acid-Base Complex Formation for Dissolution of Acids in Supercritical Carbon Dioxide" submitted to *Chemical Communications* for publication.[12] This method of dissolving acids in supercritical CO_2 may have a wide range of applications because acids are often needed for chemical reactions and separations in supercritical processes. The TBP-nitric acid complex was further characterized by other methods to evaluate their compositions and phase behavior in supercritical CO_2. The results of characterization of the complex are given in an article "Characterization of Tri-n-butylphosphate-Nitric Acid Complex – A CO_2-Soluble Extractant for Dissolution of UO_2" published in *Industrial and Engineering Chemistry Research.*[13]

One application of the TBP-nitric acid complex is for dissolution of metals and oxides in supercritical CO_2. Nitric acid is an oxidizing agent. It is known that concentrated nitric acid can oxidize solid uranium dioxide UO_2 to uranyl ions $(UO_2)^{2+}$. This reaction is important for dissolution of uranium dioxide in supercritical CO_2. For example, when a TBP-nitric acid complex dissolved in supercritical CO_2 is in contact with uranium dioxide, the acid can oxidize UO_2 to the uranyl ion followed by TBP coordination with the ion to form the $UO_2(NO_3)_2(TBP)_2$ complex. Based on our previous research, $UO_2(NO_3)_2(TBP)_2$ complex is one of the most soluble metal complexes known in the literature with a solubility around 0.45 mol L^{-1} at 40 °C and 200 atm. The solubility of the complex increases with pressure at a given temperature. When the solubility of the complex is plotted against density of supercritical CO_2 in logarithmic scale, it shows a linear relationship. The ability of the TBP-nitric acid complex for direct dissolution of

uranium dioxide in supercritical CO_2 is described in a paper "Dissolution of Uranium Dioxide in Supercritical Fluid Carbon Dioxide" published in *Chemical Communication*.[14] This supercritical fluid dissolution technique my lead to development of a dry process for treating uranium dioxide contaminated waste or even for possible recycling of spent nuclear fuels. Demonstrations of these possible applications are currently underway in Japan.

This project has provided opportunities for research as well as for education at the University of Idaho. Three graduate students received financial support from the project for their thesis research. One graduate student Xiang-Rong Ye completed his Ph.D. degree in chemistry at the University of Idaho last year. Other two graduate studies are expected to finish their Ph.D. degrees this year. An undergraduate student and two visiting scientists were also supported by this project. The project has produced 6 journal publications plus an equal number of presentations at professional meetings.

References

1. McHugh, M.A.; Krukonis, V.J. Supercritical Fluid Extraction: Principles and Practice, Butterworth-Heinemann: Oxford, U.K., **1994**.
2. Darr, J.: Poliakoff, M. Chem. Rev. **1999**, *99*, 495-541.
3. Phelps, C.L.; Smart, N.G.; Wai, C.M., *Chem. Edu.* **1996**, *12*, 1163-1168.
4. Laintz, K.E.; Wai, C.M.; Yonker, C.R.; Smith, R.D., *J. Supercrit. Fluids*, **1991**, *4*, 194-198.
5. Laintz, K.E.; Wai, C.M.; Yonker, C.R.; Smith, R.D., *Anal. Chem.* **1992**, *64*, 2875-2878.
6. Wai, C.M.; Wang, S., *J. Chromatography A*, **1997**, *785*, 369-383.
7. Carrott, M.J.; Waller, B.E.; Smart, N.G.; Wai, C.M. Chem. Commun. **1998**, 373-374.
8. Tomioka, O.; Meguro, Y.; Iso, S.; Youshida, Z.; Enokida, Y.; Yamamoto, I., *J. Nucl. Sci. Technol.* **2001**, *38*, 1097.
9. Samsonov, M.D.; Wai, C.M.; Lee, S.C.; Kulyako, Y.; Smart, N.G., *Chem. Commun.* **2001**, 1868-1869.
10. Han-Wen Cheng, Anne Rustenholtz, Richard A. Porter, Xiang R. Ye, Chien M. Wai, , *J. Chem. Eng. Data*, ASAP Web Release Date: March 2, **2004**.
11. Anne Rustenholtz, John L. Fulton, Chien M. Wai, *J. Phys. Chem. A*, **2003**, *107*, 11239-11244.
12. Shaofen Wang, Xiang-Rong Ye, Jamie Herman, Qingyong Lang, Chien M. Wai, *Chem. Comm.*, submitted on March 10, 2004.
13. Yuichi Enokida, Osamu Tomioka, Su-Chen Lee, Anne Rustenholta, Chien M. Wai, *Ind. Eng. Chem. Res.*, **2003**, *42*, 5037-5041.
14. M.D. Samsonov, C.M. Wai, Su-Chen Lee, Yuri Kulyako, N.G. Smart, *Chem. Commun.*, **2001**, 1868-1869.

II. NMR Study of Crown Ether-Water Interaction

This project started with a study of crown ether-water interaction in a low dielectric constant solvent chloroform ($\varepsilon = 4.8$ at 20 °C) using proton nuclear magnetic resonance (NMR) spectroscopy as a probe. The reason of studying crown-water interaction is that liquid-liquid extraction of metal species from aqueous solutions ($\varepsilon = 80.4$ for water at 20 °C) is often done using an organic solvent with a low dielectric constant. Another purpose of this study is to determine the influence of solvent such as a mixture of chloroform and carbon tetrachloride on the crown-water interaction. The dielectric constant (ε) of CCl_4 is about 2.2 at 20 °C. Supercritical CO_2 has a small dielectric constant and the ε value varies with density. For example, at 50 °C and 200 atm, the dielectric constant of CO_2 is about 1.4. The organic solvent mixtures cover a wide range of solvent parameters which are comparable to those of liquid and supercritical CO_2 at different densities. Some crown ethers are appreciably soluble in water leading to their partitioning between the water and organic phases. NMR measurements also enable us to obtain partition coefficients of crown ethers between water and organic solvents. These data are very useful for solvent extraction of the alkali

Proton NMR is a very precise analytical technique for measuring the amount and chemical environment of water in organic solvents. In the case of chloroform, a commercially available deuterated solvent $CDCl_3$ can be used as the solvent and proton resonance peaks of water bonded to a crown ether can be easily measured. The proton NMR spectra of unsubstituted crown ethers are simple because of their symmetrical molecular structure. Overlapping of crown ether proton resonance peaks with that of water complexed with the host molecule does not create a problem for NMR measurements. Typical NMR spectra of 18-crown-6 in the $CDCl_3$ phase after equilibration with water are shown in Figure 1. The spectra were obtained using a 500 MHz Bruker DRX500 spectrometer. The experimental details are given in our publication #1 "Partition Coefficients and Equilibrium Constants of Crown Ethers between Water and Organic Solvents Determined by Proton Nuclear Magnetic Resonance".

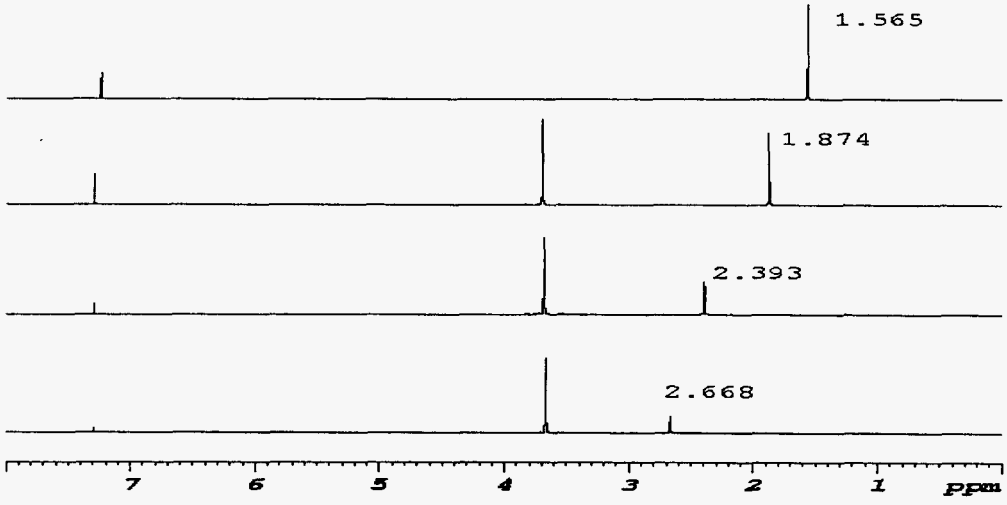

Figure 1. Typical PNMR spectra of 18-crown-6 in the $CDCl_3$ phase, the concentration of 18-crown-6 after equilibration with water, from top to bottom: 0.00 M, 0.002 M, 0.075 M, 0.153 M and H_2O resonance peak at 1.565, 1.874, 2.393, 2.668 ppm, respectively.

The 7.24 ppm proton resonance peak in Figure 1 is due to the small amount of $CHCl_3$ present in $CDCl_3$. Chemical shifts in the organic phase are calibrated by setting the chloroform chemical shift to this value. Water dissolved in chloroform has a proton resonance peak at 1.565 ppm. In the presence of a crown ether such as 18-crown-6, the water dissolved in chloroform can be bound to the crown ether to form a complex or exist as uncomplexed free water. 18-crown 6 has a single resonance peak for the ring protons at 3.65 ppm. The complexed H_2O and the free H_2O apparently undergo rapid exchange in the organic phase resulting in a single peak which shifts downfield as the crown ether concentration increases.

The equilibrium model for the partition of a crown ether (L) between water and chloroform and the formation of a crown-water complex ($L{\bullet}H_2O$) in the organic phase is represented in detail in our publication #1. An outline of our experimental measurements and calculations to obtaine the equilibrium constant of crown-water complexes in chloroform is given below. The equilibrium constant for the crown-water complex is defined as

$$K = [L{\bullet}H_2O_{(org)}]/\{[L_{(org)}][H_2O_{(org)}]\} \quad (1)$$

The fraction of crown molecules complexed to water is defined as

$$k = [L{\bullet}H_2O_{(org)}]/\{[L_{(org)}] + [L{\bullet}H_2O_{(org)}]\} \quad (2)$$

The k value can be determined from the total water $[H_2O_{(org)}]^o$ and total crown $[L_{(org)}]^o$ present in the organic phase (from NMR intensities) by the folloiwng equation

$$[H_2O_{(org)}]^o = k[L_{(org)}]^o + [H_2O_{(org)}] \quad (3)$$

From the k value, we can calculated the equilibrium constant by the following equation

$$k = K[H_2O_{(org)}]/\{1+K[H_2O_{(org)}]\} \quad (4)$$

From the NMR resonance peak shift (δ) of the H_2O peak, we can also calculate k and δ_o (the chemical shift of free water in chloroform) and δ_1 (the chemical shift of complexed water in chloroform) using the following equation

$$\delta = \delta_0 + k(\delta_1 - \delta_0)\,[L_{(org)}]^o/[H_2O_{(org)}]^o \quad (5)$$

Figure 2 shows plots of experimental data based on equations (3) and (5) for 18-crown-6 in $CDCl_3/H_2O$ system. Linear relationships are observed in these plots supporting the equilibrium assumptions made in this study.

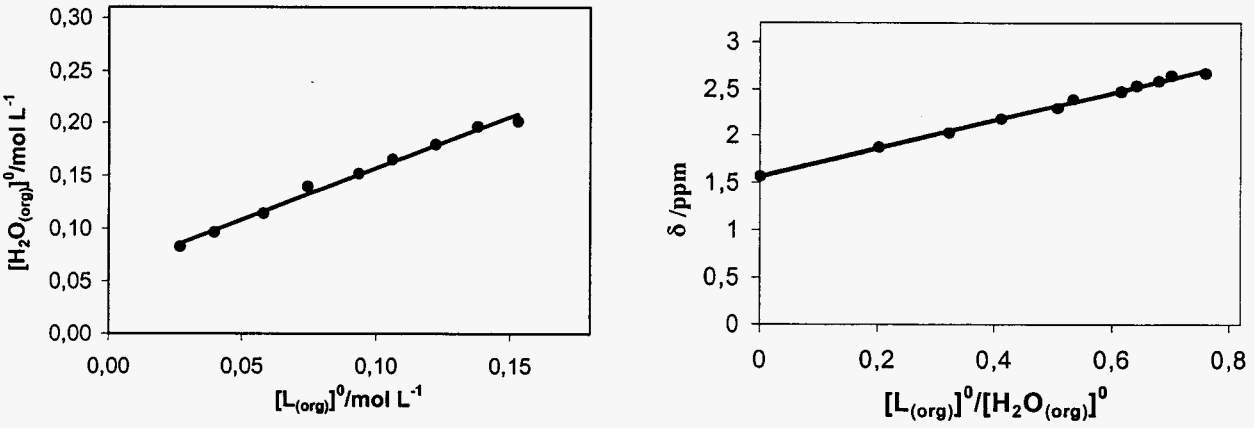

Figure 2. Linear relationship between: (a) total water and 18-crown-6 concentration in chloroform; ($[H_2O_{(org)}]^0 = 0.9704[L_{(org)}]^0 + 0.0601$; correlation coefficient r = 0.9955) (b) observed chemical shift of water and the ratio $[L_{(org)}]^o/[H_2O_{(org)}]^o$ in chloroform (eq 5) ($\delta = 1.5015[L_{(org)}]^0/[H_2O_{(org)}]^0 + 1.5611$; r = 0.9982).

Table 1 lists the equilibrium constants of various crown-water complexes in chloroform and in mixtures of chloroform and carbon tetrachloride determined by this study. The partition coefficient ($D=[L_{(aq)}]^o/[L_{(org)}]^o$) of various crown ethers between water and the organic solvent system determined by this NMR study are also given in the table.

In $CDCl_3$, the k values for unsubstituted crown ethers 12C4, 15C5, and 18C6 are 0.15, 0.54, and 0.97, respectively. This trend shows strong binding of water for 18C6 relative to the smaller rings. Substitution in crown ethers tends to lower the k value. Thus, for DCH18C6, the k value in chloroform is lowered to 0.70 compared with a value of 0.97 for the unsubstituted 18C6. In the case of DCH24C8 and DB24C8, benzyl substitution further lowers the k value compared with cyclohexyl substitution in 24C8. The equilibrium constant (K) defined by eq 4 varies from 2.78 for 12C4 to 545 for 18C6 in chloroform. The K value for the substituted (DCH18C6) crown is much lower than that of the unsubstituted (18C6) one (32 versus 545). The δ_o values for the three unsubstituted crown ethers are approximately constant (in the range of 1.53±0.04 ppm) as expected. Considering the experimental error the δ_1 value is stable.

For the individual ligands, there are several clear trends with respect to the variation of solvent composition ($CDCl_3$+CCl_4). First, the amount of free water dissolved in the organic phase decreases with increasing CCl_4 fraction in the solvent. This is expected since decreasing the solvent polarity should result in lower solubility of water in the organic phase. In all cases, the parameter k representing the fraction of ligand bound to water also decreases monotonically as the proportion of CCl_4 increases. Thus, decreasing solvent polarity also reduces water-crown complexation [$L{\cdot}H_2O_{(org)}$], leading to lower k values. This is probably caused by the combination of a lower solubility of free water in the organic phase and intrinsic solvation effects on the crown-water complex. The equilibrium constant K, which includes the concentration of unbound water and the ligand in the mixed organic phase, changes less and in an irregular fashion. Because both $[H_2O]_{org}$ and $[L]_{org}$ vary drastically with the solvent composition, the K values defined by eq 4 are not as useful as the k values for discussion in the $CHCl_3$ + CCl_4 system. In the binary solvent systems, $[H_2O]_{org}$ decreases with increasing CCl_4 fraction whereas $[L]_{org}$ changes independently in the opposite direction, resulting in irregular trends for the K values.

From the crown ether PNMR peak intensities in the organic and in the aqueous phase, we also calculated the partition coefficients $D=[L_{(aq)}]^0/[L_{(org)}]^o$ as shown in Table 1. The D values for 12C4 and 18C6 between water and chloroform are around 0.25 and that for 15C5 is somewhat lower. For the crown ethers that are appreciably soluble in water, the partition coefficients show that extraction into the aqueous phase increases exponentially as the organic solvent polarity decreases. In the case of 18C6, the D value starts at 0.25 in 100% $CHCl_3$ becomes 1.16 with a 50:50 mixture of $CHCl_3$ and CCl_4 and rises up to 48 for a 100% CCl_4 solution (Figure 3.). For the substituted crown ethers DCH18C6, DCH24C8, and DB24C8, the D values are below detection (<0.01) in the concentration range (0.06 to 0.2) mol L^{-1}. Partitioning of 18-crown-6 between water and various organic solvents has been determined by several different methods including gravimetric and conductivity measurements. PNMR actually provides a simple and rapid method for determination of crown ether partition coefficients between water and organic solvents. The D values given in Table 1 represent the first systematic measurements of such data using a PNMR technique.

Table 1. Equilibrium and chemical shift parameters by various crown ethers.[a]

Crown	% / vol $CDCl_3$[b]	k	K ($L.mol^{-1}$)	$[H_2O]_{org}$[c]	D	δ_0/ppm	δ_1/ppm
12C4	100	0.15	2.78	0.065	0.25	1.55	3.0
	75	0.10	2.79	0.039	0.34	1.43	3.0
15C5	100	0.54	25.6	0.045	0.18	1.49	2.8
	75	0.35	19.9	0.027	0.29	1.40	2.7
	50	0.25	14.2	0.024	0.71	1.29	2.8
	25	0.21	35	0.008	2.13	1.11	2.0
	0			0.00[d]	2.450	1.36	
18C6	100	0.97	545	0.060	0.25	1.52	3.1
	75	0.79	102	0.037	0.42	1.40	2.8
	50	0.63	97	0.017	1.16	1.28	2.6
	25	0.61	141	0.011	3.83	1.08	2.2
	0			0.00[d]	48.04	1.31	
DCH18C6	100	0.70	32	0.072	0.00	1.52	3.3
	50	0.58	81	0.017	0.00[d]	1.25	2.6
	25	0.40	36	0.018	0.00[d]	1.13	2.6
DCH24C8	100	0.850	93	0.060	0.00[d]	1.57	3.2
DB24C8	100	0.37	9.03	0.064	0.00[d]	1.57	2.7

[a]Typical statistical errors: k ±5%, K ±10%, $[H_2O]_{org}$ ±0.003 $mol{\cdot}l^{-1}$, D ±5%, δ_0 ±0.04 ppm, δ_1 ±0.3 ppm; [b]Volume percentage of $CDCl_3$ in CCl_4; [c]Concentration in mol L^{-1}; [d] <0.01 for the ligand concentration range 0.02-0.2 mol L^{-1}

NMR studies of crown-water complexation in liquid and in supercritical fluid CO_2 were carried out at PNNL using a capillary tubing technique developed by Dr. Clem Yonker. The results were not reproducible because of slow diffusion of crown ether and water in capillary tubing to reach equilibrium. Another spectroscopic technique Fourier Transform Infrared (FTIR) spectroscopy was chosen to study crown-water complexation in supercritical CO_2 using a high-pressure view-cell with diamond windows available in John Fulton's lab at PNNL. The results are described in the next section.

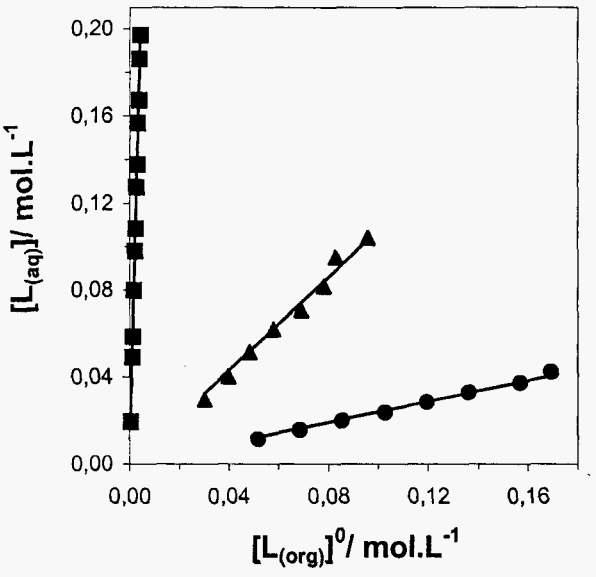

Figure 3. The partition coefficient for 18-crown-6 in , $CDCl_3$; , 50% $CDCl_3$ + CCl_4; , CCl_4.

III. FTIR Study of Crown Ether-Water Complexation in Supercritical Carbon Dioxide

Supercritical fluids have unique properties that make them highly attractive for extraction of metal ions from liquid and solid materials. Carbon dioxide is most widely used for supercritical fluid applications because of a number of advantages including (i) low toxicity, (ii) environmentally benign, (iii) low cost, (iv) moderate critical constants (T_c = 31 °C and P_c = 73.7 bar), and (v) tunable solvation strength that varies with density. Selective extraction of metal species using a non-polar solvent such as CO_2 requires special chelating agents that should possess ion recognition ability and be soluble in supercritical fluid carbon dioxide (SF-CO_2). Crown ethers have been extensively used for extraction of alkali metal and alkaline earth metal cations from aqueous solutions into organic solvents.

For the extraction of metal ions from aqueous solutions using ligands dissolved in SF-CO_2, the fluid phase will be saturated with water. Thus, water interaction with the ligand in the fluid phase plays an integral role in the extraction process. It has been reported that the extraction efficiency of alkali metal ions in conventional solvent processes depends on the solubility of water in the organic phase using macrocyclic polyethers as a complexing agent. With crown ethers, both computational simulation and spectroscopic studies show that in organic solvents, the water can bond to a macrocyclic host molecule by two different types of hydrogen bonding. The first type composes of a single hydrogen bond between one hydrogen atom of a water molecule and one oxygen atom of the crown ether cavity. In this case, the water molecule is mostly located outside the cavity. The second type occurs inside the cavity and is composed of a water molecule bridging between two different oxygen atoms of the crown cavity.

FT-IR is a sensitive and qualitative technique that has been used during the past years to study hydrogen bonding in different solvents. For example, Fulton et al. used this technique to explore hydrogen bonding of methanol dissolved in supercritical carbon dioxide and found that a weak interaction between carbon dioxide and methanol significantly reduced the amount of methanol-methanol hydrogen bonding. Johnston et al. used it to understand the solvent effect on hydrogen bonding in supercritical fluids. They were able to determine, with a good accuracy, the

equilibrium constants and other thermodynamics data for the hydrogen bond between methanol and triethylamine. The FT-IR technique has also been used by Moyer et al. to determine how water is bonded to crown ethers in carbon tetrachloride. These authors assigned vibrational bands to free water and to two different kinds of hydrogen bonds mentioned above. In this report we examine the interactions of water and 18-crown-6 in liquid and supercritical CO_2 for the purpose of establishing a basis for using this green solvent in extraction processes utilizing crown ethers as extractants.

The details of the FTIR measurements of crown-water complexation are given in our publication #2 entitled "An FTIR Study of Crown-Water Complexation in Supercritical CO2" published in the Journal of Physical Chemistry A (2003, 107, 11239-11244). According to our spectroscopic analysis, 18-crown-6 can form 1:1 complex or 2:1 complex with water in liquid and in supercritical carbon dioxide. According to our FTIR analysis, the 1:1 crown-water complex has two forms, one with H_2O located on top of the cavity with both of the hydrogen atoms bonded to the oxygen atoms of the crown ether (bridge bonding) and the other form involves only one hydrogen bond of the H_2O molecule with the crown cavity (single bondig). The structures of these crown-water complexes are illustrated in Figure 4.

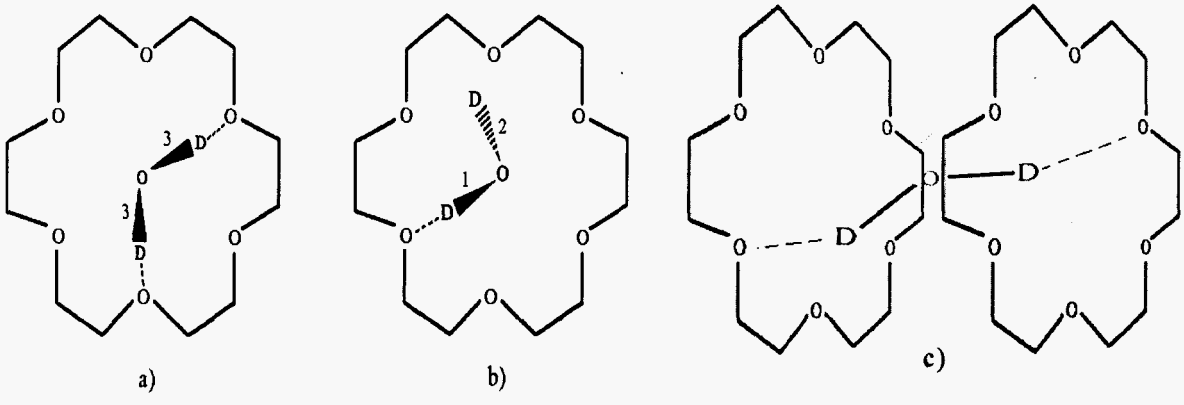

Figure 4. Schema of the three possible bonding between D_2O and 18-Crown-6. a) Bridge bonding; b) single bonding; c) a 1:2 complex in a sandwich configuration.

A typical FTIR spectrum of free and bonded D_2O with 18-crown-6 in liquid CO_2 in supercritical CO_2 is shown in Figure 5. Peaks for the free D_2O, i.e. D_2O dissolved in SF-CO_2 without the crown ether, (O-D stretching, asymmetric at 2761 cm^{-1} and symmetric at 2654 cm^{-1}) can be easily discerned and their positions are in agreement with those reported for D_2O molecules in the vapor (i.e. 2789 and 2666 cm^{-1} for the D_2O vapor). The shifts of the D_2O vibrational stretchings to lower wave numbers in SF-CO_2 relative to single molecules in the vapor phase reflect the interactions of D_2O molecules with CO_2 in the fluid phase. When 18-crown-6 was added to the CO_2 solution, three other peaks at 2733, 2679 and 2590 cm^{-1} appeared. According to the order of peak assignment of H_2O/18-crown-6 complex in carbon tetrachloride, the broad peak at 2590 cm^{-1} should correspond to the symmetrical stretch of the O-D bond involved in the two hydrogen bond bridge as illustrated in Figure 4a. The D_2O molecule with one hydrogen bonding to the cavity oxygen is expected to have two stretching bands. The sharp O-D

band at 2733 cm^{-1} should be the unbounded O-D stretching marked as 2 on Figure 5b. The bonded O-D stretching band (marked as 1 on Figure 4b) was assigned to the 2679 cm^{-1} peak, located between the symmetrical and the asymmetrical stretching bands of free water. In the FT-IR spectra of H_2O/18-crown-6 complex in CCl_4, the bonded O-H stretching band was found at a lower energy than the symmetrical stretch band of free water. We confirmed our assignment of this bonded O-D band by completing two secondary experiments. One experiment was a comparison of the FTIR spectra of 18-crown-6/H_2O and 18-crown-6/D_2O complexes in CCl_4. We confirmed the peak assignment of the former as reported in the literature and the D_2O isotopic effect altered the peak order of the latter as shown in Figure 5. In another experiment, we confirmed that the order and assignment of the various O-D bands in 18-crown-6/D_2O complex in SF-CO_2 was the same in both CCl_4 and liquid CO_2.

When the 18-crown-6 concentration exceeds 0.4 mol L^{-1} with a lower water concentration (less than 17 mmol L^{-1}), only one absorption band at 2590 cm^{-1} is observed (Figure 5). All the D_2O molecules seem to be bridge bonded to the crown ether. This observation may be explained by the formation of a 1:2 complex between D_2O and 18-crown-6 as illustrated in Figure 4c. The O-D stretching band for this kind of complex should appear at the same frequency as the bridged form of D_2O (Figure 4a configuration). Our suggestion of an 1:2 complex formation is based on the assumption that by increasing the crown ether to water ratio in SF-CO_2, we should not change the equilibrium between D_2O molecules bonded to one oxygen atom (configuration 1b) or to two oxygen atoms (configuration 1a) of the cavity. As the concentration of 18-crown-6 in the system increases, it is conceivable that the single bonded D_2O molecule (configuration 1b) would form hydrogen bonding with another crown molecule via the unbounded O-D thus leading to the formation of an 1:2 complex. The law of mass action should favor the shifting of equilibrium from a 1:1 complex to a 1:2 complex between water and 18-crown-6 in SF-CO_2. Also in figure 3c, we show, for comparison, spectra of the double bond area of 18-crown-6 (at 0.041 M and 0.123 M) and D_2O (0.049 M) at 400 bar and 40 °C. Peaks occur at the same position for both the dimmer and the monomer forms.

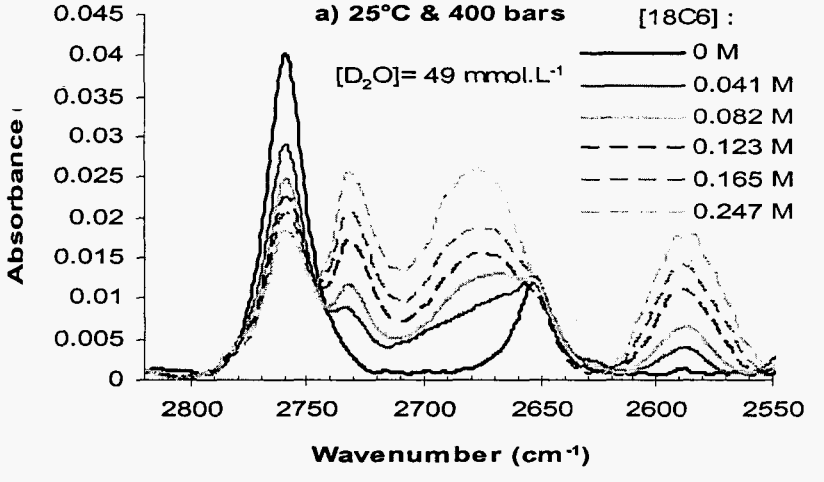

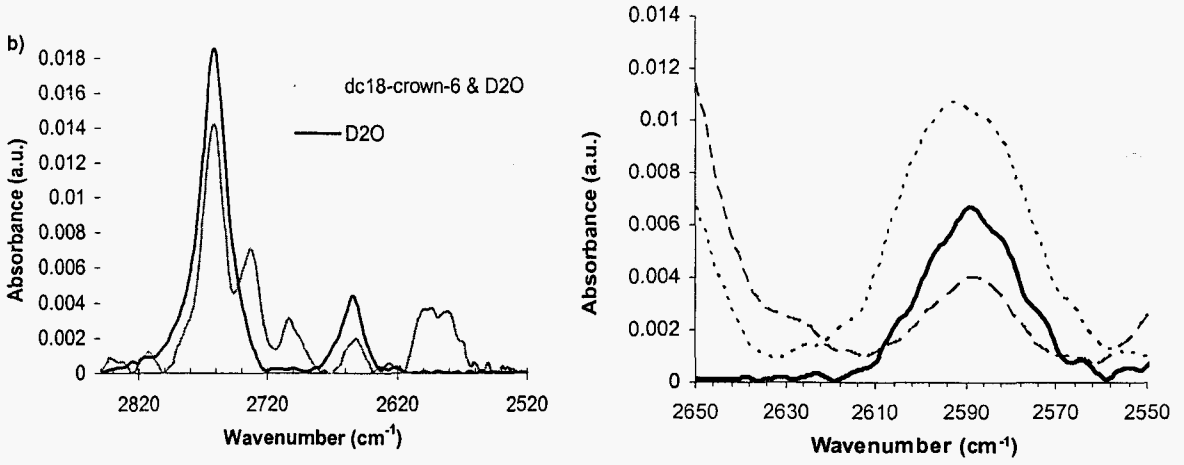

Figure 5. (a) FTIR spectrum of D_2O (49 mmol L^{-1}) in CO_2 (25 °C and 400 atm) with 18-crown-6 at different concentrations, (b) FTIR spectrum of D_2O (49 mmol L^{-1}) in CO_2 (40 °C and 400 atm) with dicyclohexano-18-crown-6 (60 mmol L^{-1}), and (c) FTIR spectrum of D_2O (49 mmol L^{-1}) and 18-crown-6 at 41 mmol L^{-1} (---) and at123 mmol L^{-1} (····) in CO_2 at 40 °C and 400 atm. The solid spectrum is for 17 mmol L^{-1} of D_2O and 40 mmol L^{-1} of 18-crown-6.

The formation of a 1:1 complex between 18-crown-6 and D_2O in the CO_2 phase at lower crown to D_2O molecular ratio was evaluated by the analysis of the FT-IR data and the equilibrium relations of the following equations:

$$18C6 + D_2O \leftrightarrows 18C6 \bullet D_2O^{single} \quad (6)$$

$$K_s = ([18C6 \bullet D_2O^{single}])/([18C6][D_2O])$$

$$18C6 + D_2O \leftrightarrows 18C6 \bullet D_2O^{bridge} \quad (7)$$

$$K_b = ([18C6 \bullet D_2O^{bridge}])/([18C6][D_2O])$$

Where K_s and K_b represent the equilibrium constants for the 1:1 complex with a single hydrogen bond (configuration 4b) and double hydrogen bonds (configuration 4a), respectively. The details are given in our publication #2.

The K values vary considerably with CO_2 density. At a constant pressure (200 bar), the K_s value decreases from 21±2 to 13±1 L mol^{-1} with increase in temperature from 25 to 60 °C. The variation of K_b with temperature is even greater for the same pressure, its value varies from 14±2 to 2±1 L mol^{-1} from 25 to 60 °C. These K values are comparable to the one reported by Moyer et al. (i.e. 15.6 (1.2) L mol^{-1}) for the 18-crown-6/H_2O complex in carbon tetrachloride. This implies that, in terms of hydrogen bonding between water and 18-crown-6, supercritical CO_2 behave as a non-polar solvent such as CCl_4 and not like chloroform. The K value of 18-crown-6/H_2O complex in chloroform was reported to be 20 times larger than that in CCl_4. The influence of density (increase in pressure from 200 to 400 bar) at a constant temperature (i.e. 40 °C) on the two equilibrium constant K_s and K_b is shown on Figure 6. An increase in density causes a decrease in the K_s and K_b values.

The molar enthalpy of a hydrogen bonding (ΔH_i) can be determined from the equilibrium constant at constant pressure by equation (4) from well known thermodynamic relations (equations 3), where T is the absolute temperature in Kelvin and R the ideal gas constant.

$$\left(\frac{\partial(\Delta G_i)}{\partial T}\right)_P = -\Delta S_i = \frac{\Delta G_i - \Delta H_i}{T} \qquad \text{and} \qquad \Delta G_i^\circ = -RT \ln K_i \quad (7)$$

$$\left(\frac{\partial(\ln K_i)}{\partial 1/T}\right)_P = -\frac{\Delta H_i}{R} \quad (8)$$

Using a linear regression on the plot of ln K versus 1/T (Figure 6), and assuming that ΔH is independent of temperature and density, the ΔH_s (for single hydrogen bond, configuration 1b) was found to be -12 ± 2 kJ mol^{-1} and ΔH_b (for bridge bonding, configuration 1a) to be -38 ± 3 kJ mol^{-1}, both at 200 bar. The complexation process is exothermic as expected for a hydrogen bonding and its value is similar to the literature values for hydrogen bonding processes in both liquid solvents and in supercritical fluids. The fact that the hydrogen bonding process is exothermic and that the bonded species are more entropically ordered explain the decrease of K values with the increase of temperature.

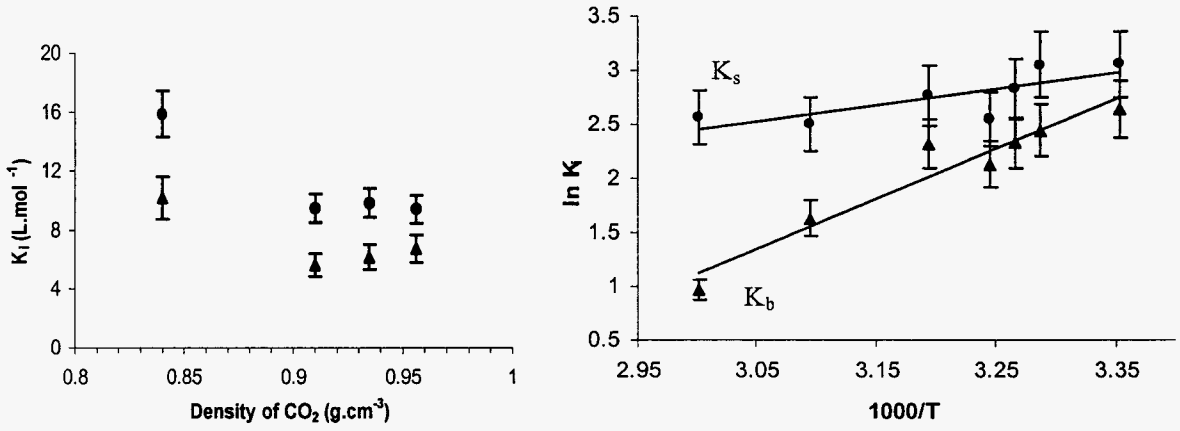

Figure 6. Left: density effect on equilibrium constants K_s (●) and K_b ( ); Pressure varies from 200 to 400 bar at constant temperature (40°C); [18C6]= 41 mmol.L^{-1}; [D_2O]= 49 mmol L^{-1} ; Right: concentration of the two isomers (i.e. single (●) and double bond ( ) between D_2O (49mmol L^{-1} total concentration in CO_2) and the 18-crown-6 (83mmol L^{-1} total concentration in CO_2) versus temperature (in Celsius).

The study has demonstrated that FT-IR is a sensitive technique for studying crown ether and water interactions in SF-CO_2. The O-D stretching vibrations for D_2O dissolved in SF-CO_2 show slight shifts to lower wave numbers relative to those found for D_2O in its vapor phase indicating interactions (salvation) of CO_2 with D_2O molecules in the supercritical fluid phase. In

the presence of 18-crown-6, D_2O forms a 1:1 complex with the macrocyclic molecule with two different configurations. The D_2O molecule can form one hydrogen bond with an oxygen atom of the crown cavity or it can be bonded to two oxygen atoms of the cavity in a bridged configuration. The equilibrium constant of the single hydrogen bond configuration is slightly greater than the two hydrogen bond configuration and both equilibrium constants decrease with increasing temperature. The enthalpy of the complex formation is -12±2 kJ mol^{-1} for the former and -38±3 kJ mol^{-1} for the latter. These values are within the range of hydrogen bonds reported in liquid solvents. At high 18-crown-6 to D_2O ratios, formation of an 1:2 complex in SF-CO_2 that involves one D_2O molecule hydrogen bonded to two crown ether molecules becomes possible.

IV. Lewis Acid-Base Complex Formation Mechanism for Dissolving water and acids in Supercritical Carbon Dioxide

The crown ether-water complex formation discussed in the previous sections involves hydrogen bonding between the crown ether oxygen atoms (electron donor) and the hydrogen atoms (electron acceptor) of the H_2O molecule. This type of complex can be considered a Lewis acid-base complex with crown ether acts as a Lewis base and water as a Lewis acid. The Lewis acid-base complex formation mechanism may provide a means of dissolving normally insoluble or slightly soluble hydrophilic compounds such as water in supercritical CO_2. This complex formation mechanism should not be limited to crown ethers as the Lewis base and water as the Lewis acid. Other compounds such as tri-n-butylphosphate with an electron donating P=O group may also be an effective Lewis base for introducing water and acids in supercritical CO_2.

Supercritical fluid processing has been a burgeoning area of research in recent years for both theoretical and practical considerations. Carbon Dioxide is the most widely used gas for supercritical fluid applications because of its moderate critical constants, nonflammable nature and environmental acceptability. However, since CO_2 is non-polar and has a low dielectric constant, supercritical CO_2 processing is limited by its poor ability to dissolve hydrophilic species. Several strategies have been developed in the past to make supercritical CO_2 more "solute-philic" including modifying CO_2 with polar solvents, utilizing water-in-CO_2 microemulsions, and complex formation approaches. Recently, dissolution of hydrophilic metal species in supercritical CO_2 has gained increasing attention because of potential applications in nuclear waste treatment, environmental remediation, semiconductor devices manufacturing, and chemical catalysis. The *in situ* chelation method for dissolving metal species in supercritical CO_2 developed by our research group in the early 1990s is widely used today for chemical and environmental studies. Several previous reports have demonstrated that the solubility of metal chelates in supercritical CO_2 can be significantly enhanced using CO_2-philic ligands such as fluorinated chelating agents and organophosphorus ligands. Among these reagents, tri-n-butylphosphate (TBP) is particularly interesting because it is a CO_2-philic Lewis base and is capable of forming stable coordination compounds with Lewis acids through the electron donating P=O group. The Lewis acid-base complex formation mechanism provides a simple method of dissolving hydrophilic acids in supercritical CO_2 using TBP as a carrier. This technique may have a wide range of applications in developing CO_2-based processes because acids are often needed for chemical reactions and separations. For this reason, we investigated Lewis acid-base complex formation with TBP as a carrier and measured the solubilities of some TBP-acid complexes in supercritical CO_2.

The complexes used in this study were prepared by shaking 5 mL of TBP (Avocado, Alfa Aesar, Ward Hill, MA) with a certain amount of an acid in a capped vial for one hour. Concentrated

nitric acid (15.5 M, Fisher, Fair Lawn, NJ), hydrochloric acid (37.4%, Fisher), and benzoic acid (Fisher) were used as received for this study. After shaking, the mixture was centrifuged for one hour and the TBP phase was removed for characterization. The acid content in the TBP phase was determined by diluting 1 mL of the TBP phase with 40 mL of water followed by NaOH (0.1 M) titration of the acid in the aqueous phase. The water content of the TBP phase was determined by Karl-Fischer titration. The TBP-acid complex has a general composition of TBP $(Acid)_x$ $(H_2O)_y$ with x and y depending on the relative amount of TBP and the acid used in the preparation. Examples of TBP-nitric acid and TBP-hydrochloric acid complexes are given in Table 1. The TBP-benzoic acid complex was prepared by dissolving a certain amount of solid benzoic acid in TBP directly. Because benzoic acid does not contain water the complex has a formula of TBP $(Acid)_x$.

Table 2. Compositions of some TBP-acid complexes prepared for this study

Initial TBP/Acid Mixture	Composition of TBP-Acid Complex
5 mL TBP + 0.82 mL nitric acid (15.5 M).	$TBP(HNO_3)_{0.7}(H_2O)_{0.7}$
5 mL TBP + 1.3 mL nitric acid (15.5 M)	$TBP(HNO_3)_{1.0}(H_2O)_{0.4}$
5 mL TBP + 1.5 mL hydrochloric acid (12.3M)	$TBP(HCl)_{0.8}(H_2O)_{2.8}$
5 mL TBP + 2 g benzoic acid	$TBP(benzoic\ acid)_{0.5}$

Proton NMR spectra of a typical TBP-hydrochloric acid complex and a TBP-nitric acid complex are given in Figure 1. The spectra were taken using a 300 MHz (Bruker) spectrometer at room temperature. In the NMR measurement of pure complexes, deuterated water was placed in an insert and fitted into an NMR tube containing a TBP-acid complex. The purpose of the D_2O insert was to lock the NMR. A trace amount of HDO present in the deuterated water allows calibration of the instrument. TBP is known to form a 1:1 complex with H_2O and the TBP-H_2O complex has a single resonance peak at about 3.9 ppm. The proton NMR spectrum of the $TBP(HCl)_{0.8}(H_2O)_{2..8}$ complex shows a single peak around 10 ppm indicating the protons of H_2O and HCl in the complex undergo rapid exchange (Figure 1a). The other 4 peaks below 4 ppm are the protons from the butyl groups of TBP. The hydrochloric acid peak in the TBP complex shifts upfield when the amount of the acid (or x value) increases in the complex. The NMR spectra of the TBP-nitric acid complexes is similar to that of TBP-hydrochloric acid complexes. Figure 2a shows the proton peaks of the $TBP(HNO_3)_{0.7}(H_2O)_{0.7}$ complex. Rapid exchange of H_2O and HNO_3 in the complex apparently takes place resulting in a single proton resonance peak at about 11.8 ppm. Formation of TBP-acid complex is not limited to hydrophilic inorganic acids. Organic acids can also form hydrogen bonded complex with TBP as illustrated by the NMR spectra of a TBP-benzoic acid complex given in Figure 3. Figure 3a shows the NMR spectrum of benzoic acid alone and Figure 3b shows the spectrum of a $TBP(benzoic\ acid)_{0.5}$ complex in $CDCl_3$. The shift of the carboxylic acid proton peak from the free benzoic acid (12.8 ppm) to the bonded acid (11.8 ppm) is obvious. Peaks at 8.1, 7.6 and 7.5 ppm in Figure 2a are protons from the benzene ring.

Understanding the solvation effect of supercritical CO_2 on the TBP-acid complexes is important for evaluating the behavior of the complex in the fluid phase. Unfortunately, the corrosive nature of the complex and the lack of a safe high-pressure NMR device in our lab prevented us from performing NMR studies of the TBP-acid complexes in supercritical CO_2. We chose to use chloroform ($CDCl_3$) to evaluate the salvation effect because chloroform has a small dielectric constant at room temperature (ε = 4.8 at 20 °C). Figure 1b shows that in the

presence of $CDCl_3$, a new peak at 7.9 ppm appears that is close to the NMR peak of free hydrochloric acid. An anti-solvent effect of chloroform probably causes a portion of the hydrochloric acid in the complex to precipitate and forming small droplets in the solvent. The bonded hydrochloric acid in TBP shifts upfield to about 10.3 ppm. Formation of small acid droplets in $CDCl_3$ was obvious because the solution turned cloudy after addition of the TBP complex to the solvent. The cloud formation was also observed when the TBP-hydrochloric acid complex was added to supercritical CO_2 using a high-pressure view-cell with quartz windows. Similar cloud formation was observed when a $TBP(HNO_3)_{0.7}(H2O)_{0.7}$ complex was added to supercritical CO_2. When the TBP-nitric acid complex was dissolved in $CDCl_3$, a free nitric acid peak appeared at 6.5 ppm and the bonded nitric acid peak shifted to 12.5 ppm as indicated by the NMR spectrum given in Figure 2b.

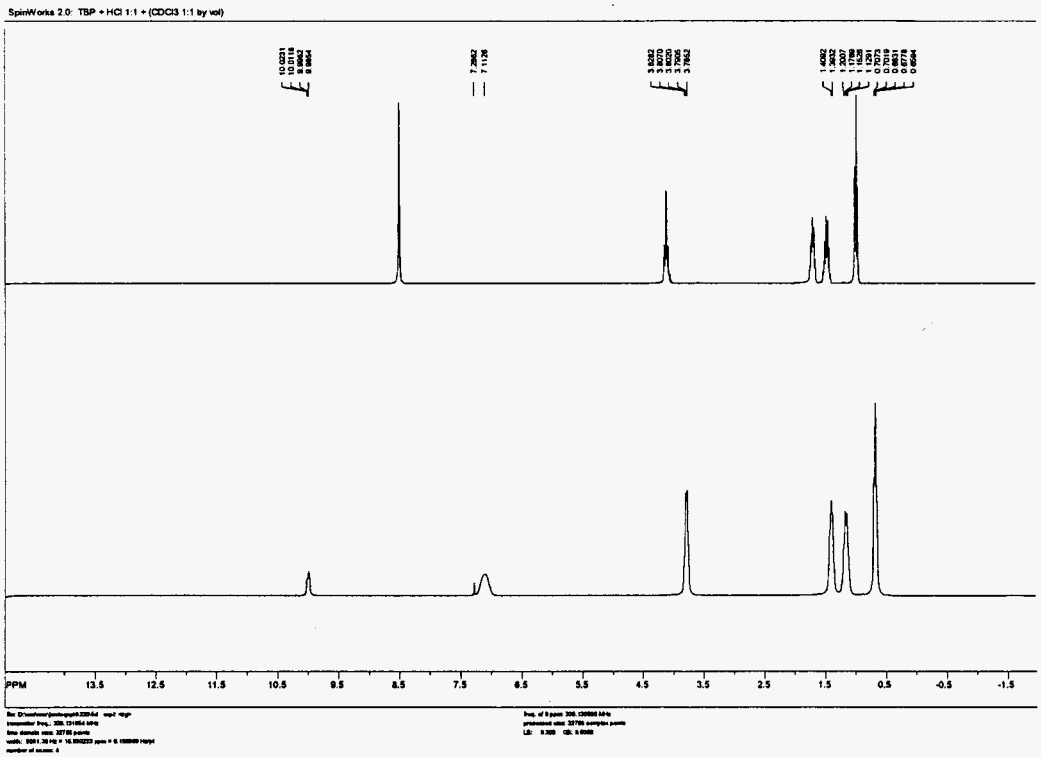

Figure 7. Proton NMR spectra of $TBP(HCl)_{0.8}(H2O)_{2.8}$ with D_2O insert (top) and in $CDCl_3$ (bottom)

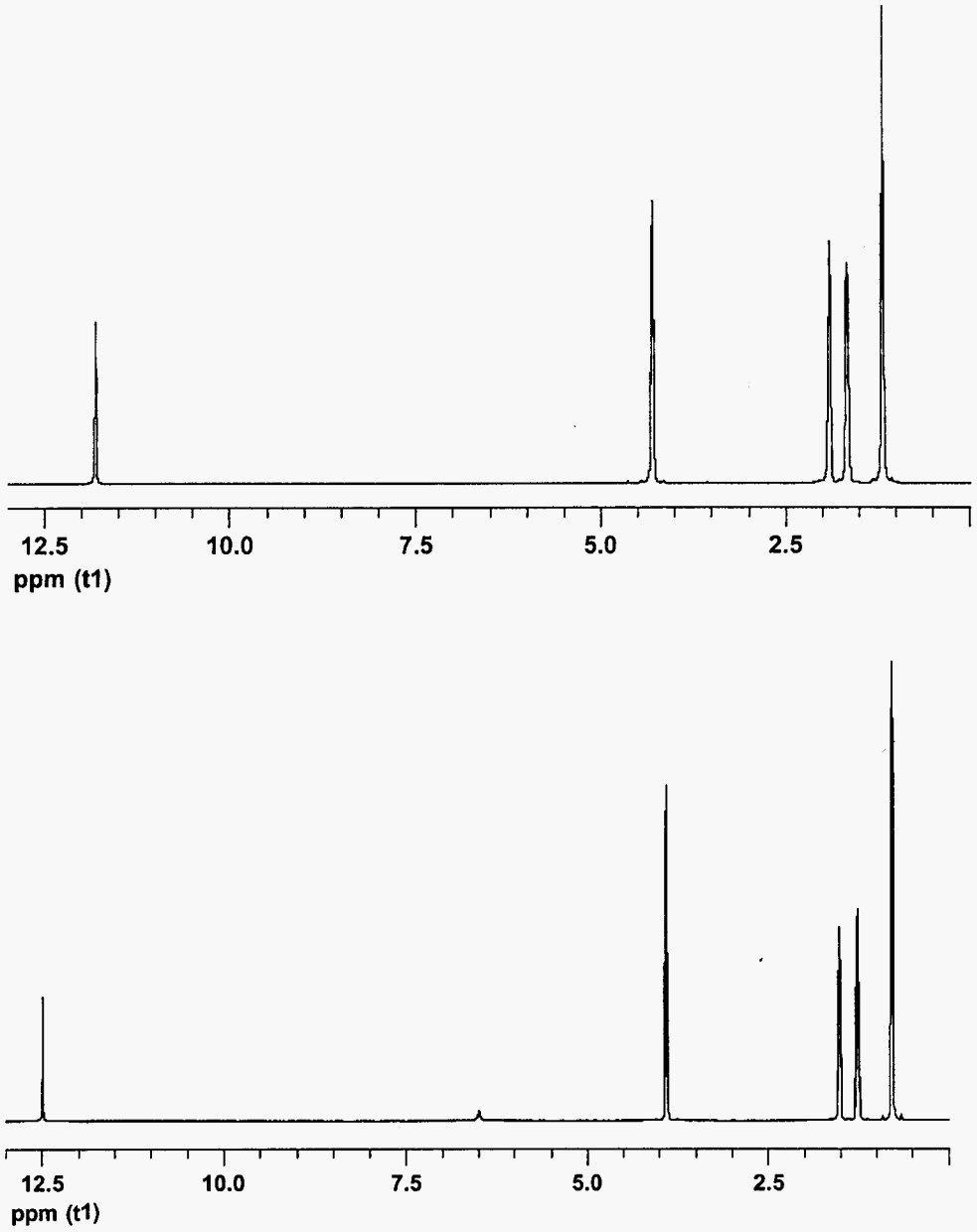

Figure 8. Proton NMR spectra of $TBP(HNO_3)_{0.7}(H_2O)_{0.7}$ with D_2O insert (top) and in $CDCl_3$ (bottom)

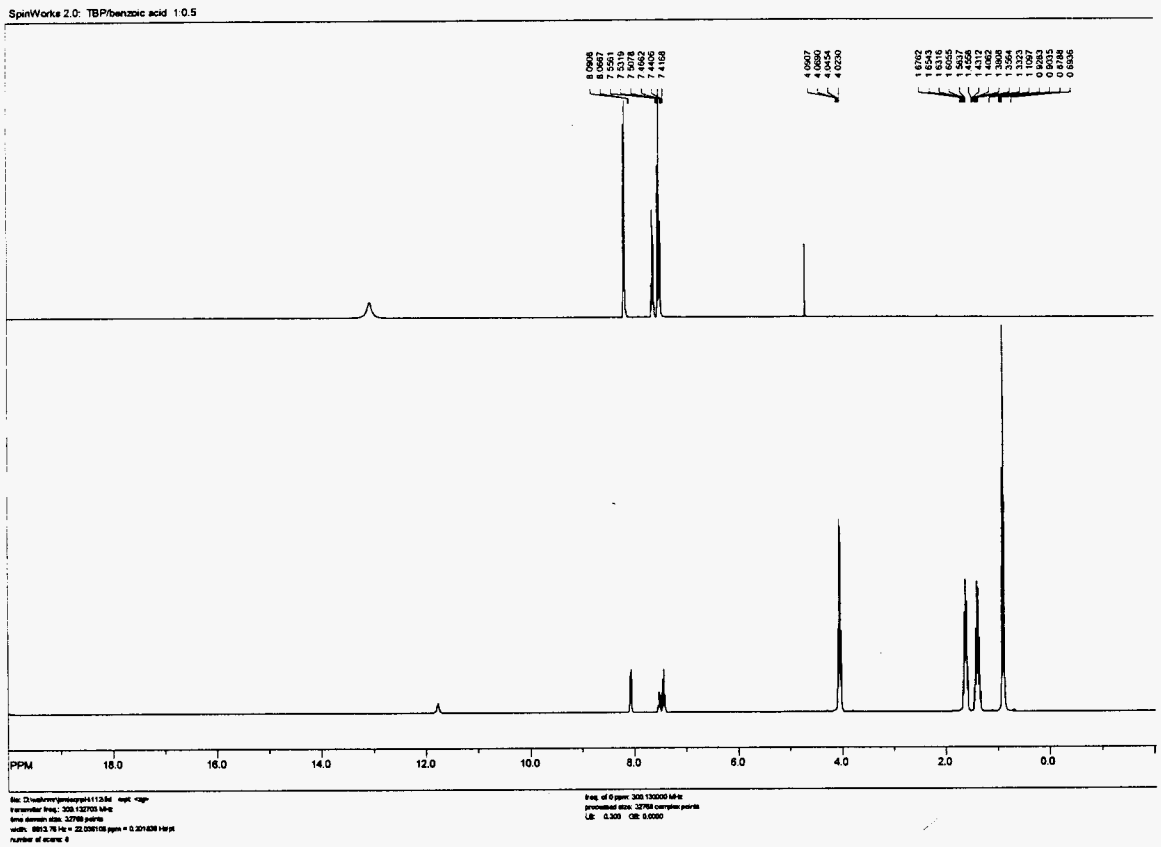

Figure 9. Proton NMR spectra of benzoic acid alone (top) and TBP(benzoic acid)$_{0.5}$ complex (bottom)

The solubilities of some TBP-acid complexes in supercritical CO_2 were measured at 40 °C by visual observation of phase behavior under different pressures using a view cell with quartz windows. Solubility data of TBP and benzoic acid are known in the literature. TBP is highly soluble in supercritical CO_2. According to Joung et al., TBP becomes miscible with supercritical CO_2 above certain pressure at a given temperature. For example, at 50 °C (323.15 K) TBP and CO_2 form one phase at pressures above 110 atm. Nitric acid and hydrochloric acid alone are not soluble in supercritical CO_2 and benzoic acid has a limited solubility in CO_2 (Table 2). When benzoic acid is bonded to TBP, the solubility of the complex is significantly enhanced. For example, the TBP(benzoic acid)$_{0.5}$ complex has a solubility of 1.3 mole% at 40 °C and 114 atm which is about an order of magnitude higher than the free acid alone in supercritical CO_2 under similar conditions. The solubilities of TBP and TBP(HCl)$_{0.8}$(H_2O)$_{2..8}$ and TBP(HNO_3)$_{0.7}$(H2O)$_{0.7}$ are in the range of 1.0-1.7 mole% in supercritical CO_2 at 40 °C and around 110 atm.

Table 3. Solubilities of some TBP-acid complexes in supercritical CO_2

Solute	Temp (°C)	P (atm)	Solubility (mole %)	Ref.
Benzoic acid	45	100	0.026	13
Benzoic acid	35	118	0.13	1
$TBP(benzoic\ acid)_{0.5}$	40	114	1.3	this study
$TBP(HNO_3)_{0.7}(H_2O)_{0.7}$	40	110	1.7	this study
$TBP(HCl)_{0.8}(H_2O)_{2..8}$	40	116	1.0	this study

* Standard deviations of solubility measurements for this study ~10%

The Lewis acid-base complex formation method described in this paper allows normally insoluble or slightly soluble acids to be dissolved in supercritical CO_2. This method is simple and can introduce a variety of acids in supercritical CO_2 for chemical reactions or separations. The method is not limited to TBP, other commercially available Lewis bases that are CO_2 soluble may also be used as carriers for introducing acids in supercritical CO_2. In principle, this method could also be used to introduce bases in supercritical CO_2 using a CO_2-philic Lewis acid. The Lewis acid-base complex formation concept can also be applied to supercritical CO_2 extraction of acids from aqueous solutions using TBP or other CO_2 soluble Lewis base as a carrier. This simple complex formation concept may have a wide range of applications and research to explore potential applications of this method in supercritical fluid processes is currently in progress.

V. Characterization of a TBP-Nitric Acid Complex for Dissolution of Uranium Dioxide in Supercritical CO_2

The Lewis acis-base complex formation method of dissolving acids particularly nitric acid in supercritical CO_2 is significant because it suggests a possibility of using this CO_2-soluble complex for dissolution of uranium dioxide directly in CO_2. In the conventional Purex (Plutonium Uranium Extraction) process, aqueous nitric acid (3-6 M) is used to dissolve and oxidize UO_2 in the spent fuel to uranyl ions $(UO_2)^{2+}$. The acid solution is then extracted with TBP in an organic solvent such as dodecane, to remove uranium as $UO_2(NO_3)_2{\cdot}2TBP$ into the organic phase. Direct dissolution of solid UO_2 in SF-CO_2 with a TBP-nitric acid complex obviously has an advantage over the conventional Purex process because it would combine dissolution and extraction steps into one with a minimum waste generation. The chemical nature of the TBP-nitric acid complex and the mechanisms of UO_2 dissolution in SF-CO_2 with the TBP-nitric acid solution are not well known. The TBP-nitric acid complex is prepared by shaking TBP with a concentrated nitric acid solution. Because water is present in the nitric acid solution, the complex is expected to have a general formula of $TBP(HNO_3)_x(H_2O)_y$, where x and y can vary depending on the relative amounts of TBP and nitric acid used in the preparation.

The solubility of water in pure TBP at room temperature is about 64 grams per liter of the solution that is close to a 1:1 mole ratio of TBP/H_2O. In the TBP/H_2O binary system, water is most likely bound to TBP through hydrogen bonding with phosphoryl oxygen forming a 1:1 complex. The bonding between TBP and H_2O in the presence of HNO_3 is unknown. Recent

molecular dynamics investigations suggest that hydronium ions or hydrogen from HNO_3 or H_2O are bonded to the oxygen of the P=O bond in TBP. Knowledge on the equilibrium compositions of the $TBP(HNO_3)_x(H_2O)_y$ complex prepared by different proportions of the initial TBP and nitric acid is essential for understanding the nature and mechanisms of UO_2 dissolution in SF CO_2. In this section, our initial results of characterizing the $TBP(HNO_3)_x(H_2O)_y$ complex using several different methods including Karl-Fischer method for water determination, conventional acid-base titration for measurement of HNO_3, nuclear magnetic resonance (NMR) spectroscopy to evaluate chemical environments of protons, and visual observation of phase behavior of the complex in SF-CO_2.

TBP was purchased from Avocado (ordered through Alfa Aesar, Ward Hill, MA). Nitric acid (69.5 % w/w) was obtained from Fisher Chemical(Fair Lawn, NJ), and was diluted to 15.5 M by deionized water. The $TBP(HNO_3)_x(H_2O)_y$ complex was prepared by mixing 98% TBP with 15.5 M nitric acid at a chosen ratio in a glass tube with a stopper. The mixture of TBP and nitric acid was manually shaken vigorously for 4 minutes, followed by centrifuging for one hour. After phase separation, portions of the TBP phase and the aqueous phase were removed with pipettes for characterization experiments. The concentration of H_2O in the TBP phase was measured by Karl-Fischer titration using an Aquacounter AQ-7 instrument (Hiranuma, Japan). The concentration of HNO_3 in the TBP phase was measured with an automatic titrator (COM-450, Hiranuma, Japan) with 0.1 M NaOH solution after adding an excess amount of deionized water to the organic phase. A typical procedure is by shaking 1 mL of the TBP phase with 50 mL of water. After phase separation, the amount of nitric acid in the aqueous phase was determined by NaOH titration. A 500 MHz NMR spectrometer (BRUKER Advance 500) was used for proton NMR measurements. Phase behavior was studied using a high-pressure view-cell system and a video camera.

The amount of HNO_3 in the complex was evaluated by the acid-base titration method described in the previous paragraph. When the molar ratio of HNO_3/TBP in the organic phase is plotted against the molar ratio of HNO_3/H_2O in the equilibrated aqueous phase, the experimental data appear to show two regions with a breaking point around unity for the HNO_3/TBP ratio (Figure 10). The data seem to suggest that there are two types of the $TBP(HNO_3)_x(H_2O)_y$ complex. The type I complex would incorporate HNO_3 rapidly into the TBP phase until a 1:1 ratio of HNO_3/TBP is reached. Beyond that point there is another region where incorporation of HNO_3 into TBP becomes slow. According to Figure 10, more than 2 molecules of HNO_3 can be associated with each TBP molecule in the complex if the organic phase is equilibriated with a concentrated nitric acid. TBP is a highly CO_2-soluble Lewis base. Inorganic acids such as nitric acid which are usually insoluble in CO_2 can be made soluble by complexation with a CO_2-soluble Lewis base such as TBP. This Lewis acid-base complex approach may provide a method of dispersing various CO_2 insoluble acids in supercritical CO_2 phase for chemical reactions.

The amount of water in the $TBP(HNO_3)_x(H_2O)_y$ complex determined by Karl-Fischer method also shows two distinct regions. When the molar ratio of HNO_3/H_2O in the TBP phase is plotted against the molar ratio of HNO_3/H_2O in the equilibrated aqueous phase, it clearly shows two different types of the $TBP(HNO_3)_x(H_2O)_y$ complex (Figure 11). In region I, the ratio of HNO_3/H_2O in the TBP phase tends to increase with increasing HNO_3/H_2O ratio in the aqueous phase. In region II, the ratio of HNO_3/H_2O in the TBP phase maintains a constant value of about 3 with increasing HNO_3/H_2O ratio in the equilibrated aqueous phase. The ratio of HNO_3/TBP in the organic phase continues to increase with increasing HNO_3/H_2O ratio in the aqueous phase as

shown in Figure 10, but the ratio of HNO_3/H_2O in the organic phase remains a constant. It appears that for the type II complex, the nitric acid incorporated into the TBP phase is in a form with a general formula of $3HNO_3 \cdot H_2O$.

The proton NMR spectra of the $TBP(HNO_3)_x(H_2O)_y$ system in supercritical CO_2 were discussed in the previous section. Formation of small nitric acid droplets due to an anti-solvent effect of supercritical CO_2 was observed when the $TBP(HNO_3)_{0.7}(H_2O)_{0.7}$ complex was dissolved in the fluid phase. The acid droplets probably started with very small particles and aggregated to certain sizes that would make the solution cloudy. This acid droplets dispersed in the supercritical CO_2 phase may be effective for oxidation of solid UO_2 to the uranyl ions $(UO_2)^{2+}$ that is followed by the formation of the CO_2-soluble $UO_2(NO_3)_2(TBP)_2$ complex. The solubility of in supercritical CO_2 is very high, reaching about 0.45 mol L^{-1} at 40 °C and 150 atm.

The phase behavior of a $TBP(HNO_3)_x(H_2O)_y$ complex in supercritical CO_2 was also evaluated by visual observation of the solution using a high-pressure view-cell. Figure 12 shows the phase boundaries of the $TBP(HNO_3)_{1.8}(H_2O)_{0.6}$ complex in supercritical CO_2 at three different temperatures with respect to pressure and mole fraction of the solute. The isothermal phase boundaries given in Figure 8 represent the transition pressures from a two-phase region into a single phase solution for the complex with mole fractions greater than 10^{-4}. At each temperature investigated there exists a maximum transition temperature above which the complex and CO_2 are miscible. For example, at 323.15 K the complex becomes miscible with SF-CO_2 at 14 MPa with any mole fractions. This implies that a large amount of the complex can be dissolved in SF-CO_2 above this specific pressure for the given temperature. The maximum phase transition temperature for the complex increases with temperature of the system varying from 11 MPa at 313.15 K to 17 MPa at 333.15 K.

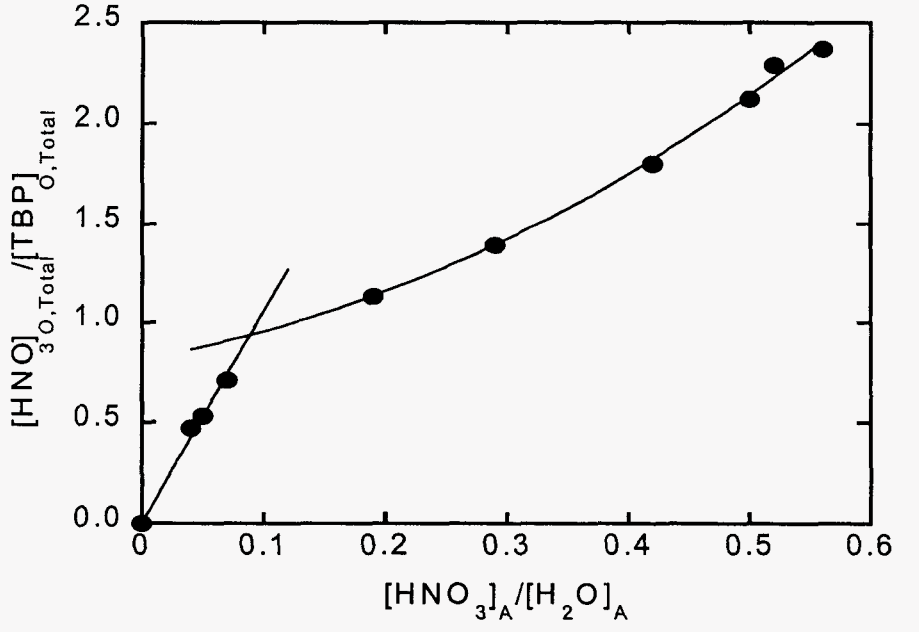

Figure 10. A plot of $[HNO_3]/[TBP]$ ratio in the TBP phase against $[HNO_3]/[H_2O]$ ratio in the equilibrated aqueous phase.

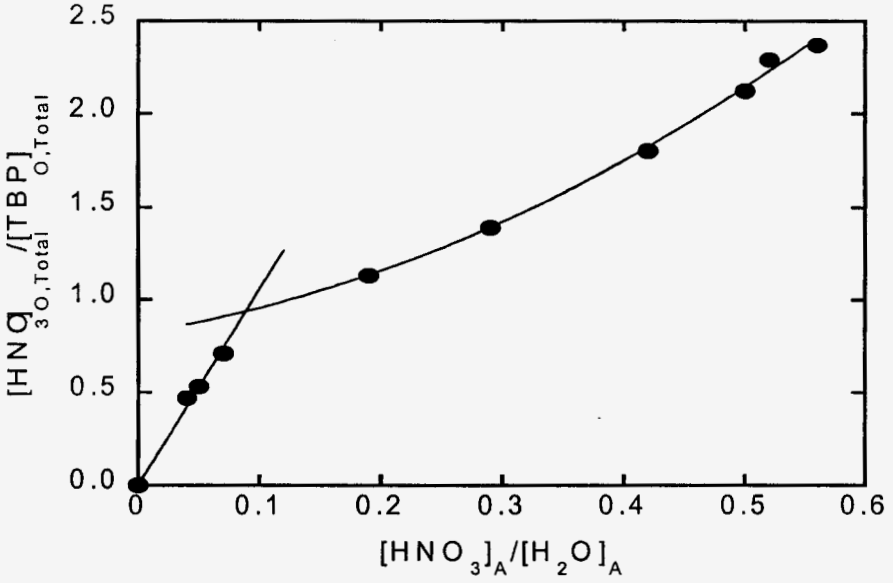

Figure 11. Molecular ratio of $[HNO_3]/[H_2O]$ in the TBP phase versus that in the equilibrated aqueous phase

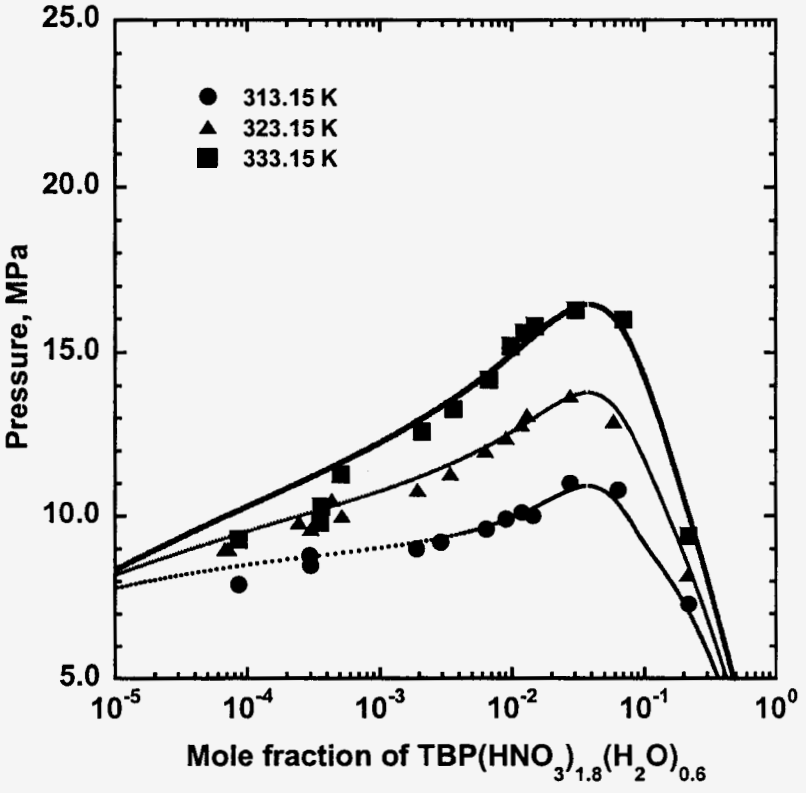

Figure 12. Phase diagram of $TBP(HNO_3)_{1.8}(H_2O)_{0.6}$ in supercritical CO_2

VI. Dissolution of Uranium Dioxide in Supercritical CO_2

Direct dissolution of solid UO_2 in supercritical CO_2 is difficult because uranium at +4 oxidation state does not form stable complexes with commonly known ligands. An oxidation step is needed to convert uranium from +4 to +6 oxidation state to make it extractable in supercritical CO_2. Recent reports show that TBP forms a complex with nitric acid which is soluble in supercritical CO_2 and is capable of dissolving lanthanide oxides and uranium oxides directly (8). The complex is prepared by mixing TBP with a concentrated nitric acid solution. Nitric acid dissolves in the TBP phase forming a complex of the general formula $TBP(HNO_3)_x(H_2O)_y$ that is separated from the remaining aqueous phase. The TBP-nitric acid complex is soluble in supercritical CO_2 and it is capable of dissolving solid uranium dioxide directly. The UO_2 dissolution process probably involves oxidation of the tetravalent uranium in UO_2 to the hexavalent uranyl followed by formation of $UO_2(NO_3)_2 \bullet 2TBP$ which is known to have a high solubility in SF-CO_2.

The solubilities of $(UO_2)(NO_3)_2 \cdot 2TBP$ in supercritical CO_2 in the temperature range 40 °C to 60 °C and pressure range 100 to 200 atm were measured using a spectroscopic method. The solubility of this important uranyl complex in supercritical CO_2 is about 0.4 mol/L at 40 °C and 200 atm. This uraniium concentration is similar to that used in the PUREX process. In comparison with $UO_2(NO_3)_2 \cdot 2TBP$, the solubility of $UO_2(TTA)_2 \cdot TBP$ in supercritical CO_2 is about an order of magnitude lower. These information indicates that uranium and transuranics in solid materials can be extracted directly by supercritical CO_2 containing a TBP-nitric acid complex.

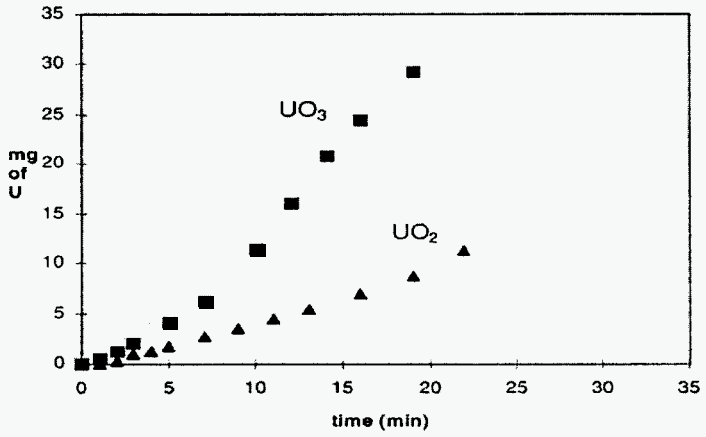

Figure 13. Dissolution of UO_2 and UO_3 in supercritical CO_2 using $TBP(HNO_3)_{0.7}(H_2O)_{0.7}$ as an extractant at 60 oC and 150 atm, flow rate = 0.4 mL/min

Dissolution of UO_2 by a TBP-nitric acid complex depends on the stoichiometry of the complex and the density of the supercritical fluid phase. For example, using a supercritical CO_2 stream containing the $TBP(HNO_3)_{0.7}(H_2O)_{0.7}$ complex that flows through a UO_2 powder with a flow rate of 0.4 mL/min, the amount of UO_2 dissolves in the supercritical CO_2 stream is shown in Figure 1. The supercritical CO_2 solution was produced by bubbling liquid CO_2 through a cell containing the $TBP(HNO_3)_{0.7}(H_2O)_{0.7}$ complex at room temperature (around 23 °C). The dissolution of UO_2 using the $TBP(HNO_3)_{1.8}(H_2O)_{0.6}$ complex in supercritical CO_2 is more rapid because of a higher nitric acid concentration provided by the complex. The alkali metals, the alkaline earth metals, and a number of transition metals can not be extracted by the TBP-nitric acid complex in supercritical CO_2. Sonification can enhance the dissolution rate of tightly packed UO_2 powders significantly probably by increasing the transport of $UO_2(NO_3)_2(TBP)_2$ from the solid surface to the supercritical fluid phase. Dissolution of UO_3 by a TBP-nitric acid complex (e.g. $TBP(HNO_3)_{0.7}(H_2O)_{0.7}$ or $TBP(HNO_3)_{1.8}(H_2O)_{0.6}$) in supercritical CO_2 is more efficiency than the dissolution of UO_2. This can be attributed to the fact that the uranium in UO_3 is already in the +6 oxidation state, thus no oxidation is required in the formation of the uranyl complex $UO_2(NO_3)_2(TBP)_2$.

In the conventional Purex (Plutonium Uranium Extraction) process, aqueous nitric acid (3-6 M) is first used to dissolve and oxidize UO_2 in the spent fuel to uranyl ions $(UO_2)^{2+}$. The acid solution is then extracted with TBP in dodecane to remove the uranium as $UO_2(NO_3)_2 \bullet 2TBP$ into the organic phase. The SF-CO_2 dissolution of UO_2 with a TBP-nitric acid complex has advantages over the conventional Purex process since it combines dissolution and extraction into one step with minimum waste generation. This green SF process that requires no aqueous solution and organic solvent may have potential applications for processing spent nuclear fuel, decontamination of UO_2 contaminated wastes, and even for processing of rare earth ores. TBP-nitric acid complex obviously has an advantage over the conventional Purex process because it would combine dissolution and extraction steps into one with a minimum waste generation. Demonstration of this Super-DIREX process (supercritical fluid direct extraction process) is currently underway in Japan involving Mitsubichi Heavy Industries, Japan Nuclear Cycle Corporation, and Nagoya University. The project is aimed at extracting uranium and plutonium from the mixed oxide fuel as well as the irradiated nuclear fuel using a TBP-nitric acid complex in supercritical CO_2.

VII. Appendix – Reprints of the Publications Derived from the Project

See Attached file

An FT-IR Study of Crown Ether−Water Complexation in Supercritical CO_2

Anne Rustenholtz,† John L. Fulton,‡ and Chien M. Wai*,†

Department of Chemistry, University of Idaho, Moscow, Idaho 83844-2343, and Fundamental Science Division, Pacific Northwest National Laboratory, P.O. Box 999, MS P8-19, Richland, Washington 99352

Received: June 24, 2003; In Final Form: September 25, 2003

In the presence of 18-crown-6, D_2O forms a 1:1 complex with the macrocyclic molecule in supercritical fluid CO_2 with two different configurations. The D_2O molecule can be bonded to two oxygen atoms of the crown cavity in a bridged configuration that is characterized by a broad peak at 2590 cm^{-1}. The D_2O molecule can also form one hydrogen bond with an oxygen atom of the crown cavity that can be characterized by two peaks at 2679 and 2733 cm^{-1}, with the former assigned to the hydrogen-bonded O−D stretching and the latter the unbonded O−D stretching. The equilibrium constants of the two configurations in supercritical CO_2 have been calculated. The enthalpy of formation is -12 ± 2 kJ mol^{-1} for the single-hydrogen-bond complex and -38 ± 3 kJ mol^{-1} for the bridged configuration complex. At high 18-crown-6 to D_2O ratios, the formation of another complex in supercritical CO_2 that involves one D_2O molecule hydrogen bonded to two 18-crown-6 molecules becomes possible.

Introduction

Supercritical fluids have unique properties that make them highly attractive for extraction of metal ions from liquid and solid materials.[1−3] Carbon dioxide is most widely used for supercritical fluid applications because of a number of advantages including (i) low toxicity, (ii) environmentally benignity, (iii) low cost, (iv) moderate critical constants (T_c = 31 °C and P_c = 73.7 bar), and (v) tunable solvation strength that varies with density. Selective extraction of metal species using a nonpolar solvent such as CO_2 requires special chelating agents that should possess ion recognition ability and be soluble in supercritical fluid carbon dioxide (SF-CO_2).[1−3] Crown ethers have been extensively used for extraction of alkali-metal and alkaline-earth-metal cations from aqueous solutions into organic solvents.[4−9] The relatively high solubility of crown ethers in liquid and supercritical CO_2 and their selectivity for the alkali-metal and the alkaline-earth-metal ions make them attractive for environmental applications such as CO_2-based nuclear waste management technology that would result in minimum liquid waste generation.

For the extraction of metal ions from aqueous solutions using ligands dissolved in SF-CO_2, the fluid phase will be saturated with water. Thus, water interaction with the ligand in the fluid phase plays an integral role in the extraction process.[2,9] It has been reported that the extraction efficiency of alkali-metal ions in conventional solvent processes depends on the solubility of water in the organic phase using macrocyclic polyethers as a complexing agent.[9] With crown ethers, both computational simulation[10] and spectroscopic studies[11,12] show that, in organic solvents, the water can bond to a macrocyclic host molecule by two different types of hydrogen bonding. The first type is composed of a single hydrogen bond between one hydrogen atom of a water molecule and one oxygen atom of the crown ether cavity. In this case, the water molecule is mostly located outside the cavity. The second type occurs inside the cavity and is composed of a water molecule bridging between two different oxygen atoms of the crown cavity.

FT-IR is a sensitive and qualitative technique that has been used during the past few years to study hydrogen bonding in different solvents.[12−16] For example, Fulton et al.[13] used this technique to explore hydrogen bonding of methanol dissolved in supercritical carbon dioxide and found that a weak interaction between carbon dioxide and methanol significantly reduced the amount of methanol−methanol hydrogen bonding. Johnston et al. used it to understand the solvent effect on hydrogen bonding in supercritical fluids.[14] They were able to determine, with a good accuracy, the equilibrium constants and other thermodynamics data for the hydrogen bond between methanol and triethylamine. The FT-IR technique has also been used by Moyer et al.[12] to determine how water is bonded to crown ethers in carbon tetrachloride. These authors assigned vibrational bands to free water and to two different kinds of hydrogen bonds mentioned above. In this paper we examine the interactions of water and 18-crown-6 in liquid and supercritical CO_2 for the purpose of establishing a basis for using this green solvent in extraction processes utilizing crown ethers as extractants.

Experimental Section

A specially designed high-pressure IR cell capable of operation to 500 bar was used for this study. The 9.2 mL internal volume cell is built in stainless steel block. The infrared beam is focused along two conical holes and passes through two small diamond windows providing a path length of 100 μm. The cell has one observation window (sapphire) sealed with a gold-plated metal V-ring seal, which allows visual determination of the number of phases present inside the cell. For quantitative analysis it is essential to avoid formation of a second aqueous phase on the beam path windows, which would interfere with data collection. A Teflon-coated magnetic stirring bar was introduced into the cell, allowing stirring of the solution while the cell was placed inside an FT-IR spectrometer.

* To whom correspondence should be addressed. E-mail: cwai@uidaho.edu.
† University of Idaho.
‡ Pacific Northwest Laboratory.

10.1021/jp035798y CCC: $25.00
Published on Web 11/15/2003

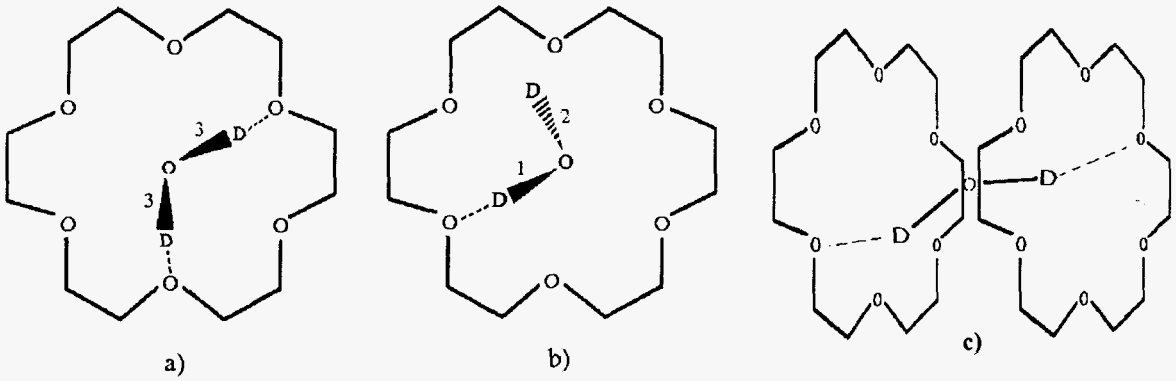

Figure 1. Scheme of the three possible bondings between D_2O and 18-crown-6: (a) bridge bonding; (b) single bonding; (c) 1:2 complex in a sandwich configuration.

A syringe pump (ISCO, model 100DX) was used to supply liquid CO_2 to the cell that was preloaded with the starting chemicals. The pressure was measured using an electronic transducer (Precise Sensor Inc., model D451-10) with a ±1 bar accuracy. The cell was placed on a lightweight ceramic stand, thermally isolated with an insulation coat, and heated using four electric cartridge heaters. The temperature was controlled with a controller (Watlow) having a ±1 °C accuracy. A Bruker IFS 66v FT-IR spectrometer with a mercury−cadmium−telluride (MCT) detector (Kolmar Technologies) was used to acquire all IR spectra. To obtain a good signal-to-noise ratio, the acquisition time was set at 5 min (corresponding to approximately 2350 scans), the scanner velocity was 80 kHz set for 4 cm^{-1} resolution. A background spectrum of the empty cell (with diamond windows) was subtracted from each sample spectrum. Deuterated water (D_2O) was used rather than H_2O to avoid overlapping of water and intense CO_2 absorption bands between 3500 and 3800 cm^{-1}. The existence of weak 18-crown-6 bands between 2760 and 2680 cm^{-1} (C−H stretch) which overlap with the D_2O signal required a spectrum of the pure crown ether in CO_2, at the same temperature and pressure, to be subtracted from the sample spectrum for background correction.

D_2O (100% D, 99.96% pure), 18-crown-6 (99.5% pure), dicyclohexano-18-crown-6 (98% pure), methanol-*d* (99.5+ atom % D), and carbon tetrachloride (99.9% pure) were purchased from Aldrich Chemical Co. and used without further purification. Carbon dioxide was obtained as supercritical fluid chromatography (SFC) grade (purity >99.99%) from Scott Specialty Gases Inc. The pure CO_2 density varies in this study between 0.66 and 1.04 g mL^{-1} by tuning the temperature between 25 and 70 °C and the pressure between 200 and 400 bar. The pure CO_2 density was determined using a reported table from the NIST (National Institute of Standards and Technology) Chemistry WebBook.

To avoid water contamination from the atmosphere, the cell was purged with nitrogen and the chemicals were handled and introduced using a glovebox purged with nitrogen. The solutions were stirred for 20−30 min to reach equilibrium after each density or concentration change. Longer equilibrium times were briefly explored, but no significant change in the IR spectra was observed. Curve fitting and other spectrum analysis and corrections have been performed with standard spectral software (OPUS, Bruker Optiks).

Results and Discussion

To study the nature of crown−water hydrogen bonding in liquid and SF-CO_2, we examined FTIR spectra of a series of mixtures with 18-crown-6 concentrations varied from 0 to 0.25 mol L^{-1} and the total D_2O concentration fixed at 49 mmol L^{-1}. The D_2O concentration was below the known solubility of water in pure CO_2[18] under our experimental conditions. This fact was supported by the observation of a single phase for all the CO_2 experiments conducted in this study.

Peak Assignment. FT-IR spectra for different crown ether concentrations (0−0.25 mol L^{-1}) and a fixed D_2O concentration (0.049 mol L^{-1}) are shown in parts a and b of Figure 2 for liquid and SF-CO_2, respectively. Peaks for the free D_2O, i.e., D_2O dissolved in SF-CO_2 without the crown ether (O−D stretching, asymmetric at 2761 cm^{-1} and symmetric at 2654 cm^{-1}), can be easily discerned, and their positions are in agreement with those reported for D_2O molecules in the vapor (i.e., 2789 and 2666 cm^{-1} for the D_2O vapor).[19] The shifts of the D_2O vibrational stretchings to lower wavenumbers in SF-CO_2 relative to those of single molecules in the vapor phase reflect the interactions of D_2O molecules with CO_2 in the fluid phase. When 18-crown-6 was added to the CO_2 solution, three other peaks at 2733, 2679, and 2590 cm^{-1} appeared. According to the order of peak assignment of H_2O−18-crown-6 complex in carbon tetrachloride,[12] the broad peak at 2590 cm^{-1} should correspond to the symmetrical stretch of the O−D bond involved in the two-hydrogen-bond bridge as illustrated in Figure 1a. The D_2O molecule with one hydrogen bond to the cavity oxygen is expected to have two stretching bands. The sharp O−D band at 2733 cm^{-1} should be the unbonded O−D stretching marked as 2 in Figure 1b. The bonded O−D stretching band (marked as 1 in Figure 1b) was assigned to the 2679 cm^{-1} peak, located between the symmetrical and the asymmetrical stretching bands of free water. In the FT-IR spectra of the H_2O−18-crown-6 complex in CCl_4, the bonded O−H stretching band was found at a lower energy than the symmetrical stretch band of free water. We confirmed our assignment of this bonded O−D band by completing two secondary experiments. One experiment was a comparison of the FTIR spectra of 18-crown-6−H_2O and 18-crown-6−D_2O complexes in CCl_4. We confirmed the peak assignment of the former as reported in the literature, and the D_2O isotopic effect altered the peak order of the latter as shown in Figure 2. In another experiment, we confirmed that the order and assignment of the various O−D bands in the 18-crown-6−D_2O complex in SF-CO_2 were the same in both CCl_4 and liquid CO_2.

We also obtained the FT-IR spectra of methanol-*d* mixed with the crown ether in supercritical CO_2 (Figure 3a). The peaks between 2860 and 3100 cm^{-1} correspond to the stretching of the C−H bonds belonging to the methanol-*d* molecule. Due to a different O−D bond energy for methanol-*d* vs D_2O, the peak maximum of the O−D stretching mode for methanol-*d* is shifted

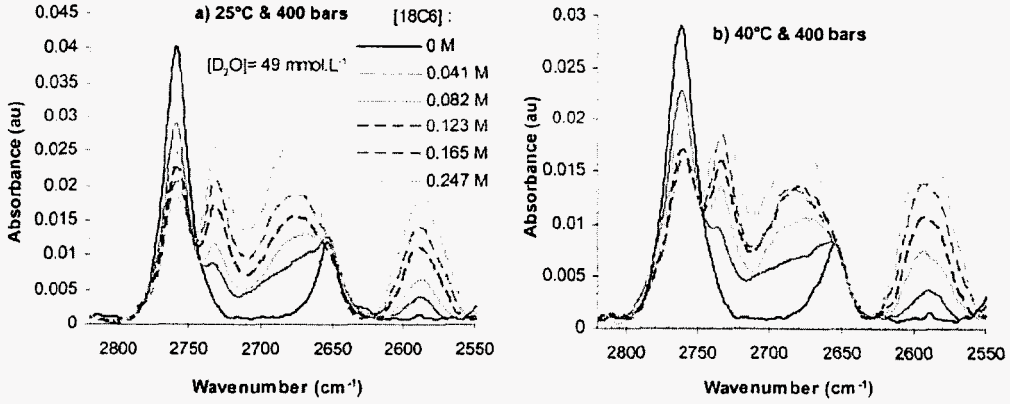

Figure 2. FT-IR spectra of free and bonded D_2O at different 18-crown-6 concentrations (0−0.25 mol L^{-1}) and at one fixed D_2O concentration (0.049 mol L^{-1}) in liquid (a, 25 °C and 400 bar) and supercritical (b, 40 °C and 400 bar) CO_2.

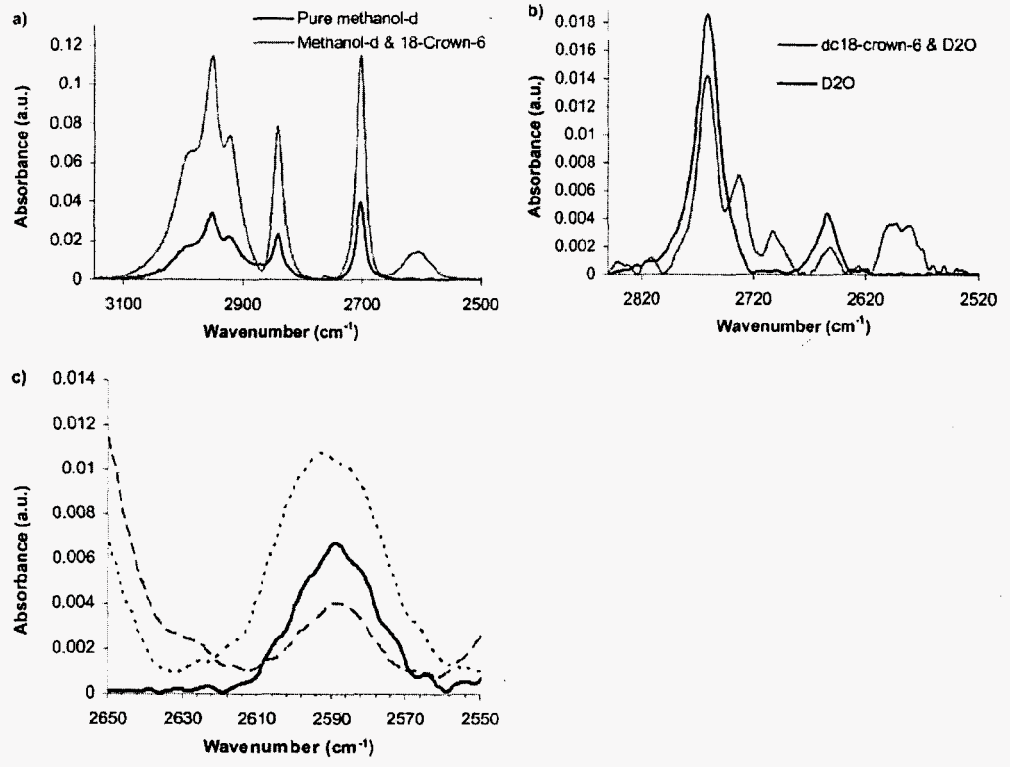

Figure 3. (a) Free methanol-*d* (0.17 mol L^{-1}) and methanol-*d* (0.17 mol L^{-1}) complexed to 18-crown-6 (0.02 mol L^{-1}) in CO_2 (40 °C and 200 bar). (b) Free D_2O (49 mmol L^{-1}) and D_2O (49 mmol L^{-1}) complexed to dicyclo-18-crown-6 (0.06 mol L^{-1}) in CO_2 (40 °C and 300 bar). (c) D_2O (respectively 17 and 49 mmol L^{-1}) complexed to 18-crown-6 (respectively at 0.40 mol L^{-1} (—), 0.041 (– – –), and 0.123 (---) mol L^{-1}) in CO_2 at, respectively, 40 °C and 200 bar and 40 °C and 400 bar.

to a higher energy. Nevertheless, both asymmetric and symmetric free O−D stretching peaks (respectively at 2841 and 2701 cm^{-1}) were observed in the spectra shown in Figure 3a. Moreover, only the bonded O−D stretching band (similar to 1 in Figure 1b) appeared at the expected position (i.e., 2609 cm^{-1}). These observations provided further support for our peak assignment.

Recent molecular dynamic simulation studies performed by Wipff et al.[20] for 18-crown-6 and water in SF-CO_2 suggest that most of the water molecules were bridge bonded to crown ether in the D_{3d} conformation. The observation of a singly bonded water to a crown complex in our experiments could be due to the flexibility of the macrocyclic molecule; 18-crown-6 can be in various conformations that may favor a singly or a doubly bonded water molecule. The 18-crown-6 cavity in dicyclohexano-18-crown-6 is forced by its geometry into the D_{3d} conformation and is supposed to be rigid. The FT-IR spectra of D_2O with and without dicyclohexano-18-crown-6 in SF-CO_2 are shown in Figure 3b. The spectrum shows that the free D_2O stretching bands are observed at 2761 (asymmetric) and 2653 (symmetric) cm^{-1}. For the D_2O with crown solution both single hydrogen bonding (at 2701 (bonded) and 2732 (unbonded) cm^{-1}) and double hydrogen bonding (at 2591 cm^{-1}) with the oxygen atoms of the macrocyclic cavity, similar to that found in 18-crown-6, are observed. The difference between our spectroscopic study and Wipff's molecular dynamic simulation may be due to differences in species concentrations and CO_2 densities used in the simulation study.

TABLE 1: Apparent Molar Absorptivity at Different CO_2 Densities[a]

pressure (bar)	199	199	200	199	200	200	199	199	301	352	403	403
temperature (°C)	70	60	50	40	35	33	31	25	40	40	40	25
density (g mL^{-1})	0.659	0.723	0.784	0.840	0.860	0.870	0.888	0.914	0.911	0.930	0.957	1.035
ϵ_1 (L mol^{-1} cm^{-1})	10	11	13	16	17	18	20	20	18	19	20	24
ϵ_2 (L mol^{-1} cm^{-1})	45	52	60	68	73	74	80	79	74	78	81	93
ϵ_3 (L mol^{-1} cm^{-1})			42	41	41	42	44	44	39	37	35	39
ϵ_4 (L mol^{-1} cm^{-1})	527	517	504	489	484	480	477	469	481	482	481	463
ϵ_5 (L mol^{-1} cm^{-1})	296	288	278	269	264	262	260	254	266	268	268	255

[a] ϵ_1, free D_2O asymmetric (2761 cm^{-1}) stretching band; ϵ_2, free D_2O symmetric (2654 cm^{-1}) stretching band; ϵ_3, doubly bonded D_2O to crown band (at 2593 cm^{-1}); ϵ_4 and ϵ_5, C−H stretch band of 18-crown-6 at 2872 and 2947 cm^{-1}, respectely.

1:2 Complex Formation. When the 18-crown-6 concentration exceeds 0.4 mol L^{-1} with a lower water concentration (less than 17 mmol L^{-1}), only one absorption band at 2590 cm^{-1} is observed (Figure 3c). All the D_2O molecules seem to be bridge bonded to the crown ether. This observation may be explained by the formation of a 1:2 complex between D_2O and 18-crown-6 as illustrated in Figure 1c. The O−D stretching band for this kind of complex should appear at the same frequency as that of the bridged form of D_2O (Figure 1a configuration). Our suggestion of 1:2 complex formation is based on the assumption that, by increasing the crown ether to water ratio in SF-CO_2, we do not change the equilibrium between D_2O molecules bonded to one oxygen atom (configuration 1b) or to two oxygen atoms (configuration 1a) of the cavity. As the concentration of 18-crown-6 in the system increases, it is conceivable that the singly bonded D_2O molecule (configuration 1b) would form a hydrogen bond with another crown molecule via the unbonded O−D, thus leading to the formation of a 1:2 complex. The law of mass action should favor the shifting of equilibrium from a 1:1 complex to a 1:2 complex between water and 18-crown-6 in SF-CO_2. Also in Figure 3c, we show, for comparison, spectra of the double bond area of 18-crown-6 (at 0.041 and 0.123 M) and D_2O (0.049 M) at 400 bar and 40 °C. Peaks occur at the same position for both the dimer and the monomer forms.

The sandwich form (configuration 1c) is a probable conformation for the 1:2 complex, but other configurations (e.g., from offset to perpendicular) can be envisaged. Formation of 1:2 complexes has been reported for crown ether extraction of metal ions from aqueous solutions where a metal ion can bind to two crown cavities to form a sandwich complex. We are not aware of any previous report regarding 1:2 complex formation between water and crown molecules. Our experimental data indicate that, with increasing crown to D_2O ratios in the SF-CO_2 system, the intensities of the single-hydrogen-bond D_2O stretching peaks (2733 and 2679 cm^{-1}) decreases and that of the peak at 2590 cm^{-1} increases. Although the 1:2 complex forms at high crown to D_2O ratios, we cannot distinguish the bridging 1:1 complex (configuration 1a) and the 1:2 complex (configuration 1c) from the FT-IR spectra.

Molar Absorptivity Calculation. A number of experimental parameters (e.g., path length change, radiation of the cell, etc.) can influence molar absorptivity values in addition to pressure and temperature effects in SF-CO_2 as reported in the literature.[22] Therefore, for quantitative discussion of FT-IR data, molar absorptivity should be evaluated for each SF-CO_2 condition.[21]

The molar absorptivities for free D_2O dissolved in CO_2 (Table 1 and Figure 4) were determined by the analysis of FT-IR spectra with pure D_2O of known concentrations. The apparent molar absorptivity of D_2O, in liquid and supercritical CO_2, increases with the fluid density. This behavior is similar to that reported for pyrene and anthracene[21] in CO_2 solutions. In our system, the molar absorptivity for the asymmetric stretching band of the free D_2O at 2761 cm^{-1} is more than doubled for an

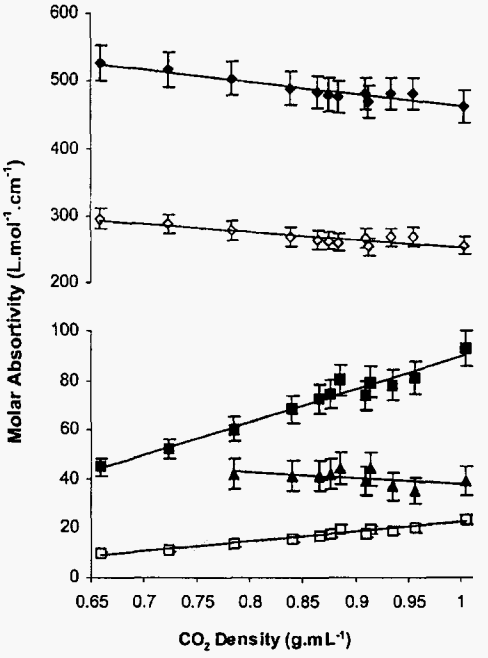

Figure 4. Apparent molar absoptivity at different CO_2 densities: (■) free D_2O asymmetric (ϵ_1 at 2761 cm^{-1}) stretching bands; (□) free D_2O symmetric (ϵ_2 at 2654 cm^{-1}) stretching bands; (▲) doubly bonded D_2O to crown (at 2593 cm^{-1}); (◆, ◇) C−H stretch band of 18-crown-6 at 2872 and 2947 cm^{-1}, respectively.

increase in CO_2 density from 0.66 to 1.04 g mL^{-1}. The molar absorptivities of the C−H stretching vibrations of pure 18-crown-6 dissolved in CO_2 at its maximum intensity (2872 cm^{-1}) and at 2947 cm^{-1} are also given in Figure 4. A 20% decrease in molar absorptivity is observed for both wavenumbers when the CO_2 density varies from 0.65 to 1.0 g mL^{-1}. Because of the stability of those C−H stretches, this decrease might reflect changes in molecular absorptivities due to experimental parameters and needs to be considered to determine true molecular absorptivities. Molar absorptivity changes for free D_2O stretching vibrations might be caused by a change in solute−solvent interaction and in solvent refractive index.

The molar absorptivity of the bridging 1:1 complex was determined in the following way. We assumed that the molar absorptivities of the 1:1 bridge complex and the 1:2 complex were similar. Thus, the molar absorptivity of the bridged 1:1 complex could be obtained from the region with high 18-crown-6 to D_2O ratios in SF-CO_2. Its value (Table 1 and Figure 4) at 2593 cm^{-1} does not seem to be affected by the change in density. However, the weak solubility limit of 18-crown-6 at low CO_2 density did not permit this calculation for a density below 0.8 g mL^{-1}.

Equilibrium Constants and Enthalpy Calculations. The formation of a 1:1 complex between 18-crown-6 and D_2O in

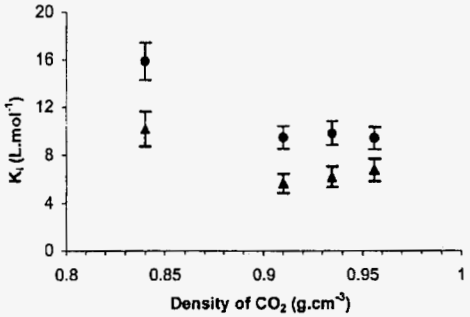

Figure 5. Density effect on equilibrium constants K_s (●) and K_b (▲). The pressure varies from 200 to 400 bar at constant temperature (40 °C). [18C6] = 41 mmol.L^{-1}. [D_2O] = 49 mmol L^{-1}.

the CO_2 phase at a lower crown to D_2O molecular ratio was evaluated by the analysis of the FT-IR data and the equilibrium relations of the following equations:

$$18C6 + D_2O \leftrightarrows 18C6{\cdot}D_2O^{single} \quad (1)$$

$$K_s = ([18C6{\cdot}D_2O^{single}])/([18C6][D_2O])$$

$$18C6 + D_2O \leftrightarrows 18C6{\cdot}D_2O^{bridge} \quad (2)$$

$$K_b = ([18C6{\cdot}D_2O^{bridge}])/([18C6][D_2O])$$

where K_s and K_b represent the equilibrium constants for the 1:1 complex with a single hydrogen bond and double hydrogen bonds, respectively. The total bonded water concentration for equilibrium constant calculations was calculated from the free water concentration (deduct from its molar absortivity) and the total concentration introduced in the cell. The K values vary considerably with CO_2 density. At a constant pressure (200 bar), the K_s value decreases from 21 ± 2 to 13 ± 1 L mol^{-1} with an increase in temperature from 25 to 60 °C. The variation of K_b with temperature is even greater for the same pressure; its value varies from 14 ± 2 to 2 ± 1 L mol^{-1} from 25 to 60 °C. These K values are comparable to the one reported by Moyer et al. (i.e., 15.6(1.2) L mol^{-1}) for the 18-crown-6−H_2O complex in carbon tetrachloride. This implies that, in terms of hydrogen bonding between water and 18-crown-6, liquid CO_2 and supercritical CO_2 behave as nonpolar solvents such as CCl_4 and not chloroform. The K value of the 18-crown-6−H_2O complex in chloroform was reported to be 20 times larger than that in CCl_4.

The influence of density (increase in pressure from 200 to 400 bar) at a constant temperature (i.e., 40 °C) on the two equilibrium constants K_s and K_b is shown in Figure 5. An increase in density causes a decrease in the K_s and K_b values.

The molar enthalpy of a hydrogen bond (ΔH_i) can be determined from the equilibrium constant at constant pressure by eq 4 from well-known thermodynamic relations (eq 3),[17] where T is the absolute temperature in (K) and R the ideal gas constant.

$$\left(\frac{\partial(\Delta G_i)}{\partial T}\right)_P = -\Delta S_i = \frac{\Delta G_i - \Delta H_i}{T} \quad \text{and} \quad \Delta G_i^\circ = -RT \ln K_i \quad (3)$$

$$\left(\frac{\partial(\ln K_i)}{\partial(1/T)}\right)_P = -\frac{\Delta H_i}{R} \quad (4)$$

Using a linear regression on the plot of ln K versus $1/T$ (Figure 6), and assuming that ΔH is independent of temperature and

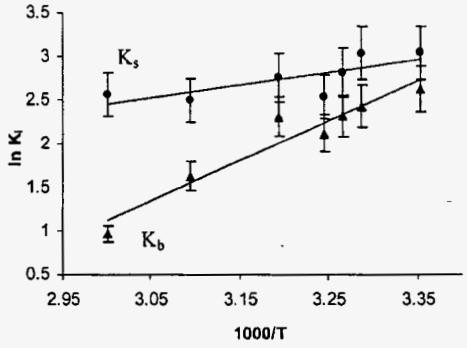

Figure 6. Dependence of ln K_s (●) and ln K_b (▲) on 1000/T at 200 bar for [18C6] = 41 mmol L^{-1} and [D_2O] = 49 mmol L^{-1}.

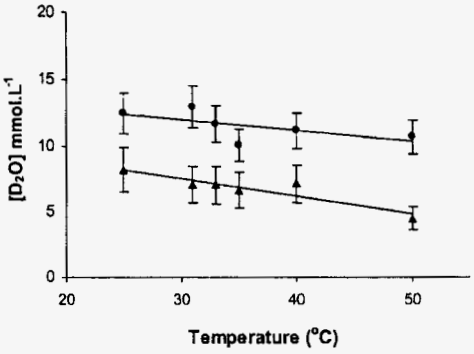

Figure 7. Concentration of the two isomers (i.e., single bond (●) and double bond (▲)) between D_2O (49 mmol L^{-1} total concentration in CO_2) and the 18-crown-6 (83 mmol L^{-1} total concentration in CO_2) versus temperature (°C).

density, the ΔH_s (for a single hydrogen bond, configuration 1b) was found to be −12 ± 2 kJ mol^{-1} and ΔH_b (for bridge bonding, configuration 1a) to be −38 ± 3 kJ mol^{-1}, both at 200 bar. The complexation process is exothermic as expected for hydrogen bonding, and its value is similar to the literature values for hydrogen-bonding processes in both liquid solvents and supercritical fluids. The facts that the hydrogen-bonding process is exothermic and that the bonded species are more entropically ordered explain the decrease of K values with the increase of temperature.

Isomeric Ratio of the Crown−Water Complex. The relative concentrations of the singly bonded and the doubly bonded water−crown complexes change with temperature as shown in Figure 7. At a low crown to water mole ratio (about 0.8), the trend is similar for both isomers. When the temperature is increased from 25 to 50 °C at 200 bar, the concentrations of both the singly bonded and the doubly bonded complexes tend to decrease (Figure 7). The decrease for the doubly bonded complex is perhaps slightly faster than the decrease for the singly bonded complex. This can be explained by an entropy effect; i.e., at higher temperatures the more disordered form should be favored.

At a high crown to water mole ratio (i.e., superior to 1.7), the concentration of the bridged species decreases whereas the concentration of the single-bond species increases when the temperature increases from 25 to 50 °C at a fixed pressure of 200 bar (Figure 8). This observation also appears to support the formation of a 1:2 complex. As expected in terms of entropy, at higher temperatures the 1:2 complex form probably would break down to form a singly bonded 1:1 crown−D_2O complex and unbonded crown ether. Thus, even if the singly bonded species dissociate with rising temperature, the total amount still increases due to the breakdown of the 1:2 complex form.

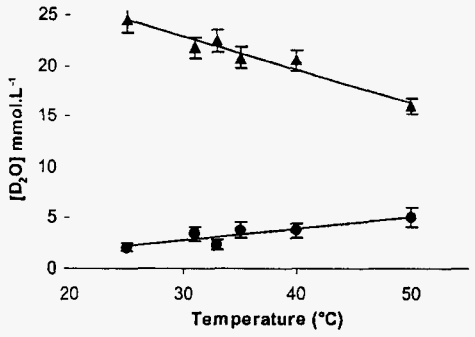

Figure 8. Concentration of the two isomers (i.e., single bond (●) and double bond (▲) between D_2O (49 mmol L^{-1} total concentration in CO_2) and the 18-crown-6 (41 mmol L^{-1} total concentration in CO_2) versus temperature (°C).

Conclusions

FT-IR is a sensitive technique for studying crown ether and water interactions in SF-CO_2. The O−D stretching vibrations for D_2O dissolved in SF-CO_2 show slight shifts to lower wavenumbers relative to those found for D_2O in its vapor phase, indicating interactions (salvation) of CO_2 with D_2O molecules in the supercritical fluid phase. In the presence of 18-crown-6, D_2O forms a 1:1 complex with the macrocyclic molecule with two different configurations. The D_2O molecule can form one hydrogen bond with an oxygen atom of the crown cavity, or it can be bonded to two oxygen atoms of the cavity in a bridged configuration. The equilibrium constant of the single-hydrogen-bond configuration is slightly greater than the two-hydrogen-bond configuration, and both equilibrium constants decrease with increasing temperature. The enthalpy of the complex formation is -12 ± 2 kJ mol^{-1} for the former and -38 ± 3 kJ mol^{-1} for the latter. These values are within the range of hydrogen bonds reported in liquid solvents. At high 18-crown-6 to D_2O ratios, formation of a 1:2 complex in SF-CO_2 that involves one D_2O molecule hydrogen bonded to two crown ether molecules becomes possible.

Acknowledgment. This work was supported by the DOE Office of Environment Management, EMSP Program (Grant No. DE-FG07-98ER 14913). Work by J.L.F. was supported by the Office of Energy Research, Office of Basic Energy Sciences, Chemical Sciences Division of the U.S. Department of Energy, under Contract DE-AC06-76RLO 1830 with Pacific Northwest National Laboratory.

References and Notes

(1) Lin, Y.; Smart, N. G.; Wai, C. M. *Trends Anal. Chem.* **1995**, *14* (3), 123.
(2) Wai, C. M.; Lin, Y.; Brauer, R. D.; Wang, S.; Beckert, W. F. *Talanta* **1993**, *40*, 1325.
(3) Laintz, K. E.; Wai, C. M.; Yonker, C. R.; Smith, *R. D. Anal. Chem.* **1992**, *64* (22), 2875.
(4) Iwacho, T.; Sadakane, A.; Tôei, K. Bul. *Chem. Soc. Jpn.* **1978**, *51* (2), 629.
(5) Kolthoff, I. M. *Can. J. Chem.* **1981**, *59*, 1548.
(6) Shamsipur, M.; Popov, A. I. *J. Phys. Chem.* **1987**, *91*, 447.
(7) Kolthoff, I. M.; Chantooni, M. K., Jr. *J. Chem. Eng. Data* **1997**, *42*, 49.
(8) Talanova, G. G.; Elkarim, N. S. A.; Talanov, V. S.; Hanes R. E., Jr.; Hwang, H.; Bartsch, R. A.; Rogers, R. D. *J. Am. Chem. Soc.* **1999**, *121*, 11281.
(9) Dietz, M. L.; Horwitz, E. P.; Rhoads, S.; Bartsch, R. A.; Krzykawski, *J. Solvent Extr. Ion Exch.* **1996**, *14* (1), 1.
(10) Rhangino, G.; Romano, S.; Lehn, J. M.; Wipff G. *J. Am. Chem. Soc.* **1985**, *107*, 7873.
(11) Northlander, E. H.; Burns J. H. *Inorg. Chim. Acta* **1986**, *115*, 31.
(12) Bryan, S. A.; Willis, R. R.; Moyer, B. A. *J. Phys. Chem.* **1990**, *94*, 5230.
(13) Fulton, J. L.; Yee, G. G.; Smith, R. D. *J. Am. Chem. Soc.* **1991**, *113*, 8327.
(14) Gupta, R. B.; Combes, J. R.; Johnston, K. P. *J. Phys. Chem.* **1993**, *97*, 707.
(15) Yamamoto, M.; Iwai, Y.; Nakajima, T.; Arai Y. *J. Phys. Chem. A* **1999**, *103*, 3525.
(16) Xu, Q.; Han, B.; Yan, H. *J. Phys. Chem. A* **1999**, *103*, 5240.
(17) O'Shea, K. E.; Kirmse, K. M.; Fox, M. A.; Johnston, K. P. *J. Phys. Chem.* **1991**, *95*, 7863.
(18) Jackson, K.; Bowman, L. E.; Fulton J. L. *Anal. Chem.* **1995**, *67*, 2368.
(19) *Molecular spectra & molecular structure. Infrared and Raman Spectra of polyatomic molecules*; Herzberg, G.; Ed.: Van Norstrand Reinhold Ltd. Co.: New York, 1945; p 282.
(20) Vayssière, P.; Wipff, G. *Phys. Chem. Chem. Phys.* **2003**, *5*, 127.
(21) Rice, J. K.; Niemeyer, E. D.; Bright F. V. *Anal. Chem.* **1995**, *67*, 4354.
(22) Gorbaty, Y. E.; Bondarenko, G. V. *Rev. Sci. Instrum.* **1993**, *64*, 2346.

COMMUNICATION

ChemComm www.rsc.org/chemcomm

Lewis acid-base complex formation for dissolution of acids in supercritical CO_2

Joanna Shaofen Wang, Xiang-Rong Ye, Jamie Herman, Qingyong Lang and Chien M. Wai*

Department of Chemistry, University of Idaho, Moscow, Idaho 83844, USA. E-mail:cwai@uidaho.edu

Hydrophilic acids can be dissolved in supercritical CO_2 by a Lewis acid-base complex formation method using a CO_2-philic base tri-*n*-butylphosphate as a carrier.

Supercritical fluid processing has been a burgeoning area of research in recent years for both theoretical and practical considerations. Carbon dioxide (CO_2) is the most widely used gas for supercritical fluid applications because of its moderate critical constants, nonflammable nature and environmental acceptability. However, since CO_2 is non-polar and has a low dielectric constant, supercritical CO_2 (SC-CO_2) processing is limited by its poor ability to dissolve hydrophilic species. Several strategies have been developed in the past to make SC-CO_2 more "solute-philic" including modifying CO_2 with polar solvents, utilizing water-in-CO_2 microemulsions, and complex formation approaches.[1] Recently, dissolution of hydrophilic metal species in SC-CO_2 has gained increasing attention because of potential applications in nuclear waste treatment, environmental remediation, semiconductor devices manufacturing, and chemical catalysis.[2] The *in situ* chelation method for dissolving metal species in SC-CO_2 developed by our research group in the early 1990s is widely used today for chemical and environmental studies.[3] Several previous reports have demonstrated that the solubility of metal chelates in SC-CO_2 can be significantly enhanced using CO_2-philic ligands such as fluorinated chelating agents and organophosphorus ligands.[2a,3a] Among these reagents, tri-*n*-butylphosphate (TBP) is particularly interesting because it is a CO_2-philic Lewis base and is capable of forming stable coordination compounds with Lewis acids through the electron donating P=O group.[4] The Lewis acid-base complex formation mechanism provides a simple method of dissolving hydrophilic acids in SC-CO_2 using TBP as a carrier. This technique may have a wide range of applications in developing CO_2-based processes because acids are often needed for chemical reactions and separations. The general Lewis acid-base concept of introducing hydrophilic species in SC-CO_2 should not be limited to TBP. In principle, other CO_2 soluble Lewis bases and Lewis acids could also be used as carriers for dissolution of acid or base counterparts in SC-CO_2. This communication presents some examples of Lewis acid-base complexes using TBP as a carrier and their solubilities in SC-CO_2.

The complexes used in this study were prepared by shaking 5 mL of TBP (Aldrich, Miwaukee, MI) with a certain amount of an acid in a capped vial for one hour. Concentrated HNO_3 (15.5 M, Fisher, Fair Lawn, NJ), HCl (12.3 M, Fisher), and benzoic acid (Fisher) were used as received for this study. After shaking, the mixture was centrifuged for one hour and the TBP phase was removed for characterization. The acid content in the TBP phase was determined by diluting 1 mL of the TBP phase with 40 mL of water followed by NaOH (0.1 M) titration of the acid in the aqueous phase. The water content of the TBP phase was determined by Karl-Fischer titration. The TBP-acid complex has a general composition of TBP $(Acid)_x$ $(H_2O)_y$ with x and y depending on the relative amount of TBP and the acid used in the preparation. Examples of TBP-HNO_3 and TBP-HCl complexes are given in Table 1. The TBP-benzoic acid complex was prepared by dissolving a certain amount of solid benzoic acid in TBP directly. Because benzoic acid does not contain water the complex has a formula of TBP $(Acid)_x$.

Table 1 Compositions of some TBP-acid complexes prepared for this study

Initial TBP/acid mixture	Composition of TBP-acid complex
5 mL TBP + 0.82 mL HNO_3 (15.5 M)	$TBP(HNO_3)_{0.7}(H_2O)_{0.7}$
5 mL TBP + 1.3 mL HNO_3 (15.5 M)	$TBP(HNO_3)_{1.0}(H_2O)_{0.4}$
5 mL TBP + 1.5 mL HCl (12.3 M)	$TBP(HCl)_{0.8}(H_2O)_{2.8}$
5 mL TBP + 2 g benzoic acid	$TBP(benzoic\ acid)_{0.5}$

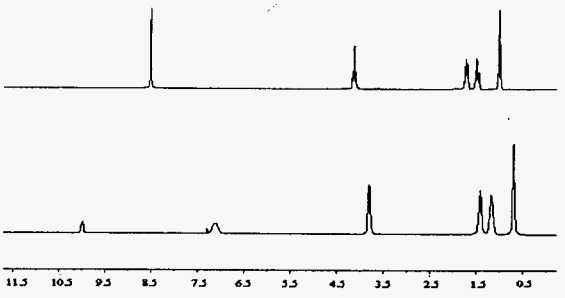

Fig. 1(a) Proton NMR spectra of $TBP(HCl)_{0.8}(H_2O)_{2.8}$ with D_2O insert (top) and in $CDCl_3$ (bottom)

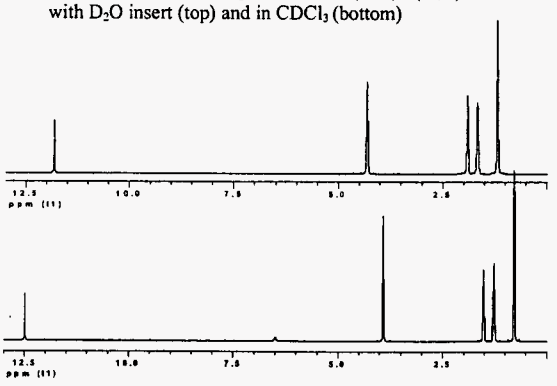

Fig. 1(b) Proton NMR spectra of $TBP(HNO_3)_{0.7}(H_2O)_{0.7}$ with D_2O insert (top) and in $CDCl_3$ (bottom)

Proton NMR spectra of a typical TBP-HCl complex (a) and a TBP-HNO_3 complex (b) are given in Fig. 1. The spectra were taken using a 300 MHz (Bruker) spectrometer at room temperature. In the NMR measurement of pure complexes, deuterated water was placed in an insert and fitted into an NMR tube containing a TBP-acid complex. The purpose of the D_2O

† Electronic Supplementary Information (ESI) available: [details of any supplementary information available should be included here]. See http://www.rsc.org/suppdata/cc/b0/b000000a/

insert was to lock the NMR. A trace amount of HDO present in the deuterated water allows calibration of the instrument. TBP is known to form a 1:1 complex with H_2O and the TBP-H_2O complex has a single resonance peak at about 3.9 ppm. The proton NMR spectrum of the $TBP(HCl)_{0.8}(H_2O)_{2.8}$ complex shows a single peak around 8.5 ppm indicating the protons of H_2O and HCl in the complex undergo rapid exchange (Fig. 1(a), top). The other 4 peaks below 4 ppm are the protons from the butyl groups of TBP. The HCl peak in the TBP complex shifts downfield when the amount of the acid (or x value) increases in the complex. The NMR spectra of the TBP-HNO_3 complexes are similar to that of TBP-HCl complexes. Fig. 1(b) shows the proton peaks of the $TBP(HNO_3)_{0.7}(H_2O)_{0.7}$ complex. Rapid exchange of H_2O and HNO_3 in the complex apparently takes place resulting in a single proton resonance peak at about 11.8 ppm. Formation of TBP-acid complex is not limited to hydrophilic inorganic acids. Organic acids can also form hydrogen bonded complex with TBP as illustrated by the NMR spectra of a TBP-benzoic acid complex given in Fig. 2. Fig. 2 (top) shows the NMR spectrum of benzoic acid in CCl_4 with D_2O insert and Fig. 2 (bottom) shows the spectrum of a $TBP(benzoic\ acid)_{0.5}$ complex with D_2O insert. The shift of the carboxylic acid proton peak from the free benzoic acid (13 ppm) to the bonded acid (11.8 ppm) is obvious. Peaks at 8.1, 7.6 and 7.4 ppm in Fig. 2 are protons from the benzene ring.

Table 2 Solubilities of some TBP-acid complexes in supercritical CO_2

Solute	Temp (°C)	P (atm)	Solubility (mole%)	Ref.
Benzoic acid	45	120	0.12	5
Benzoic acid	35	120	0.13	1*a*
$TBP(benzoic\ acid)_{0.5}$	40	120	2.4	this study
$TBP(HNO_3)_{0.7}(H_2O)_{0.7}$	40	112	1.7	this study
$TBP(HCl)_{0.8}(H_2O)_{2.8}$	40	116	1.0	this study

* Standard deviations of solubility measurements for this study ~10%

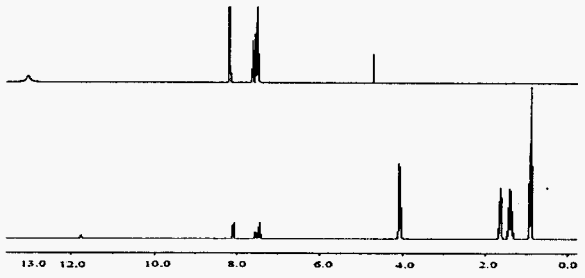

Fig. 2 Proton NMR spectra of benzoic acid alone in CCl_4 with D_2O insert (top) and $TBP(benzoic\ acid)_{0.5}$ complex with D_2O insert (bottom)

Understanding the solvation effect of SC-CO_2 on the TBP-acid complexes is important for evaluating the behavior of the complex in the fluid phase. Unfortunately, the corrosive nature of the complex and the lack of a safe high-pressure NMR device in our lab prevented us from performing NMR studies of the TBP-acid complexes in SC-CO_2. We chose to use chloroform ($CDCl_3$) to evaluate the salvation effect because chloroform has a small dielectric constant at room temperature (ε = 4.8 at 20 °C). Fig. 1(a), (bottom) shows that in the presence of $CDCl_3$, a new peak at 7.1 ppm appears that is attributed to the presence of free HCl. An anti-solvent effect of chloroform probably causes a portion of the HCl in the complex to precipitate and forming small droplets in the solvent. The bonded HCl in TBP shifts downfield to about 10.0 ppm. Formation of small acid droplets in $CDCl_3$ was obvious because the solution turned cloudy when the TBP-HCl complex was added to the solvent. The cloud formation was also observed when the TBP-HCl complex was added to SC-CO_2 using a high-pressure view-cell with quartz windows. Similar cloud formation was observed when a $TBP(HNO_3)_{0.7}(H_2O)_{0.7}$ complex was added to SC-CO_2. When the TBP-HNO_3 complex was dissolved in $CDCl_3$, a free HNO_3 peak appeared at 6.5 ppm and the bonded HNO_3 peak shifted to 12.5 ppm as indicated by the NMR spectrum given in Fig. 1(b), (bottom).

The solubilities of some TBP-acid complexes in SC-CO_2 were measured at 40 °C by visual observation of phase behavior under different pressures using a view cell with quartz windows. Solubility data of TBP and benzoic acid are known in the literature. TBP is highly soluble in SC-CO_2. According to Joung *et al.*, TBP becomes miscible with SC-CO_2 above certain pressure at a given temperature.[6] For example, at 50 °C (323.15 K), TBP and CO_2 form one phase at pressures above 110 atm. Hydrochloric acid and nitric acid are not soluble in SC-CO_2 and benzoic acid has a limited solubility in CO_2 (Table 2). When benzoic acid is bonded to TBP, the solubility of the complex is significantly enhanced. For example, the $TBP(benzoic\ acid)_{0.5}$ complex has a solubility of 2.4 mole% at 40 °C and 120 atm which is about an order of magnitude higher than the free acid alone in SC-CO_2 under similar conditions. The solubilities of TBP and $TBP(HCl)_{0.8}(H_2O)_{2.8}$ and $TBP(HNO_3)_{0.7}(H_2O)_{0.7}$ are in the range of 1.0-1.7 mole% in SC-CO_2 at 40 °C and around 115 atm.

The Lewis acid-base complex formation method described in this paper allows normally insoluble or slightly soluble acids to be dissolved in SC-CO_2. This method is simple and can introduce a variety of acids in SC-CO_2 for chemical reactions or separations. The method is not limited to TBP, other commercially available Lewis bases that are CO_2 soluble may also be used as carriers for introducing acids in SC-CO_2. In principle, this method could be used to introduce bases in SC-CO_2 using a CO_2-philic Lewis acid. The Lewis acid-base complex formation concept may also be applied to SC-CO_2 extraction of acids from aqueous solutions using TBP or other CO_2 soluble Lewis base as a carrier. Research to explore potential applications of this method in supercritical fluid processes is currently in progress.

This work was supported by the Idaho NSF-EPSCoR Program and by a DOE-EMSP Program.

Notes and references

1 *(a)* J. M. Dobbs, J. M. Wong, R. J. Lahiere and K. P. Johnston, *Ind. Eng. Chem. Res.*, 1987, **26**, 56; *(b)* J. L. Fulton, D. M. Pfund, J. B. McClain, T. J. Romack, E. E. Maury, J. R. Combes, E. T. Samulski, J. M. DeSimone and M. Capel, *Langmuir*, 1995, **11**, 4241; *(c)* K. P. Johnston, K. L. Harrison, M. J. Clarke, S. M. Howdle and M. P. Heitz, *Science*, 1996, **271**, 624; *(d)* J. Darr and M. Poliakoff, *Chem. Rev.*,1999, **99**, 495; *(e)* C. M. Wai, Metal Processing in Supercritical Carbon Dioxide, in *Supercritical Fluid Technology in Materials Science and Engineering*, Y. P. Sun, ed., Marcel Dekker, 2002, p.351-386.

2 *(a)* C. M. Wai, Supercritical Fluid Extraction Technology for Nuclear Waste Management, in *Hazardous and Radioactive Waste Treatment Technologies Handbook*, C.H. Oh, ed., CRC Press, Boca Raton, Florida, 2001, p.5.1-5.3; *(b)* C. Kersch, M. J. E. van Roosmalen, G. F. Woerlee and G. J. Witkamp, *Ind. Eng. Chem. Res.*, 2000, **39**, 4670; *(c)* C. A. Bessel, G. M. Denison, J. M. DeSimone, J. DeYoung, S. Gross, C. K. Schauer and P. M. Visintin, *J. Am. Chem. Soc.*, 2003, **125**, 4980; *(d)* M. Ji, X. Chen, C. M. Wai and J. L. Fulton, *J. Am. Chem. Soc.*, 1999, **121**, 2631.

3 *(a)*K. E. Laintz, C. M. Wai, C. R. Yonker and R. D. Smith, *J. Supercrit. Fluids*, 1991, **4**, 194; *(b)* K. E. Laintz, C.M. Wai, C. R. Yonker and R. D. Smith, *Anal. Chem.*,1992, **64**, 2875.

4 Y. Enokida, O. Tomika, S. C. Lee, A. Rustenholtz and C. M. Wai, *Ind. Eng. Chem. Res.*, 2002, **42**, 5037.

5 W. J. Schmitt and R. C. Reid, *J. Chem. Eng. Data*, 1986, **31**, 204.

6 S. N. Joung, S. J. Yoon, J. Park, S. Y. Kim and K. Yoo, *J. Chem. Eng. Data*, 1999, **44**, 1034.

Nuclear Laundry Using Supercritical Fluid Solutions

Joanna Shaofen Wang, Moonsung Koh, and Chien M. Wai*

Department of Chemistry, University of Idaho, Moscow, Idaho 83844-2343

Cobalt and other metals, spiked onto lab coats, can be removed by supercritical fluid carbon dioxide (SC-CO_2) containing mixed chelating agents Cyanex 302 and dithiocarbamate, as well as by a water-in-CO_2 microemulsion. The extraction efficiencies for both methods can exceed 90%. The mixed-ligand approach suggests that effective metal extraction can be developed using two different ligands contributing to the solubility and stability of the resulting metal chelates in SC-CO_2. The water-in-CO_2 microemulsion method does not require chelating agents. This approach significantly reduces the amount of liquid waste generation. Dynamic extraction time, flow rate, temperature of outlet restrictor, and collection solvent must be taken into consideration for the recovery efficiency. The potential of utilizing supercritical fluid solutions for cleaning ^{60}Co-contaminated protective coats used by nuclear power plant workers is discussed.

Introduction

Supercritical fluid carbon dioxide (SC-CO_2) has been extensively studied in the past two decades and has come to be recognized as an environmentally friendly solvent for the dissolution of organic compounds that has been traditionally done using organic solvents. In recent years, the studies of supercritical fluid extraction (SFE) techniques for using CO_2 as a solvent to remove metal species from solids have also been reported by various research groups.[1-9] Metal ions do not dissolve in nonpolar SC-CO_2 because of the charge neutralization requirement and weak solute−solvent interactions. Wai and co-workers first reported in the early 1990s that, using an organic chelating agent such as diethyldithiocarbamate [$(C_2H_5)_2NCS_2^-$, DDC], metal ions could be extracted by SC-CO_2 as dithiocarbamate complexes.[2] Fluorination of the terminal ethyl groups of metal dithiocarbamate complexes was found to enhance the solubility in SC-CO_2 by 2−3 orders of magnitude.[1] This discovery has been one of the key developments in supercritical fluid research. Later, many fluorinated chelating agents including fluorinated β-diketones and fluorinated polymers with various chelating heads were used for dissolution of metal species in SC-CO_2 using this in situ chelation/SFE method.[3-9] Other types of chelating agents, particularly organophosphorus reagents, such as tri-*n*-butyl phosphate, bis(2,4,4-trimethylpentyl)monothiophosphinic acid (Cyanex 302), etc., also form CO_2-soluble complexes with various metal species.[10-12] These ligands and chelating agents have been used to extract transition metals, lanthanides, and actinides from solid samples of different matrixes in SC-CO_2. After SFE, depressurizing the supercritical fluid solution results in rapid precipitation of the solutes (metal chelates) from the solvent, leaving decontaminated samples behind. This in situ chelation/SFE method is obviously attractive for removing toxic metals and radioisotopes from contaminated substances.

The radioactive contamination level on protective coats worn by nuclear power plant workers is generally required to be kept below 4 Bq/cm^2.[13] Above this level, washing of contaminated coats is often required. The main radioactive isotope in contaminated protective coats is ^{60}Co, which emits β (E_{max} 0.32 MeV) and γ (1.173 and 1.333 MeV) radiations with a half-life of 5.26 years. The contaminated protective coats are commonly washed with water and detergent to remove the radioactive contamination. However, treatment of the wastewater from the conventional nuclear laundry becomes an environmental problem.

More recently, water-in-CO_2 microemulsions have been shown to be an effective medium for transporting metal ions in SC-CO_2.[5] Relatively high concentrations of metal salts can be dissolved in the water core of the microemulsion and dispersed in the CO_2 phase. The water-in-CO_2 microemulsions are dynamic in nature, and exchange of contents in the water core can take place effectively during collisions. Because of their small size and dynamic nature, these microemulsions show great promise as transporting media for removing metal species from solid materials into SC-CO_2. Using the CO_2 microemulsion to remove metal species from porous solid materials requires only a small amount of water. In comparison with a conventional washing or acid leaching process, which usually requires large quantities of water, the CO_2 microemulsions technique could greatly minimize liquid waste generation. Thus, water-in-CO_2 microemulsion may be regarded as a new solvent for decontamination of radioactive materials. In this paper, we report our recent results regarding SFE of cobalt and other metals from lab coats using in situ chelation/SFE with Cyanex 302 and a dithiocarbamate reagent as extractants. A synergistic effect of the two chelating agents for removing cobalt and other transition metals is described. The results are compared with that obtained using a water-in-CO_2 microemulsion as a medium for removing these metals from fabric matrixes.

Experimental Section

Reagents and Materials. Cyanex 302 (Cytec Industries Inc.) and bis(2,4,4-trimethylpentyl)phosphinic acid (Cyanex 272, Cytec Industries Inc.) were used as supplied (Figure 1). Instrument grade carbon dioxide (Oxarc, Spokane, WA) was used in all experiments. Nitric acid (J. T. Baker) was Ultrex grade ultrapure reagent. Sodium diethyldithiocarbamate [$(C_2H_5)_2NCS_2^-Na^+$, NaD-

* To whom correspondence should be addressed. Tel.: (208) 885-6787. Fax: (208) 885-6173. E-mail: cwai@uidaho.edu.

10.1021/ie030509d CCC: $27.50
Published on Web 00/00/0000 **PAGE EST: 6**

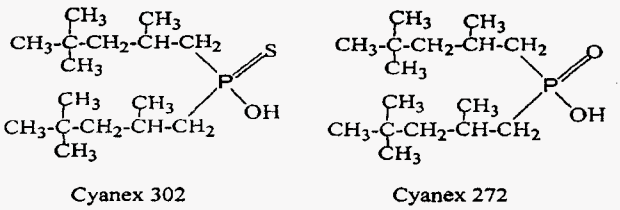

Figure 1. Structure of Cyanex 302 and Cyanex 272.

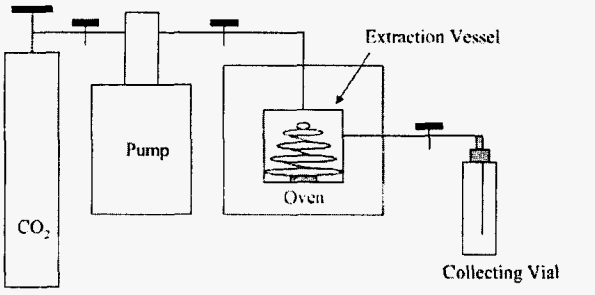

Figure 2. Extraction apparatus used in CO_2 microemulsions and in situ chelation/SFE.

DC] (J. T. Baker) was used as received. Dibutyldithiocarbamate ammonia salt, $[(C_4H_9)_2NCS_2^-\ N^+(CH_3)_4$, DBDC] was synthesized in our laboratory. The details of the synthetic procedure are given in the literature.[8] A commercial liquid detergent (Liqui-Nox) was used for conventional laundry (Alconox, Inc., White Plains, NY). Ammonia pyrrolidinedithiocarbamate $[(CH_2)_4NCS_2^-N^+H_4$, APDC] and other chemicals, including $Sr(NO_3)_2$, $La(NO_3)_3{\cdot}H_2O$, and $Eu(NO_3)_3{\cdot}H_2O$ salts were obtained from Aldrich Chemical Co. (Milwaukee, WI). Sodium bis(2-ethylhexyl) sulfosuccinate (AOT, Aldrich Chemical Co.) and perfluoropolyether phosphate (PFPE-PO_4) (KDP-4413, Lot No. E88576-64, DuPont Co.) were used as received. All other reagents and solvents used in this study were of analytical grade. Deionized water (Millipore Milli-Q system, Bedford, MA) was used for the preparation of all aqueous solutions. Standard solutions of cobalt chloride and nitrate solutions of Cu, Cd, Pb, and Zn were prepared from atomic absorption spectroscopy standards (EM Science, a Division of EM Industries, Inc., Cherry Hill, NJ).

Instrumentation. The apparatus for the SFE experiments (Figure 2) includes the following: a liquid CO_2 tank, a high-pressure syringe pump, an extraction cell, and a collection vial. SFC-grade CO_2 was supplied with a syringe pump (Isco, model 260D, Lincoln, NB). The experiments were performed with a stainless steel extraction vessel (35.3 mL) maintained at a desired temperature by placing it in a thermostatic oven. The flow rate of the extraction fluid was controlled by the Isco pump. At the oven exit, a stainless steel tube (316 SS, $^1/_{16}$-in. o.d. and 0.030-in. i.d.) with a length of 20 cm was used as the pressure restrictor for the exit CO_2.

A high-pressure view cell (16.8-mL volume and 5-cm path length) with sapphire windows was used to evaluate the solubility and stability of the water-in-CO_2 microemulsions. A high-pressure fiber-optic cell equipped with a CCD array UV–visible spectrometer was used for in situ spectroscopic measurements. Descriptions of the view cell and fiber-optic system are given in the literature.[14,15]

Metal Extraction with Chelating Agents. A 10-μL sample of a standard solution containing 1000 ppm each of Co, Cd, Cu, Pb, and Zn were spiked on pieces (0.6×4 cm^2) of fabrics cut from a laboratory coat. After evaporation to dryness, the fabric sample was placed on the stainless steel rack in the extraction vessel as shown in Figure 2. The system was preheated prior to the experiments. A 300-mg sample of Cyanex 302 or 272 was added to the extraction vessel. A 10-mg sample of sodium diethyldithiocarbamate was added afterward. After the addition of 30 μL of water to the sample, the system was pressurized. A magnetic stirrer was used and set at 300 rpm. Experimental conditions were set for 20-min static extraction followed by 30-min dynamic extraction using neat CO_2 at 40 °C and 200 atm with agitation. The flow rate was measured by the pump controller, which was set at ~0.5 ± 0.1 mL/min by adjusting the outlet valve. The extracted metal chelates were collected in a collection vial containing 20 mL of hexane at the exit. A heating gun was used to maintain a warm environment for the outlet valve and tubing to avoid plugging of the system. When the extraction was completed, the fabric sample was removed from the extraction cell and treated with 2 mL of 50% nitric acid. The trapped solution was back-extracted by 2 mL of 50% nitric acid. After phase separation, the aqueous solutions were diluted to 10 mL and subsequently analyzed by inductively coupled plasma-atomic emission spectroscopy (ICP-AES).

Metal Extraction with CO_2 Microemulsion. The conditions for making stable water-in-CO_2 microemulsions were investigated by the high-pressure view cell system. The surfactants [15 mM (235 mg) AOT, and 30 mM (920 mg) PFPE-PO_4] were introduced into a high-pressure view cell (volume, 16.86 mL). A certain amount of water was then added to make a desired W value (W = $[H_2O]$/[surfactant], between 10 and 20). After that, the system was filled with CO_2 to a fixed pressure (100–200 atm) and temperature. The system was stirred with a minimagnetic bar for ~15 min. If a stable water-in-CO_2 microemulsion was formed, the fluid phase became optically transparent.

Changing pressure, temperature and W value will affect the stability of the microemulsion in supercritical CO_2. For example, if pressure is reduced to the cloud point, the optically transparent solution becomes cloudy, indicating the microemulsion no longer exists due to aggregation of water and surfactants. Formation of the CO_2 microemulsion is reversible. When the pressure is increased above the cloud point, the microemulsion solution becomes transparent again. When the W value exceeds a certain value, the optically transparent microemulsion disappears and the solution becomes cloudy at a given constant temperature and pressure.

After understanding the stability of the microemulsion system, the extraction of metals with the CO_2 microemulsion was performed using a high-pressure system shown in Figure 2. A lab coat sample spiked with metal ions was held on a stainless steel rack placed in the extraction cell. AOT and PFPE-PO_4 were added to the extraction cell. The cell was heated to 40 °C. This was followed by addition of an accurate known amount of water to make a W value of 15, and the system was then pressurized to 200 atm and stirred to form a water-in-CO_2 microemulsion. A GC oven was used as a thermostat, and a thermacouple was used to control and monitor temperature. After a period of contact time, the system was depressurized and the fabric sample was removed from the system, treated with 2 mL of 50% HNO_3, and diluted for chemical analysis.

Table 1. In Situ Chelation/SFE[a] of Metal Ions from Spiked Lab Coat Samples Using Cyanex 302, Cyanex 272, and NaDDC

Cyanex 302 (mg)	NaDDC (mg)	extraction efficiency (%)				
		Co	Cd	Cu	Pb	Zn
300		53 ± 5	78 ± 8	87 ± 5	62 ± 4	48 ± 6
	10	44 ± 8	49 ± 3	71 ± 5	32 ± 5	35 ± 4
300	10	93 ± 5	91 ± 4	98 ± 4	94 ± 3	92 ± 3
blank		0.001	0.002	0.002	0.003	0.003

Cyanex 272 (mg)	NaDDC (mg)	extraction efficiency (%)				
		Co	Cd	Cu	Pb	Zn
300		52 ± 3	61 ± 5	88 ± 4	61 ± 5	77 ± 8
300	10	95 ± 3	92 ± 4	92 ± 3	98 ± 5	93 ± 6
blank		0.002	0.001	0.002	0.004	0.002

[a] SFE conditions: 10 μg of each element, 20-min static extraction followed by 30-min dynamic extraction at 40 °C and 200 atm with agitation. A 30-μL aliquot of water was added to the sample prior to the SFE. The extraction results were calculated based on the residue part and samples were in triplicate runs.

Metal Analysis. A Perkin-Elmer Optima 3000XL with an axially mounted torch ICP-AES was used to analyze the extracted metals. Calibration standards were prepared using certified standards of individual elements acquired from Aldrich Chemical Co. and Fisher Scientific. Sets of three to five different concentrations of the standards were used to establish calibration curves. To minimize matrix effects, blank and standard solutions were closely matched with the samples. Blanks and standards of known concentrations were run periodically through the ICP-AES analyses as quality control checks.

Results and Discussion

SFE of Metal Species Using Organophosphorus Reagents. The results of the experiments show that organophosphorus reagents Cyanex 302 and Cyanex 272 have good solubilities in SC-CO_2 that make them suitable for SFE of trace metals.[12] At 60 °C, the solubilities of Cyanex 302 are 40 (0.13 mol L^{-1}) and 110 g L^{-1} (0.36 mol L^{-1}) at 200 and 300 atm, respectively.[12] The results of SFE of Co^{2+}, Cd^{2+}, Cu^{2+}, Pb^{2+}, and Zn^{2+} from a spiked lab coat sample at 40 °C and 200 atm using either Cyanex 302 or 272 as an extractant are shown in Table 1; the extraction efficiencies for Co^{2+}, Cd^{2+}, Cu^{2+}, Pb^{2+}, and Zn^{2+} spiked on a lab coat using Cyanex 302 were 53, 78, 87, 62, and 48%, respectively. The metal extraction efficiencies using Cyanex 272 as an extractant were about the same as those of Cyanex 302, generally in the range 50–90%, according to Table 1.

SFE of Metal Species with Dithiocarbamate Reagents. One ligand system that has been extensively studied for SFE of metal species in the literature is the derivatives of dithiocarbamic acid of the general form R_2NCS_2X, where R is an alkyl group and X is a cation, which can be an alkali metal ion, an ammonium ion, or an alkylammonium ion.[1,2,7,8,16,17] Dithiocarbamate derivatives are effective extractants for preconcentration of trace elements from aqueous solutions by solvent extraction.[18] A widely used dithiocarbamte reagent for this purpose is NaDDC, which is able to extract over 40 metal species from aqueous solutions into organic solvents. One problem with using DDC as an extractant in SFE of metals is the low solubility of metal–DDC chelates in SC-CO_2. For example, the solubility of Co-$(DDC)_2$ in SC-CO_2 at 50 °C and 100 atm is 2.4 × 10^{-6} mol L^{-1}.[1] The solubility of NaDDC in neat CO_2 is also small, about 1.5 × 10^{-4} mol L^{-1} at 50 °C and 100 atm[1] and 1.5 × 10^{-3} mol L^{-1} at 60 °C and 200 atm.[19] With 10 mg (4.44 × 10^{-5} mol) of NaDDC at 40 °C and 200 atm, using neat CO_2, the extraction efficiencies of Co^{2+}, Cd^{2+}, Cu^{2+}, Pb^{2+}, and Zn^{2+} were around 30–70%, according to Table 1. The concentration of NaDDC in the 35.3 mL extraction cell was probably near saturation at 40 °C and 200 atm for these experiments.

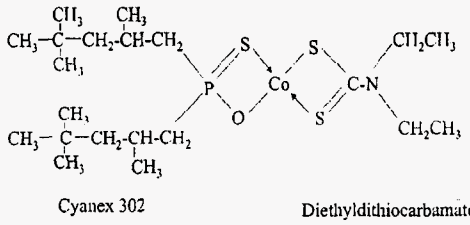

Figure 3. Possible structure of a Co(II)–Cyanex 302–DDC complex.

SFE of Metal Species with Mixed Chelating Agents. A surprising observation made in this study is that when a small amount of NaDDC (10 mg) was mixed with Cyanex 302 or 272, the extraction efficiencies for the metal ions were increased significantly (see Table 1). The extraction efficiencies for Co^{2+}, Cd^{2+}, Cu^{2+}, Pb^{2+}, and Zn^{2+} from the lab coat samples at 40 °C and 200 atm were 93, 91, 98, 94, and 92%, respectively. Similar results were observed when 300 mg of Cyanex 272 was mixed with 10 mg of NaDDC for SFE of metals in the same matrix. When two or more different chelating agents are used as extractants for metal species, sometimes the net extraction efficiency is enhanced. A synergistic extraction effect is well known in solvent extraction systems but has not been reported in SFE systems. The cause of synergistic extraction is often complicated, but it may be associated with the formation of a more stable and soluble complex in SC-CO_2 involving two chelating agents.

The form of the Co–Cyanex 302 complex is generally $CoR_2(HR)$,[20] CoR(HR) or $CoR_2(HR)_2$,[21] where HR is the protonated form of Cyanex 302. The metal complexes formed by Cyanex 302 have good solubilities in SC-CO_2 with reasonable formation constants. At 60 °C, the solubilities of Cu–Cyanex 302 are 0.9 (2.4 × 10^{-3} mol L^{-1}) and 7.8 g L^{-1} (2.1 × 10^{-2} mol L^{-1}) at 200 and 300 atm, respectively.[12] The formation constant (log K) of $CdR_2(HR)$ was reported to be ~7.02 by Almela et al.[20] It is known that diethyldithiocarbamate can form very stable chelates with metal ions but with low solubilities in SC-CO_2.[1,18] For example, the stability constant values (log K) for $Cu(DDC)_2$, $Cd(DDC)_2$, and $Co(DDC)_2$ are 26.26, 19.22, and 15.0, respectively.[18] The solubilities of these metal–DDC chelates in SC-CO_2 are small, in the order of 10^{-6} mol/L. If a cobalt complex is formed with the two different chelating agents as shown in Figure 3, it probably would have a solubility larger than the $Co(DDC)_2$ complex and a stability higher than the Co–Cyanex complex. This is probably the cause of the synergistic effect observed in the mixed Cyanex 302 and NaDDC system. Using a mixture of Cyanex 302 (300 mg) and Na–DDC (10 mg), near-quantitative extraction of cobalt and other metal ions spiked on the lab coat samples was achieved.

When the amount of NaDDC was increased from 2 (8.88 × 10^{-6} mol) to 10 mg (4.44 × 10^{-5} mol) with a fixed amount of Cyanex 302 (300 mg), the extraction efficiency increased accordingly (Table 2). With an

Table 2. Comparison of the Mixed-Ligand Effect Using Different Amounts of Dithiocarbamate Chelating Agents with a Fixed Amount of Cyanex 302[a]

Cyanex 302 (300 mg) plus	amt (mg)	amt (mol)	extraction efficiency (%)				
			Co	Cd	Cu	Pb	Zn
NaDDC	2	8.88×10^{-6}	16 ± 3	24 ± 4	42 ± 8	42 ± 5	10 ± 4
NaDDC	5	2.22×10^{-5}	19 ± 4	37 ± 7	45 ± 4	58 ± 4	23 ± 3
NaDDC	10	4.44×10^{-5}	93 ± 5	91 ± 4	98 ± 4	94 ± 3	92 ± 3
NaDDC	20	8.88×10^{-5}	94 ± 3	96 ± 2	90 ± 5	91 ± 3	90 ± 4
DBDC	2.5	8.88×10^{-6}	40 ± 5	41 ± 4	45 ± 3	49 ± 4	43 ± 5
DBDC	6.2	2.22×10^{-5}	42 ± 3	57 ± 3	51 ± 5	64 ± 4	50 ± 3
DBDC	12.3	4.44×10^{-5}	89 ± 3	93 ± 5	91 ± 5	90 ± 4	91 ± 3
DBDC	24.7	8.88×10^{-5}	91 ± 5	90 ± 3	94 ± 4	92 ± 4	93 ± 2
APDC	1.5	8.88×10^{-6}	22 ± 2	33 ± 4	28 ± 3	23 ± 3	20 ± 2
APDC	3.6	2.22×10^{-5}	32 ± 5	64 ± 3	23 ± 2	37 ± 4	40 ± 4
APDC	7.3	4.44×10^{-5}	55 ± 3	66 ± 4	62 ± 5	63 ± 4	48 ± 5
APDC	14.6	8.88×10^{-5}	64 ± 7	58 ± 5	64 ± 6	65 ± 3	46 ± 4

[a] SFE conditions: 10 μg of each element, 20-min static extraction followed by 30-min dynamic extraction at 40 °C and 200 atm with agitation. A 30-μL aliquot of water was added to the sample prior to the SFE. Matrix, lab coat.

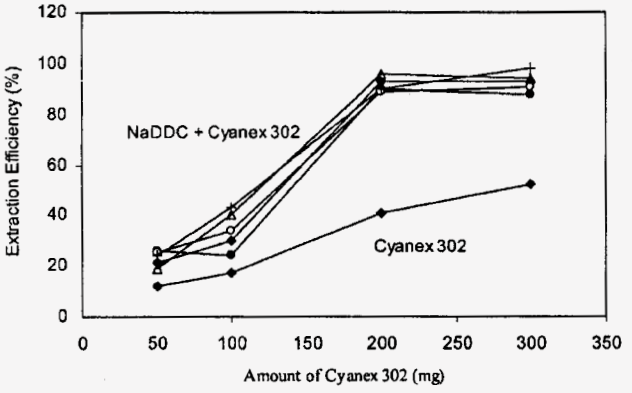

Figure 4. Extraction efficiency of Co and other metals using DDC with varying amounts of Cyanex 302: (◆) Co, (+) Cu, (△) Cd, (●) Pb, and (○) Zn. The amount of Cyanex 302 increased from 50, 100, and 200, to 300 mg and the amount of NaDDC was fixed at 10 mg (4.44×10^{-5} mol). SFE conditions: 20-min static extraction followed by 30-min dynamic extraction at 40 °C and 200 atm using neat CO_2 with agitation. A 30-μL aliquot of water was added to the sample prior to the SFE. Matrix, lab coat.

increase in NaDDC from 10 to 20 mg (8.88×10^{-5} mol), the extraction efficiency did not show a detectable increase, indicating that 10 mg of NaDDC was sufficient for the mixed-ligand extraction. Other dithiocarbamate chelating agents were also tested in combination with Cyanex 302 for the extraction of the spiked metal ions from lab coat samples in SC-CO_2. DBDC and APDC were chosen because both were reported in the literature as chelating agents for metal extraction in SC-CO_2.[16,19] Addition of DBDC (12.3 mg, 4.44×10^{-5} mol) to Cyanex 302 (300 mg) showed about the same results as those of NaDDC + Cyanex 302 mixed system (Table 2). When APDC was added to Cyanex 302, the results were not as good as the NaDDC + Cyanex 302 mixed system.

With a fixed amount of NaDDC (10 mg), increasing Cyanex 302 tends to increase the extraction efficiency of the metals spiked in the lab coat samples. Figure 4 shows the correlation between the extraction efficiencies of the metal ions and the amount of Cyanex 302 added. With 10 mg of NaDDC, the extraction efficiencies of these metal ions increase with increasing amount of Cyanex 302 from 50 to 200 mg and reach a plateau above that. The curve for cobalt extraction with only Cyanex 302 is also given in Figure 4. The efficiency of cobalt extraction with Cyanex 302 alone is about half of that with a small amount of NaDDC (10 mg) in 200 mg of Cyanex 302.

Table 3. Recovery of Metal Ions from SFE System

	extraction efficiency[a] (%)				
	Co	Cd	Cu	Pb	Zn
residue	6.2	1.2	5.1	4.9	3.2
trapped	74	93	93	90	92
cell + tubing	4.5	4.1	4.4	4.0	3.5
total	85 ± 4	98 ± 7	102 ± 4	99 ± 5	98 ± 3

[a] Extraction conditions: 30 μg of each element, 300 mg of Cyanex 302, and 10 mg of NaDDC, $T = 40$ °C, $P = 200$ atm, static time 30 min, dynamic time 4 h, and flow rate 0.4–0.6 mL/min. Results were based on triplicate runs.

All of the results given in Table 1 and Table 2 were obtained by SC-CO_2 extraction with agitation as described in the Experimental Section. According to Figure 4, over 90% of the spiked metal ions can be removed from the lab coat samples under the specified experimental conditions (200 mg of Cyanex 302 and 10 mg of NaDDC). Without agitation, the extraction efficiency for cobalt was less then 60% under the same SC-CO_2 extraction conditions. Agitation appears necessary to obtain reproducible results and to enhance the extraction efficiency of metal ions in this system.

Recovery of Metal Complexes. Recovery of extracted metal complexes was studied using lab coat samples spiked with 30 μg each of Co, Cd, Cu, Pb, and Zn. The SFE conditions remained the same, i.e., 40 °C and 200 atm. Hexane was used as the trapping solvent. Flow rate was controlled around 0.5 ± 0.1 mL/min. The static extraction time was set at 30 min followed by dynamic extraction time of up to 7 h (with ~200 mL of CO_2). The recovery results indicated that there was little difference if dynamic flushing time was longer than 4 h (120 mL of CO_2); i.e., 4 h of dynamic flush was enough for quantitative recovery. Three portions of SFE sample, i.e., residue lab coat, trapped solution, and extraction cell and tubing, were collected and analyzed by ICP-AES. The extraction cell and tubing were washed with 50% nitric acid for ICP analysis similar to that of analyzing the lab coat sample. The majority of the metals were found in the trap solution after dynamic flushing. The lab coat sample and the walls of the cell and tubing usually contained a small percentage of metals, according to the results given in Table 3.

Several factors must also be considered for satisfactory metal recovery: (1) trapping solvent volume must be maintained at a certain level. This means a small addition of trap solvent during SFE is necessary. (2) The trap solvent should have a high solvating power for the analytes. Hexane is a good choice as a collection solvent

in this case. (3) The outlet valve and the restrictor above the solvent should be in a warm environment in order to avoid plugging during the SFE process. In our experiments, a heating gun was used in the dynamic extraction to keep the outlet valve warm. (4) Flow rate is another factor important for satisfactory recovery of solutes. If the flow rate is too high, incomplete trapping of solutes will occur. If the flow rate is too low, poor recovery can also occur, because the restrictor tends to be plugged or because of insufficient fluid to carry the analytes out of the system. Flow rate in our experiments was controlled at ~0.5 ± 0.1 mL/min. Common restrictors used in SFE[20] were usually 50-μm i.d. that were easy to plug. We used a larger i.d. (0.030 in.) restrictor in our SFE recovery. The restrictor should be immersed into the middle of the trap solution. Our experimental results indicate that, following the recommended conditions, quantitative recovery of the metals can be achieved.

Water-in-CO_2 Microemulsion Extraction of Metal Species. Recently, water-in-CO_2 microemulsions have been developed for transporting polar compounds in SC-CO_2. Nanometer-sized water drops can be stabilized by CO_2-soluble surfactants to form microemulsions that are uniformly dispersed in SC-CO_2 over an extended period of time. These surfactants are amphiphilic molecules containing a hydrophilic headgroup and a CO_2-philic tail. The tails are usually fluorinated groups, and the molecular size and shape of the head and tail are designed to favor aggregation. The size of the microemulsions depends on the molar ratio of water-to-surfactant (W) present in the SC-CO_2 solution. Typically, the diameters of the spherical droplets of surfactant-encapsulated water are from a few nanometers to 50 nm. These solutions are thermodynamically stable and optically transparent since structures of this size are poor scatterers of light.

AOT is known to form stable microemulsions as reported in many water-in-oil microemulsion studies.[22,23] However, microemulsions stabilized by AOT are not soluble in SC-CO_2. Ji et al.[24] used two surfactants, AOT and PFPE-PO_4, to form water-in-CO_2 microemulsions. The fluorinated surfactant PFPE-PO_4 acts like a cosurfactant to make the AOT microemulsion soluble in SC-CO_2. The PFPE-PO_4 surfactant used by Ji et al. has a general structure of $CF_3O[OCF(CF_3)CF_2]_n(OCF_2)_m$-$OCF_2CH_2OCH_2CH_2O-PO(OH)_2$ and an average molecular weight of 870. Using a mixture of AOT and PFPE-PO_4, the resulting water-in-CO_2 microemulsion is stable with W values up to 40 at 40 °C and 200 atm.

A water-in-CO_2 microemulsion can interact with metal ions in solid materials and remove them from the solid matrix into the water core. In our experiments, 235 mg (0.015 M) of AOT, 920 mg of PFPE-PO_4, and 182 μL of water were used to form a microemulsion in an extraction cell of 35.3 mL. The W value was ~15. At 40 °C and 200 atm, ~40 μL of water can be dissolved in CO_2, which should be subtracted from the amount of water added to the system for the W value calculation. Lab coat samples were prepared by spiking 10 μL of a standard solution containing 1000 ppm of Co^{2+}, Cd^{2+}, Cu^{2+}, Pb^{2+}, and Zn^{2+}. The experiments were performed at 40 °C and 200 atm with stirring.

Experimental results given in Table 4 indicate that 15 min of mixing time may not be enough for stabilizing the microemulsion and extraction of metal ions from the fabric samples. A mixing time of 30 min gave good extraction results for removing the metal ions from the

Table 4. Extraction of Metal Ions Using Water-in-CO_2 Microemulsion

extraction efficiency (%)					
Co	Cd	Cu	Pb	Zn	conditions[a]
95 ± 5	94 ± 6	93 ± 3	91 ± 5	92 ± 4	60 min, AOT + PFPE-PO_4
94 ± 4	96 ± 5	92 ± 4	89 ± 3	91 ± 6	30 min, AOT + PFPE-PO_4
88 ± 4	88 ± 3	86 ± 2	86±5	67 ± 7	15 min, AOT + PFPE-PO_4
<1	<1	<1	<1	<1	60 min, blank

extraction efficiency (%)				
Co	Eu	La	Sr	conditions
95±5	94±7	96±6	94±4	60 min, AOT + PFPE-PO_4
<1	<1	<1	<1	60 min, blank

[a] Conditions: 10 μg of each element, [AOT] = 0.015 M (235 mg), [PFPE-PO_4] = 920 mg (460 μL), [H_2O] = 0.225 M (142 μL), cell V = 35.3 mL, W = 15, T = 40 °C, P = 200 atm, 1-h stirring, matrix lab coat, and triplicate runs.

Table 5. Recovery of Metal Ions from Water-in-CO_2 Microemulsion

	extraction efficiency[a] (%)				
	Co	Cd	Cu	Pb	Zn
residue	4	8	7	5	4
trapped	87	88	91	90	92
total	91 ± 4	96 ± 5	98 ± 3	95 ± 4	96 ± 5

[a] SFE conditions: 30 μg of each element, T = 40 °C, P = 200 atm, [AOT] = 0.015 M (235 mg), [PFPE-PO_4] = 920 mg (460 μL), [H_2O] = 0.225 M (142 μL), cell V = 35.3 mL, W = 15, matrix lab coat, 0.5-h microemulsion formation time, 1-h extraction time, dynamic extraction overnight (~180 mL of CO_2), and flow rate 0.4 mL/min.

matrix. To ensure a good extraction of metals from lab coat samples, 30–60 min of mixing time is needed. According to the results given in Table 4, over 90% of the spiked metal species can be extracted by the microemulsion after 1 h of mixing time. Another microemulsion extraction experiment was done with cobalt (Co^{2+}), strontium (Sr^{2+}), and lanthanides (La^{3+} and Eu^{3+}) spiked on a lab coat sample. Blank extraction under the same conditions was also tested, which indicated that the system background was below the detection limits. In the presence of the water-in-CO_2 microemulsion, effective removal of these metal ions from the fabric sample was observed. The recovery of the metal ions from the microemulsion was also investigated. In this study, 30 μg of each element were spiked on the lab coat. The system was stirred for 1.5 h for microemulsion formation and extraction. After that, the system was flushed with CO_2 at 40 °C and 200 atm overnight, which usually consumed ~180 mL of CO_2. The flow rate was controlled at ~0.4 mL/min, and a heating gun was used to keep the outlet valve and restrictor warm during the entire dynamic flush. The results given in Table 5 suggested that satisfactory metal ions recovery from the microemulsion system could be achieved using a long dynamic flushing.

Experiments were also performed using conventional water and detergent washing of the same lab coat samples (0.6 × 4 cm^2 size) spiked with the metal ions as described in the SC-CO_2 experiments. The sample was submerged in 5 mL of tap water placed in a vial (2.3-cm i.d. and 9.5 cm high with a cap) with a small amount of detergent (Liqui-Nox 0.3 mL). This volume of water was necessary for effective agitation of the sample using a magnetic stirrer. The washing time was 30 min. After that, the sample was rinsed 3 times with water (3 min of stirring each time). The total volume of the wastewater generated in the washing procedure was

~20 mL. After the washing, the cobalt remaining in the fabric was found to be 8 and 11% of the amount initially spiked on the sample based on duplicate experiments. The efficiency of conventional laundry is similar to the water-in-CO_2 microemulsion extraction, but the amount of wastewater generated in the former case is 2 orders of magnitude greater. Low levels of radioisotopes in diluted aqueous solutions are usually removed by adsorption, coprecipitation, or solvent extraction and concentrated in a small volume for their final disposal. Nuclear laundry using supercritical fluid solutions can greatly simplify the wastewater treatment procedure. Methods for disposal of radioactive wastes are known in the literature.[25]

Conclusion

This study has demonstrated that cobalt (Co^{2+}) and other metal ions spiked on a lab coat can be removed satisfactorily by a mixture of Cyanex 302 and dithiocarbamate, as well as by a water-in-CO_2 microemulsion. The efficiency of removing metal ions using either method is greater than 90%. It should be pointed out that, when treating ^{60}Co-contaminated samples, the mass of the radioisotope involved is actually extremely small. Assuming each lab coat contains a total of 1×10^5 Bq, the total mass of the isotope is only $\sim 7.6 \times 10^{-12}$ mol. The cobalt concentrations tested in this study should be sufficient for treating real ^{60}Co-contaminated protective coats. The microemulsion approach described in this paper does not need chelating agents. However, fluorinated surfactants required for the microemulsion formation are expensive. If inexpensive and effective surfactants for water-in-CO_2 microemulsion formation could be developed in the future, the microemulsion approach would be attractive for nuclear laundry applications. Synergistic extraction using Cyanex 302 and NaDDC is interesting for SFE of metal species. This mixed-ligand approach suggests that effective metal extractants can be developed using two ligands, one contributing to solubility and the other to stability of the resulting metal chelates in SC-CO_2. Using this approach, synthesis of stable CO_2-philic ligands such as fluorinated ligands may not be necessary. The discussion presented in this paper was based on the results obtained from lab coat samples spiked with cobalt and other metal ions. Different chemical forms of metal species may exist in real contaminated protective coats that might require additional reagents or pretreatment steps for effective SC-CO_2 extraction. Research along these directions is currently in progress.

Acknowledgment

This work was supported by DOE Office of Environmental Management, EMSP Program (Grant DE-FG07-98ER14913) and by Idaho NSF-EPSCoR Program. M.K. was on leave from Nuclear Engineering Department, Kyung-Hee University, South Korea.

Literature Cited

(1) Laintz, K. E.; Wai, C. M.; Yonker, C. R.; Smith, R. D. Solubility of Fluorinated Metal Dithiocarbamates in Supercritical Carbon Dioxide. *J. Supercrit. Fluids* **1991**, *4*, 194.

(2) Laintz, K. E.; Wai, C. M.; Yonker, C. R.; Smith, R. D. Extraction of Metal Ions from Liquid and Solid Materials by Supercritical Carbon Dioxide. *Anal. Chem.* **1992**, *64*, 2875.

(3) Lin, Y.; Wai, C. M. Supercritical Fluid Extraction of Lanthanides with Fluorinated β-Diketones and Tributyl Phosphate. *Anal. Chem.* **1994**, *66*, 1971.

(4) Yazdi, A.; Beckman, E. Design of Highly CO_2-Soluble Chelating Agents for Carbon Dioxide Extraction of Heavy Metals. *J. Mater. Res.* **1995**, *10* (3), 530.

(5) Yates, M. Z.; Apodaca, D. L.; Campbell, M. L.; Birnbaum, E. R.; Mecleskey, T. M. Metal Extractions Using Water in Carbon Dioxide Microemulsions. *Chem. Commun.* **2001**, 25.

(6) Laintz, K. E.; Tachikawa, E. Extraction of Lanthanides from Acidic Solution Using Tributyl Phosphate Modified Supercritical Carbon Dioxide. *Anal. Chem.* **1994**, *66*, 2190.

(7) Wang, J.; Marshall, W. D. Metal Separation by Supercritical Fluid Extraction with On-Line Detection by Atomic Absorption Spectrometry. *Anal. Chem.* **1994**, *66*, 3900.

(8) Wang, J.; Marshall W. D. Recovery of Metals from Aqueous Media by Extraction with Supercritical Carbon Dioxide. *Anal. Chem.* **1994**, *66*, 1658.

(9) Wai, C. M.; Wang, S. Separation of Metal Chelates and Organometallic Compounds by SFC and SFE/GC. *J. Biochem. Biophys. Methods* **2000**, *43*, 273.

(10) Lin, Y.; Smart, N. G.; Wai, C. M. Supercritical Fluid Extraction of Uranium and Thorium from Nitric Acid Solutions with Organophosphorus Reagents. *Environ. Sci. Technol.* **1995**, *29*, 2706.

(11) Lin, Y.; Smart, N. G.; Wai, C. M. Supercritical Fluid Extraction and Chromatography of Metal Chelates and Organometallic Compounds. *Trends Anal. Chem.* **1995**, *14*, 123.

(12) Smart, N. G.; Carleson, T. E.; Elshani, S.; Wang S.; Wai, C. M. Extraction of Toxic Heavy Metals Using Supercritical Fluid Carbon Dioxide Containing Organophosphorus Reagents. *Ind. Eng. Chem. Res.* **1997**, *36*, 1819.

(13) Radiation Safety Requirements for Radionuclide Laboratories, Guide 6.1, July, http://www. stuk.fi/saannosto/st6_1e.pdf.

(14) Hunt, F.; Ohde, H.; Wai, C. M. A High-Pressure Fiber-Optic Reactor with CCD Array UV−Vis Spectrometer for Monitoring Chemical Processes in Supercritical Fluids. *Rev. Sci. Instrum.* **1999**, *70 (12)*, 4661.

(15) Ohde, H.; Wai, C. M.; Kim, H.; Kim, J.; Ohde, M. Hydrogenation of Olefins in Supercritical CO_2 Catalyzed by Palladium Nanoparticles in a Water-in-CO_2 Microemulsion. *J. Am. Chem. Soc.* **2002**, *124*, 4540.

(16) Wai, C. M.; Wang, S.; Yu, J. J. Solubility Parameters and Solubilities of Metal Diothiocarbamates in Supercritical Carbon Dioxide. *Anal. Chem.* **1996**, *68*, 3516.

(17) Laintz, K. E.; Yu, J. J.; Wai, C. M. Separation of Metal Ions with Sodium Bis(trifluoroethyl)dithiocarbamate Chelation and Supercritical Fluid Chromatography. *Anal. Chem.* **1992**, *64*, 311.

(18) Wai, C. M. Preconcentration of Trace Elements by Solvent Extraction. In *Preconcentration Techniques for Trace Elements*; CRC Press: Boca Raton, FL, 1991; Chapter 4, pp 111−119.

(19) Wai, C. M.; Wang, S.; Liu, Y.; Lopez-Avila, V.; Beckert, W. F. Evaluation of Dithiocarbamates and β-diketones as Chelating Agents in Supercritical Fluid Extraction of Cd, Pb, and Hg from Solid Samples. *Talanta* **1996**, *43*, 2083.

(20) Almela, A.; Elizalde, M. P. Correlation of the Extraction Constants of the System Cd(II)-H_3PO_4/Cyanex 302-Kerosene at Different Ionic Strengths, *Fluid Phase Equilib.* **1998**, *153*, 243.

(21) Menoyo, B.; Elizalde, M. P. Extraction of Cobalt (II) by Cyanex 302. *Solvent Extr. Ion Exch.* **1997**, *5(1)*, 97.

(22) Bartscherer, K. A.; Minier, M.; Renon, H. Microemulsion in Compressible Fluids: a Review. *Fluid Phase Equilib.* **1995**, *107*, 93.

(23) Gale, R. W.; Fulton, J. L.; Smith, R. D. Organized Molecular Assemblies in the Gas Phase: Reverse Micelles and Microemulsions in Supercritical Fluids. *J. Am. Chem. Soc.* **1987**, *109*, 920.

(24) Ji, M.; Chen, X.; Wai, C. M.; Fulton, J. L. Synthesizing and Dispersing Silver Nanoparticles in a Water-in-Supercritical Carbon Dioxide Microemulsion. *J. Am. Chem. Soc.* **1999**, *121*, 2631.

(25) Oh, C. H., Ed. *Hazardous and Radioactive Waste Treatment Technologies Handbook*; CRC Press: Boca Raton, FL, 2001.

Received for review June 18, 2003
Revised manuscript received January 20, 2004
Accepted January 20, 2004

IE030509D

Partition Coefficients and Equilibrium Constants of Crown Ethers between Water and Organic Solvents Determined by Proton Nuclear Magnetic Resonance

Han-Wen Cheng, Anne Rustenholtz, Richard A. Porter, Xiang R. Ye, and Chien M. Wai*

Department of Chemistry, University of Idaho, Moscow, Idaho 83844-2343

The extraction of water by several crown ethers into chloroform + carbon tetrachloride mixtures has been investigated using a proton NMR technique. The equilibrium is well described by formation of a 1:1 water−crown complex in rapid exchange with uncomplexed ligand and water. The fraction (k) of crown ether complexed with water increases with crown cavity size, varying from (15 ±1)% for 12-crown-4 to (97 ± 5)% for 18-crown-6. Addition of carbon tetrachloride to chloroform lowers the k value for all crown ethers in equilibrium with water, and the value is close to zero in pure CCl_4. The partition coefficient follows the opposite trend: the amount of crown ether in the organic phase increases with the percentage of CCl_4 in this phase. The chemical shifts of free and complexed water also vary with solvent composition. Interaction of water with crown ether depends on solvation environment and may play a significant role in liquid−liquid extraction of metal ions using macrocyclic polyethers as extractants.

Introduction

Solvent extraction processes for the removal or separation of metal ions from aqueous solutions have been extensively studied using a variety of acidic, anionic, or neutral extractants.[1−6] Macrocyclic compounds, such as crown ethers and calixarene-crowns, are excellent neutral extractants with high efficiency and selectivity for a number of metal cations, including the alkali metal ions.[1,7−9] We are interested in the equilibria involved in the extraction of cesium ions from aqueous solution into a supercritical CO_2 phase, using crown ethers and calixarene-crowns. As part of this project, we are studying extraction of cesium salts into solvents of low dielectric constant, with solubility parameters in the range of possible solubility parameters for supercritical CO_2.[3] The equilibria of cesium salts with the above ligands have been studied extensively in organic solvents, usually with relatively high relative permittivity (>10).[10] In these studies, the specific role of the water which is dissolved in the organic solvents is generally not discussed in detail. In one study, it was noted that the description of the resulting equilibria must take into account the fact that the organic phase is saturated with water.[11] In a second study, it was found that the extraction efficiency of alkali metal ions increases with the solubility of water in the organic phase.[12] This is ascribed to increased solubility of the counteranion in the water-saturated organic phase. In another study,[13] the equilibrium constant between water and 18-crown-6 (18C6) has been determined in CCl_4 by FTIR. The effects of solvent polarity or crown ether cavity size have not been discussed. Neither was the partition coefficient.

For organic solvents with a high relative permittivity, equilibration of the solvent with water yields a water concentration in the solvent which is high compared to the typical concentrations of the extracting agents and the extracted ions. Therefore, the water concentration is relatively independent of the concentrations of these other components. By contrast, the solubility of water in chloroform (relative permittivity 4.8 at 20 °C) is about 0.06 $mol \cdot L^{-1}$ at normal ambient temperature, which is more comparable to the concentrations of other species extracted from a water phase. Water solubility varies from 0.02 to 0.2 $mol \cdot L^{-1}$ in supercritical CO_2, depending on the temperature and the pressure applied.

Proton nuclear magnetic resonance (NMR) is a very precise analytical technique for measuring the amount and chemical environment of water in organic solvents. Early NMR studies by de Jong et al.[14] and Golovkova et al.[15] have shown that various crown ethers interact with water to form 1:1 complexes in $CHCl_3$. An IR study by Moyer et al. has likewise demonstrated formation of a 1:1 water−crown ether complex in CCl_4.[13] A compilation of data for complexes of crown ethers with neutral molecules has been carried out by Izatt et al.[16]

The purpose of this paper is to determine the influence of solvent (mixtures of $CHCl_3$ and CCl_4) on those interactions using NMR techniques. These solvent mixtures cover a wide range of solvent parameters which are comparable to those of liquid and supercritical CO_2 at different densities. Some of the crown ethers used in this study are appreciably soluble in water, leading to their partitioning between the water and organic phases. NMR measurements also enable us to obtain partition coefficients of crown ethers between water and organic phases.

Experimental Section

The crown ethers dibenzyl-24-crown-8 (DB24C8), dicyclohexano-24-crown-8 (DCH24C8), dicyclohexano-18-crown-6 (DCH18C6), 12-crown-4 (12C4), 15-crown-5 (15C5), and 18-crown-6 (18C6) were purchased from Aldrich Chemical Co. and used without further purification. To carry out the NMR measurement, chloroform was used in its deuterated form (99.5% $CDCl_3$). The water phase contained 5% D_2O by volume.

Solutions of the crown ethers, in the concentration range (0.02 to 0.2) $mol \cdot L^{-1}$, in the $CDCl_3$ + CCl_4 mixtures were

* E-mail: cwai@uidaho.edu.

10.1021/je034195c CCC: $27.50
Published on Web 00/00/0000 PAGE EST: 4.8

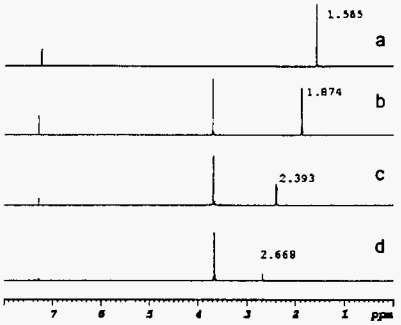

Figure 1. Typical NMR spectra of 18-crown-6 in the $CDCl_3$ phase. The concentrations of 18-crown-6 after equilibration with water are 0.00 M, 0.002 M, 0.075 M, and 0.153 M (from top to bottom) for the water peaks at (1.565, 1.874, 2.393, and 2.668) ppm, respectively.

equilibrated with an equal volume of the D_2O-enriched water by shaking with a wrist-type shaker for 2 h or more. The mixtures were then centrifuged for 1 h. The studies involving 15C5, 18C6, and DCH18C6 in solvents containing high percentages of CCl_4 required longer shaking time to get consistent data. Several shaking times (from 2 h to 24 h) were tested; after 12 h no change was observed. These procedures were conducted at ambient temperatures which were within the range (25 ± 1) °C.

NMR measurements for the solvent experiments were carried out using a 500 MHz Bruker DRX500 spectrometer. To obtain quantitative results, the pulse interval was set to 11.3 s (acquisition time 3.3 s, relaxation delay 8 s) and the pulse width was 30° (corresponding to a 2 μs relation time) in all systems (organic, aqueous, with or without chelator agent). Chemical shifts in the organic phase were calibrated by setting the chloroform chemical shift to 7.24 ppm. For the solvent mixtures containing CCl_4, the chloroform resonance shifts upfield (lower ppm) as CCl_4 is added. The magnitude of this effect was measured by comparing the solvent mixtures at constant field, that is, with the field lock turned off. The shift between 100% $CHCl_3$ and 25% $CHCl_3$ was 0.14 ppm. Therefore, an upfield correction was added for the mixed solvent samples run with a $CDCl_3$ field lock. The intensity (based on integrated area calculations for all data) of the water peaks in the NMR spectra was corrected for the 5% D_2O (by volume) present in the water phase. For the 100% CCl_4 mixture, an insert filled up with benzene-d_6 has been used as a reference for the intensity and the chemical shift, which was set at 7.15 ppm.

Typical NMR spectra for 18C6 in the $CDCl_3$ phase are shown in Figure 1. For the unsubstituted crown ethers, there is only a single resonance for the ring protons, generally in the region between (3 and 4) ppm. A singlet resonance for water appears at a chemical shift which moves downfield as the ligand concentration is increased. As noted above, the observed water and ligand resonances are averages which result from the rapid equilibrium between uncomplexed ligand and water and the complex $L{\cdot}H_2O_{(org)}$. Figure 1 shows the trend of the chemical shift for the water resonance associated with 18C6 concentration in $CDCl_3$. The concentration of the ligand in the organic phase has been corrected for its solubility in the aqueous phase on the basis of NMR measurements of its partition between the two phases.

The purities of the substituted crown ethers were assessed by determining the relative areas of the various resonances of the crown ethers, under conditions such that there is no overlap with the water peak. The ratios agreed with the theoretical values to better than 1%. All spectra were relatively free of artifacts, indicating a purity of crown ethers of 99% or better.

Calculations

The equilibrium model for the extraction is straightforward. Representing the crown ether ligand by L and the organic phase by (org), we have

$$H_2O_{(aq)} \rightleftharpoons H_2O_{(org)} \quad (1)$$

$$L_{(aq)} \rightleftharpoons L_{(org)} \quad (2)$$

$$H_2O_{(org)} + L_{(org)} \rightleftharpoons L{\cdot}H_2O_{(org)} \quad (3)$$

where $L{\cdot}H_2O_{(org)}$ represents a ligand–water complex. We define

$$K = [L{\cdot}H_2O_{(org)}]/\{[L_{(org)}][H_2O_{(org)}]\} \quad (4)$$

to be the equilibrium constant corresponding to eq 3 on the basis of concentrations ([ ], in $mol{\cdot}L^{-1}$). Because of equilibrium 1, the concentration $[H_2O_{(org)}]$ is independent of the ligand concentration. Therefore, the ratio $[L{\cdot}H_2O_{(org)}]/[L_{(org)}]$ is independent of the ligand concentration. Likewise, k, the fraction of ligand molecules complexed to water as defined in eq 5 is independent of the ligand concentration.

$$k = [L{\cdot}H_2O_{(org)}]/\{[L_{(org)}] + [L{\cdot}H_2O_{(org)}]\} \quad (5)$$

When $[L{\cdot}H_2O_{(org)}]$ is expressed in terms of $K[L_{(org)}][H_2O_{(org)}]$, the constant k is related to K by

$$k = K[H_2O_{(org)}]/\{1 + K[H_2O_{(org)}]\} \quad (6)$$

The initial total ligand concentration $[L_{(init)}]^\circ$ is calculated from the total mass of ligand dissolved in a known volume of the organic phase during the preparation of the solutions. By material balance, at equilibrium

$$[L_{init}]^\circ = [L_{(aq)}] + [L_{(org)}] + [L{\cdot}H_2O_{(org)}] \quad (7)$$

For the crown ethers containing additional organic groups (benzyl and cyclohexyl), the term $[L_{(aq)}]$, representing extraction of the ligand into the aqueous phase, is negligible. Because of the rapid exchange of complexed and uncomplexed water in the organic phase, only the totals

$$[L_{(org)}]^\circ = [L_{(org)}] + [L{\cdot}H_2O_{(org)}] \quad (8)$$

and

$$[H_2O_{(org)}]^\circ = [H_2O_{(org)}] + [L{\cdot}H_2O_{(org)}] \quad (9)$$

can be measured directly, where $[H_2O_{(org)}]^\circ$ and $[L_{(org)}]^\circ$ are the total concentrations of water (uncomplexed and complexed water) and ligand (free and complexed ligand) present in the organic phase, respectively.

When the material balance relations (eqs 8 and 9) are combined with eq 5, the linear relation

$$[H_2O_{(org)}]^\circ = k[L_{(org)}]^\circ + [H_2O_{(org)}] \quad (10)$$

can be derived. According to eq 10, a plot of $[H_2O_{(org)}]^\circ$ versus $[L_{(org)}]^\circ$ should yield a straight line and the slope gives the value k. From k and $[H_2O_{(org)}]$, the equilibrium constant K can be obtained from eq 6.

As noted above, the equilibrium between $H_2O_{(org)}$ and $L{\cdot}H_2O_{(org)}$ determines the observed NMR chemical shift δ of

Table 1. Equilibrium and Chemical Shift Parameters of Various Crown Ethers[a]

crown	% vol $CDCl_3$[b]	k	K (L·mol^{-1})	$[H_2O]_{org}$[c]	D	δ_0/ppm	δ_1/ppm
12C4	100	0.15	2.78	0.065	0.25	1.55	3.0
	75	0.10	2.79	0.039	0.34	1.43	3.0
15C5	100	0.54	25.6	0.045	0.18	1.49	2.8
	75	0.35	19.9	0.027	0.29	1.40	2.7
	50	0.25	14.2	0.024	0.71	1.29	2.8
	25	0.21	35	0.008	2.13	1.11	2.0
	0			0.00[d]	2.450	1.36	
18C6	100	0.97	545	0.060	0.25	1.52	3.1
	75	0.79	102	0.037	0.42	1.40	2.8
	50	0.63	97	0.017	1.16	1.28	2.6
	25	0.61	141	0.011	3.83	1.08	2.2
	0			0.00[d]	48.04	1.31	
DCH18C6	100	0.70	32	0.072	0.00	1.52	3.3
	50	0.58	81	0.017	0.00[d]	1.25	2.6
	25	0.40	36	0.018	0.00[d]	1.13	2.6
DCH24C8	100	0.850	93	0.060	0.00[d]	1.57	3.2
DB24C8	100	0.37	9.03	0.064	0.00[d]	1.57	2.7

[a] Typical statistical errors (based on linear regressions): k, ±5%; K, ±10%; $[H_2O]_{org}$, ±0.003 mol·L^{-1}; D, ±5%; δ_0, ±0.04 ppm; δ_1, ±0.3 ppm. [b] Volume percentage of $CDCl_3$ in CCl_4. [c] Concentration in moles per liter. [d] <0.01 for the ligand concentration range 0.02–0.2 mol·L^{-1}.

water in chloroform. Denoting δ_0 = the chemical shift of pure water in the organic solvent and δ_1 = the chemical shift of complexed water, we have

$$(\delta - \delta_0)/(\delta_1 - \delta_0) = [L{\cdot}H_2O_{(org)}]/[H_2O_{(org)}]^\circ \quad (11)$$

Combining eq 11 with eqs 6 and 8 and rearranging produces the linear relation between δ and $[L_{(org)}]^\circ/[H_2O_{(org)}]^\circ$

$$\delta = \delta_0 + k(\delta_1 - \delta_0)[L_{(org)}]^\circ/[H_2O_{(org)}]^\circ \quad (12)$$

According to eq 12, δ_0 and δ_1 can be determined by linear regression once k is known.

The NMR data required for obtaining equilibrium (k and K) and chemical shift parameters (δ_0 and δ_1) are the intensities of the water and the ligand peaks ($[H_2O_{(org)}]^\circ$ and $[L_{(org)}]^\circ$) and the chemical shift (δ) of the water peak in the organic phase. For the NMR intensity measurements, the water peak in the aqueous phase or the $CHCl_3$ peak in the organic phase can be used as the reference. At 25 °C, the density of water is known and the concentration of 95% water by volume is 52.8 mol·L^{-1}. Using the $CHCl_3$ peak as the reference, the amount of $CHCl_3$ in $CDCl_3$ must be known. The results represented in Table 1 were obtained using the water peak as the reference. A few experiments were done by adding a known amount of $CHCl_3$ to $CDCl_3$ as the reference. The results are consistent with those obtained using the water peak as the reference within the experimental uncertainty. The intensities of the ligand peaks in the aqueous phase were also measured to evaluate their partition coefficients (D) and for correction of ligand concentrations in the organic phase.

It should be noted that eq 12 differs from the classic complex equilibrium equations derived from the work of Benesi and Hildebrand[20] and Deranleau,[21] which are derived for a single-phase system containing two interacting components. As pointed out in the Calculations section, because of equilibrium 1, $[H_2O_{(org)}]$ is constant. As an incidental consequence, $[H_2O_{(org)}]^\circ$ cannot go to zero. This enables an extrapolation of eq 12 to zero ligand concentration to get the value of δ_0. Also, two separate quantities $[H_2O_{(org)}]^\circ$ and $[L_{(org)}]^\circ$ appear which vary together, since increasing $[H_2O_{(org)}]^\circ$ increases $[L_{(org)}]^\circ$. Unlike the case in the previous work, none of the individual species can be measured.

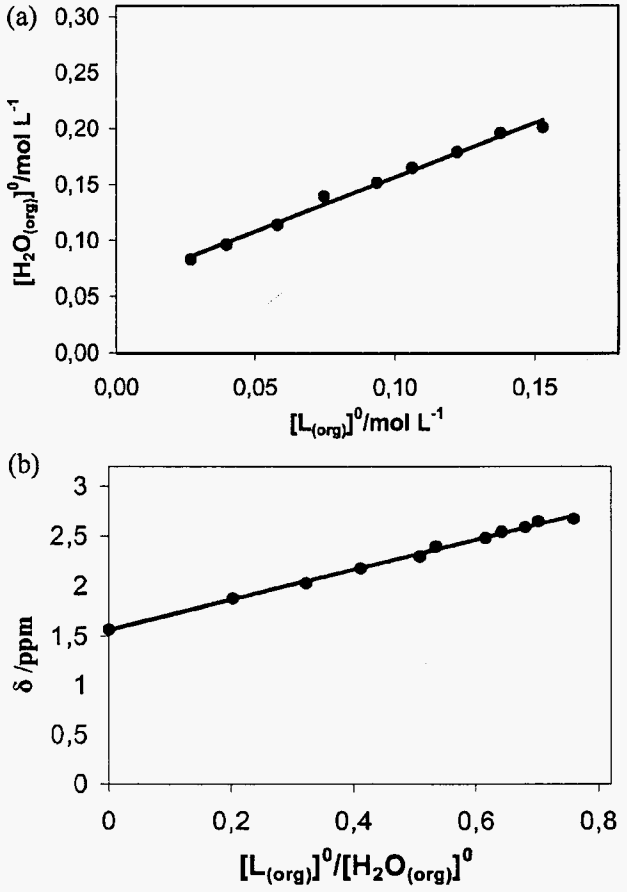

Figure 2. Linear relationship between (a) the total water and 18-crown-6 concentrations in chloroform ($[H_2O_{(org)}]^\circ$ = 0.9704-$[L_{(org)}]^\circ$ + 0.0601; correlation coefficient r = 0.9955) and between (b) the observed chemical shift of water and the ratio $[L_{(org)}]^\circ/[H_2O_{(org)}]^\circ$ in chloroform (eq 7) (δ = 1.5015$[L_{(org)}]^\circ/[H_2O_{(org)}]^\circ$ + 1.5611; r = 0.9982).

Results and Discussion

Parts a and b of Figure 2 show plots based on eqs 10 and 12, respectively, for 18C6 in $CDCl_3$. Results for the other ligands are similar. The linear relations obtained in every case verify that the water–ligand equilibrium is well described by formation of a 1:1 complex. Figure 2a yields a slope of 0.970 ± 0.04 (corresponding to k) and an intercept

of 0.060 ± 0.003 (corresponding to $[H_2O]_{org}$) based on our regression analysis (R^2 = 0.991) and according to eq 10. The free (uncomplexed) water dissolved in chloroform is about 0.06 mol·L^{-1} for the H_2O + $CDCl_3$ + 18C6 system at room temperature (25 ± 1) °C. This value is confirmed by the analysis of a solution of water saturated chloroform-*d*. The concentration of the total water in the organic phase, $[H_2O]_{org} + L\cdot[H_2O]_{org}$, depends on the ligand concentration as shown in Figure 2a. About 97% of the ligands in the organic phase are complexed with water. The intercept of Figure 2b gives the chemical shift of uncomplexed water in chloroform δ_0 = (1.56 ± 0.02) ppm. From the slope of Figure 2b, the chemical shift of the water complexed with 18C6 in $CDCl_3$, δ_1, was calculated to be (3.1 ± 0.3) ppm.

Results for the equilibrium and NMR chemical shift parameters for the six crown ethers studied by this work are summarized in Table 1. In $CDCl_3$, the k values for unsubstituted crown ethers 12C4, 15C5, and 18C6 are 0.15, 0.54, and 0.97, respectively. This trend shows strong binding of water for 18C6 relative to the smaller rings. Substitution in crown ethers tends to lower the k value. Thus, for DCH18C6, the k value in chloroform is lowered to 0.70 compared with a value of 0.97 for the unsubstituted 18C6. In the case of DCH24C8 and DB24C8, benzyl substitution further lowers the k value compared with cyclohexyl substitution in 24C8. The equilibrium constant (K) defined by eq 4 varies from 2.78 for 12C4 to 545 for 18C6 in chloroform. The K value for the substituted (DCH18C6) crown is much lower than that of the unsubstituted (18C6) one (32 versus 545). The δ_0 values for the three unsubstituted crown ethers are approximately constant (in the range 1.53 ± 0.04 ppm), as expected. Considering the experimental error, the δ_1 value is stable.

For the individual ligands, there are several clear trends with respect to the variation of solvent composition ($CDCl_3$ + CCl_4). First, the amount of free water dissolved in the organic phase decreases with increasing CCl_4 fraction in the solvent. This is expected, since decreasing the solvent polarity should result in lower solubility of water in the organic phase. In all cases, the parameter k representing the fraction of ligand bound to water also decreases monotonically as the proportion of CCl_4 increases. Thus, decreasing solvent polarity also reduces water–crown complexation $[L\cdot H_2O_{(org)}]$, leading to lower k values. This is probably caused by the combination of a lower solubility of free water in the organic phase and intrinsic solvation effects on the crown–water complex. The equilibrium constant K, which includes the concentration of unbound water and the ligand in the mixed organic phase, changes less and in an irregular fashion. Because both $[H_2O]_{org}$ and $[L]_{org}$ vary drastically with the solvent composition, the K values defined by eq 4 are not as useful as the k values for discussion in the $CHCl_3$ + CCl_4 system. In the binary solvent systems, $[H_2O]_{org}$ decreases with increasing CCl_4 fraction whereas $[L]_{org}$ changes independently in the opposite direction, resulting in irregular trends for the K values.

From the crown ether NMR peak intensities in the organic and in the aqueous phases, we also calculated the partition coefficients $D = [L_{(aq)}]^\circ/[L_{(org)}]^\circ$ as shown in Table 1. The D values for 12C4 and 18C6 between water and chloroform are around 0.25, and that for 15C5 is somewhat lower. For the crown ethers that are appreciably soluble in water, the partition coefficients show that extraction into the aqueous phase increases exponentially as the organic solvent polarity decreases. In the case of 18C6, the D value starts at 0.25 in 100% $CHCl_3$, becomes 1.16 with a 50:50 mixture of $CHCl_3$ and CCl_4, and rises up to 48 for a 100% CCl_4 solution (Figure 3). For the substituted crown ethers DCH18C6, DCH24C8, and DB24C8, the D values are below detection (<0.01) in the concentration range (0.06 to 0.2) mol·L^{-1}. Partitioning of 18-crown-6 between water and various organic solvents has been determined by several different methods including gravimetric and conductivity measurements.[17–19] NMR actually provides a simple and rapid method for determination of crown ether partition coefficients between water and organic solvents. The D values given in Table 1 represent the first systematic measurements of such data using a NMR technique.

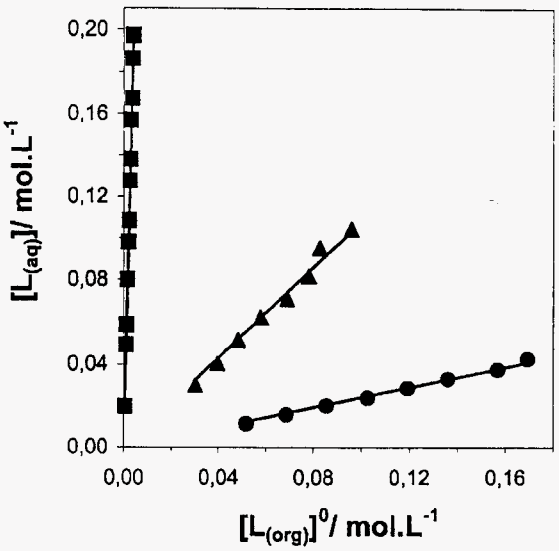

Figure 3. Determination of the partition coefficient for 18-crown-6 in (●) $CDCl_3$, (▲) 50% $CDCl_3$ + CCl_4, and (■) CCl_4.

The NMR studies performed by Golovkova et al.[15] in $CDCl_3$ investigated several compounds also covered in our work (15C5, 18C6, and DCH18C6). In their work, single-phase measurements were made with a constant water concentration and varying ligand concentrations. Analysis was based on the chemical shift employing eq 11. The chemical shift δ_1 for the pure complex $L\cdot H_2O$ was determined by extrapolation to infinite ligand concentration. Their results for K deviate widely from ours, sometimes by an order of magnitude. We feel that their extrapolation method is subject to considerable error because (1) the dependence of the chemical shift on ligand concentration is nonlinear and, (2) on the basis of the δ_1 values we obtained, the range of concentrations they employed was insufficient. Our calculational method involved only the use of linear regression analysis; thus, it is more accurate.

The chemical shifts δ_0, representing isolated water molecules in the organic solvent, can be measured by equilibrating the organic solvent with pure water. For 18C6, the δ_0 values decrease from 1.56 ppm in pure chloroform to 1.08 ppm in the $CHCl_3$ + CCl_4 mixture with 25% $CHCl_3$ by volume. Similar trends are observed for the other crown ether systems. For 15C5 and DCH18C6, the δ_0 values decrease, respectively, from 1.49 ppm to 1.52 ppm in pure chloroform and from 1.11 ppm to 1.08 ppm in the $CHCl_3$ + CCl_4 mixture with 25% $CHCl_3$ by volume. Those results follow the general trend of an upfield shift for water in solvents of decreasing polarity. The values of δ_0 and δ_1 in Table 1 were found using a linear regression plot of δ versus $[L_{(org)}]^\circ/[H_2O_{(org)}]^\circ$ according to eq 12 and using the k values predetermined. Those results agree well with preceding measurements involving no crown ethers.

δ_1 represents the chemical shift of water in the crown–water complex. The error on δ_1 values includes the error on k; therefore, the δ_1 value is less accurate than the δ_0 one. In the 18C6 series, δ_1 decreases monotonically with decreasing solvent polarity from 3.1 ppm in pure chloroform to 2.2 ppm in the $CHCl_3 + CCl_4$ mixture with 25% $CHCl_3$ by volume. The trends of δ_1 for the other crown ethers are less clear. Generally, there is an upfield shift as the solvent polarity decreases. This does not seem obvious, however, for the weakly binding ligands 12C4 and 15C5.

Complexation of water with crown ether depends strongly on the nature of the solvents. The difference in solvation environment of chloroform and carbon tetrachloride is reflected in the degree of crown–water complexation and the chemical shifts of free water and the crown–water complex described in this NMR study. Interaction between water and crown ether is likely to affect complex formation of the crown ether with metal ions during liquid–liquid extraction. Crown ethers have been extensively investigated for selective extraction of the alkali metal and the alkaline earth metal ions from aqueous solutions. The solvation effects of water and solvent molecules on metal–crown complexation are not well understood. NMR studies may provide very useful information for understanding such interactions. Solvation effects can be studied using different conventional solvents. Conventional solvents offer discontinued changes in solvation environment and often involve other variables that are difficult to control experimentally. Further studies of water–crown interactions in a system with a tunable solvation environment, supercritical fluid carbon dioxide, are currently in progress in our laboratory.

Literature Cited

(1) Izatt, R. M.; Pawlak, K.; Bradshaw, J. S. Thermodynamic and Kinetic Data for Macrocycle Interaction with Cations and Anions. *Chem. Rev.* **1991**, *91*, 1721–2085.

(2) Dietz, M. L.; Bond, A. H.; Hay, B. P.; Chiarizia, R.; Huber, V. J.; Herlinger, A. W. Ligand Reorganization Energies as a Basis for the Design of Synergistic Metal Ion Extraction Systems. *Chem. Commun.* **1999**, *13*, 1177–78.

(3) Phelps, C. L.; Smart, N. G.; Wai, C. M. Past, Present, and Possible Future Applications of Supercritical Fluid Extraction Technology. *J. Chem. Educ.* **1996**, *12*, 1163–1168.

(4) Steed, J. W.; Junk, P. C. Stabilisation of Sodium Complexes of 18-Crown-6 by Intramolecular Hydrogen Bonding. *J. Chem. Soc., Dalton Trans.* **1999**, *13*, 2141–2146.

(5) Horwitz, E. P.; Schulz, W. W. In *Metal-Ion Separation and Preconcentration*; Bond, A. H., Dietz, M. L., Rogers, R. D., Eds.; ACS Symposium Series 716; American Chemical Society: Washington, DC; Chapter 2, pp 20–50.

(6) Yakshin, V. V.; Vilkova, O. M. Extraction of Metals from Nitrate-Chloride Mixed Solutions Using Crown Ethers. *Russ. J. Inorg. Chem.* (Engl. Transl.) **1998**, *43* (10), 1629–1632; *Zh. Neorg. Khim.* **1998**, *43* (10), 1753–1755.

(7) Muzet, N.; Engler, E.; Wipff, W. Demixing of Binary Water-Chloroform Mixtures Containing Ionophoric Solutes and Ion Recognition at a Liquid–Liquid Interface: A Molecular Dynamics Study. *J. Phys. Chem. B* **1998**, *102* (52), 10772–10788.

(8) Marchand, A. P.; McKim, A. S.; Kumar, K. A. Synthesis and Alkali Metal Ppicrate Extraction Capabilities of Novel, Cage-Functionalized Diazacrown Ethers. Effects of Host Preorganization on Avidity and Selectivity Toward Alkali Metal Picrates in Solution. *Tetrahedron* **1998**, *54* (44), 13421–13426.

(9) Barakat, N.; Burgard, M.; Asfari, Z.; Vicens, J.; Montavon, G.; Duplatre, G. Solvent Extraction of Alkaline-Earth Ions by Dicarboxylated Calix[4]arenas. *Polyhedron* **1998**, *17* (20), 3649–3656.

(10) Mei, E.; Dye, J. L.; Popov, A. I. Cesium-133 Nuclear Magnetic Resonance Study of Crown and Cryptate Complexes of Cesium-(1+) Ion in Nonaqueous Solvents. *J. Am. Chem. Soc.* **1976**, *98*, 1619–20. (b) Mei, E.; Popov, A. I.; Dye, J. L. Cesium-133 Nuclear Magnetic Resonance Study of Complexation by Cryptand C222 in Various Solvents: Evidence for Exclusive and Inclusive Complexes. *J. Am. Chem. Soc.* **1977**, *99*, 6532–6536. (c) Thuéry, M. N.; Bryan, J. C.; Lamare, V.; Dozol, J. F.; Asfari, Z.; Vicens, J. Crown Ether Conformations in 1,3-Calix[4]arene bis(Crown Ethers): Crystal Structures of a Caesium Complex and Solvent Adducts and Molecular Dynamics Simulations. *J. Chem. Soc., Dalton Trans.* **1997**, *22*, 4191–4202.

(11) de Namor, A. F. D.; Yelarde, F. J. S.; Casal, A. R.; Pugliese, A.; Goitia, M. T.; Montero, M.; Lopez, F. F. The First Quantitative Assessment of the Individual Processes Involved in the Extraction of Alkali-Metal Picrates by Ethyl p-*tert*-Butylcalix(4)arene-tetraethanoate in the Water-Benzonitrile Solvent System. *J. Chem. Soc., Faraday Trans.* **1997**, *93* (22), 3955–3959.

(12) Dietz, M. L.; Horwitz, E. P.; Rhoads, S.; Bartsch, R. A.; Krzykawski, J. Extraction of Cesium from Acidic Nitrate Media Using Macrocyclic Polyethers: The Role of Organic Phase Water. *Solvent Extr. Ion Exch.* **1996**, *14* (1), 1–12.

(13) Bryan, S. A.; Willis, R. R.; Moyer, B. A. Hydration of 18-Crown-6 in Carbon Tetrachloride: Infrared Spectral Evidence for an Equilibrium between Monodentate and Bidentate Forms of Bound Water in the 1:1 Crown–Water Adduct. *J. Phys. Chem.* **1990**, *94*, 5230–5233.

(14) de Jong, F.; Reinhoudt, D. N.; Smit, C. J. On the Role of Water in the Complexation of Alkylammonium Salts by Crown Ethers. *Tetrahedron Lett.* **1976**, *17*, 1371–74.

(15) Golovkova, L. P.; Telyatnik, A. I.; Bidzilya, V. A. Investigation of the Interaction of Macrocyclic Polyethers with Water by PMR Spectroscopy. *Theor. Exp. Chem.* (Eng. Transl.) **1984**, *20*, 219–222; *Teor. Eksp. Khim.* **1984**, *20*, 231–234.

(16) Izatt, R. M.; Bradshaw, J. S.; Pawlak, K.; Bruening, R. L.; Tarbet, B. J. Thermodynamic and Kinetic Data for Macrocycle Interaction with Neutral Molecules. *Chem. Rev.* **1992**, *92*, 1261–1354 and further references therein.

(17) Frensdorff, H. K. Salt Complexes of Cyclic Polyethers. Distribution Equilibriums. *J. Am Chem. Soc.* **1971**, *93*, 4684–4688.

(18) Inou, Y.; Amano, F.; Okado, N.; Ouchi, M.; Tai, A.; Hakushi, T.; Liu, Y.; Tong, L. Thermodynamics of Solvent Extraction of Metal Picrates with Crown Ethers: Enthalpy–Entropy Compensation. Part 1. Stoicheiometric 1:1 Complexation. *J. Chem. Soc., Perkin Trans. 2* **1990**, *7*, 1239–1246.

(19) Kolthoff, I. M. Ionic Strength Effect on Extraction of Potassium Complexed with Crown Ether 18-Crown-6. Preliminary Communication. *Can. J. Chem.* **1981**, *59*, 1548–1551.

(20) Benesi, H. A.; Hildebrand, J. H. Conformational Analysis. XVIII. 1,3-Dithianes. Conformational Preferences of Alkyl Substituents and the Chair-Boat Energy Difference. *J. Am. Chem. Soc.* **1969**, *91*, 2703–2715.

(21) Deranleau, D. A. Theory of the Measurement of Weak Molecular Complexes. I. General Considerations. *J. Am. Chem. Soc.* **1969**, *91*, 4044–4049.

Received for review October 6, 2003. Accepted January 23, 2004. This work was supported by the DOE Office of Environmental Management, EMSP Program, under Contract Number DE-FG07-98ER14913.

JE034195C

Characterization of a Tri-*n*-butyl Phosphate−Nitric Acid Complex: a CO_2-Soluble Extractant for Dissolution of Uranium Dioxide

Youichi Enokida,[†] Osamu Tomioka,[†] Su-Chen Lee,[‡] Anne Rustenholtz,[‡] and Chien M. Wai*[,‡,§]

Research Center for Nuclear Materials Recycle, Nagoya University, Nagoya 4648603, Japan, Department of Chemistry, University of Idaho, Moscow, Idaho 83844, and Venture Business Laboratory, Nagoya University, Nagoya 4648603, Japan

Tri-*n*-butyl phosphate (TBP) reacts with nitric acid to form a hydrogen-bonded complex TBP-$(HNO_3)_x(H_2O)_y$ that is highly soluble in supercritical fluid carbon dioxide (SF-CO_2). The value of x can be up to 2.5, whereas the value of y varies between 0.4 and 0.8 determined by acid−base and Karl Fischer titrations. The protons of HNO_3 and H_2O in the complex undergo rapid exchange and exhibit a singlet resonance peak in NMR spectra. When the complex is dissolved in a low dielectric constant solvent, small droplets of nitric acid are formed that can be detected by NMR. Phase behavior studies indicate that the complex forms a single phase with SF-CO_2 above a certain pressure for a given temperature. This CO_2-soluble Lewis acid−base complex provides a method of introducing nitric acid in SF-CO_2 for effective dissolution of uranium dioxide, lanthanide oxides, and perhaps other metal oxides.

Introduction

Recent reports show that tri-*n*-butyl phosphate (TBP) forms a solution with nitric acid that is soluble in supercritical fluid carbon dioxide (SF-CO_2) and capable of dissolving lanthanide oxides and uranium oxides.[1−5] The ability of this CO_2-philic TBP−nitric acid solution to dissolve solid uranium dioxide (UO_2) directly in SF-CO_2 suggests a potential new technique for reprocessing of spent nuclear fuels and for treatment of nuclear wastes. The UO_2 dissolution process in SF-CO_2 probably involves oxidation of the tetravalent U in UO_2 to the hexavalent $(UO_2)^{2+}$ by nitric acid followed by formation of $UO_2(NO_3)_2$·2TBP.[4] The product $UO_2(NO_3)_2$·2TBP identified from the supercritical fluid dissolution process is known to have a very high solubility in CO_2.[6,7]

In the conventional Purex (plutonium−uranium extraction) process, aqueous nitric acid (3−6 M) is used to dissolve and oxidize UO_2 in the spent fuel to uranyl ions $(UO_2)^{2+}$. The acid solution is then extracted with TBP in an organic solvent such as dodecane to remove uranium as $UO_2(NO_3)_2$·2TBP into the organic phase.[8] Direct dissolution of solid UO_2 in SF-CO_2 with a TBP−nitric acid complex obviously has an advantage over the conventional Purex process because it would combine dissolution and extraction steps into one with a minimum waste generation. Demonstration of this super-DIREX process (supercritical fluid direct extraction process) is currently underway in Japan involving Mitsubichi Heavy Industries, Japan Nuclear Cycle Corp., and Nagoya University. The project is aimed at extracting uranium and plutonium from the mixed oxide fuel as well as the irradiated nuclear fuel using a TBP−nitric acid complex in SF-CO_2.

The chemical nature of the TBP−nitric acid complex and the mechanisms of UO_2 dissolution in SF-CO_2 with the TBP−nitric acid solution are not well-known. The TBP−nitric acid complex is prepared by shaking TBP with a concentrated nitric acid solution. Because water is present in the nitric acid solution, the complex is expected to have a general formula of TBP-$(HNO_3)_x(H_2O)_y$, where x and y can vary depending on the relative amounts of TBP and nitric acid used in the preparation. Two types of the complexes, one with $x = 0.7$ and the other with $x = 1.8$, were reported in the literature for direct dissolution of uranium dioxide in SF-CO_2.[3−5] In the former case with a HNO_3/TBP ratio of 0.7, the complex was found to cause cloudiness of the supercritical fluid phase, indicating formation of small acid water droplets released from the complex probably as a result of an antisolvent effect of SF-CO_2.[4]

The solubility of water in pure TBP at room temperature is about 64 g/L of the solution, which is close to a 1:1 molar ratio of TBP/H_2O. In the TBP−H_2O binary system, water is most likely bound to TBP through hydrogen bonding with phosphoryl oxygen, forming a 1:1 complex. The bonding between TBP and H_2O in the presence of HNO_3 is unknown. Recent molecular dynamics investigations suggest that hydronium ions or hydrogen from HNO_3 or H_2O are bonded to the oxygen of the P=O bond in TBP.[9,10] Knowledge on the equilibrium compositions of the TBP$(HNO_3)_x$-$(H_2O)_y$ complex prepared by different proportions of the initial TBP and nitric acid is essential for understanding the nature and mechanisms of UO_2 dissolution in SF-CO_2.

In this paper, we report our initial results of characterizing the TBP$(HNO_3)_x(H_2O)_y$ complex using several different methods including the Karl Fischer method for water determination, conventional acid−base titration for measurement of HNO_3, nuclear magnetic resonance (NMR) spectroscopy to evaluate chemical environments

* To whom correspondence should be addressed. Tel.: (208) 885-6787. Fax: (208) 885-6173. E-mail: cwai@uidaho.edu.

[†] Research Center for Nuclear Materials Recycle, Nagoya University.

[‡] University of Idaho.

[§] Venture Business Laboratory, Nagoya University.

10.1021/ie030010j CCC: $25.00
Published on Web 09/18/2003

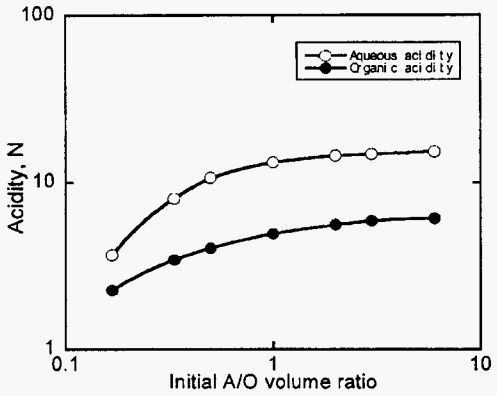

Figure 1. Acidities of the aqueous and organic phases. The *x* axis is the initial volume ratios of 15.5 M HNO_3 to 98% TBP. (○) Aqueous acidity is defined as moles of H^+ per liter of aqueous solution. (●) Organic acidity is defined as moles of H^+ per liter of organic solution.

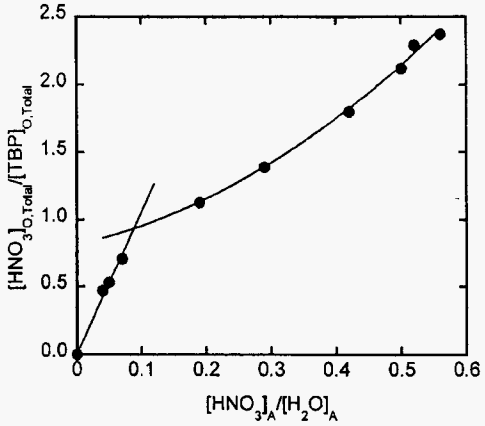

Figure 2. Plot of the $[HNO_3]/[TBP]$ ratio in the TBP phase against the $[HNO_3]/[H_2O]$ ratio in the equilibrated aqueous phase.

of protons, and visual observation of the phase behavior of the complex in SF-CO_2.

Experimental Section

TBP was purchased from Avocado (ordered through Alfa Aesar, Ward Hill, MA). Nitric acid [69.5% (w/w)] was obtained from Fisher Chemical (Fair Lawn, NJ) and was diluted to 15.5 M by deionized water. The TBP-$(HNO_3)_x(H_2O)_y$ complex was prepared by mixing 98% TBP with 15.5 M nitric acid at a chosen ratio in a glass tube with a stopper. The mixture of TBP and nitric acid was manually shaken vigorously for 4 min, followed by centrifuging for 1 h. After phase separation, portions of the TBP phase and the aqueous phase were removed with pipets for characterization experiments.

The concentration of H_2O in the TBP phase was measured by Karl Fischer titration using an Aqua-counter AQ-7 instrument (Hiranuma, Japan). The concentration of HNO_3 in the TBP phase was measured with an automatic titrator (COM-450, Hiranuma, Japan) with a 0.1 M NaOH solution after adding an excess amount of deionized water to the organic phase. A typical procedure is by shaking 1 mL of the TBP phase with 50 mL of water. After phase separation, the amount of nitric acid in the aqueous phase was determined by NaOH titration. A 500 MHz NMR spectrometer (Bruker Advance 500) was used for proton NMR (PNMR) measurements. The phase behavior was studied using a high-pressure view-cell system purchased from Taiatsu Techno Co. (Tokyo, Japan) and a video camera.

Results and Discussion

1. Characterization of the TBP$(HNO_3)_x(H_2O)_y$ Complex by Titration Methods. The amount of HNO_3 in the complex was evaluated by the acid–base titration method described in the Experimental Section. Figure 1 shows the acidity of the TBP phase (organic phase) with respect to the initial nitric acid/TBP ratio. The organic phase acidity (closed circles) and the acidity of the equilibrated aqueous phase (open circles) are shown in Figure 1. A significant fraction of the HNO_3 in the initial acid solution can be incorporated into the TBP phase, resulting in an acidity of the organic phase greater than 3 M for all of the cases shown in Figure 1. If the initial volume ratio of nitric acid/TBP is unity or higher, the acidity of the TBP phase exceeds 6 M. The high acidity carried by the TBP phase is important for dissolving uranium dioxide, lanthanide oxides, and perhaps other metal oxides in SF-CO_2.

When the molar ratio of HNO_3/TBP in the organic phase is plotted against the molar ratio of HNO_3/H_2O in the equilibrated aqueous phase, the experimental data appear to show two regions with a breaking point of around unity for the HNO_3/TBP ratio (Figure 2). The data seem to suggest that there are two types of the TBP$(HNO_3)_x(H_2O)_y$ complex. The type I complex would incorporate HNO_3 rapidly into the TBP phase until a 1:1 ratio of HNO_3/TBP is reached. Beyond that point, there is another region where incorporation of HNO_3 into TBP becomes slow. According to Figure 2, more than two molecules of HNO_3 can be associated with each TBP molecule in the complex if the organic phase is equilibriated with a concentrated nitric acid. TBP is a highly CO_2-soluble Lewis base. Inorganic acids such as nitric acid which are usually insoluble in CO_2 can be made soluble by complexation with a CO_2-soluble Lewis base such as TBP. This Lewis acid–base complex approach may provide a method of dispersing various CO_2-insoluble acids in the SF-CO_2 phase for chemical reactions.

The amount of water in the TBP$(HNO_3)_x(H_2O)_y$ complex determined by the Karl Fischer method also shows two distinct regions. When the molar ratio of HNO_3/H_2O in the TBP phase is plotted against the molar ratio of HNO_3/H_2O in the equilibrated aqueous phase, it clearly shows two different types of the TBP-$(HNO_3)_x(H_2O)_y$ complex (Figure 3). In region I, the ratio of HNO_3/H_2O in the TBP phase tends to increase with increasing HNO_3/H_2O ratio in the aqueous phase. In region II, the ratio of HNO_3/H_2O in the TBP phase maintains a constant value of about 3 with increasing HNO_3/H_2O ratio in the equilibrated aqueous phase. The ratio of HNO_3/TBP in the organic phase continues to increase with increasing HNO_3/H_2O ratio in the aqueous phase as shown in Figure 2, but the ratio of HNO_3/H_2O in the organic phase remains a constant. It appears that, for the type II complex, the nitric acid incorporated into the TBP phase is in a form with a general formula of $3HNO_3 \cdot H_2O$.

2. Characterization of the Complex by PNMR Spectroscopy. PNMR spectra of the TBP$(HNO_3)_x$-$(H_2O)_y$ complex at room temperature were taken using an insert technique. Deuterated water (D_2O) was placed

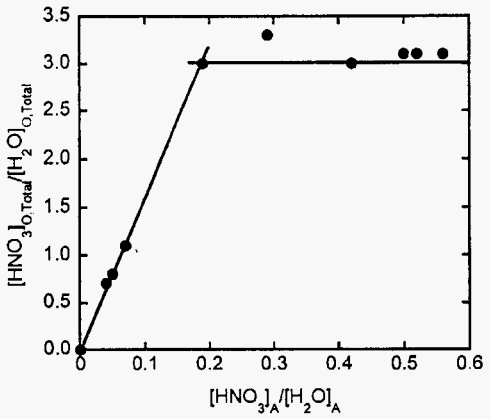

Figure 3. Molecular ratio of $[HNO_3]/[H_2O]$ in the TBP phase versus that in the equilibrated aqueous phase.

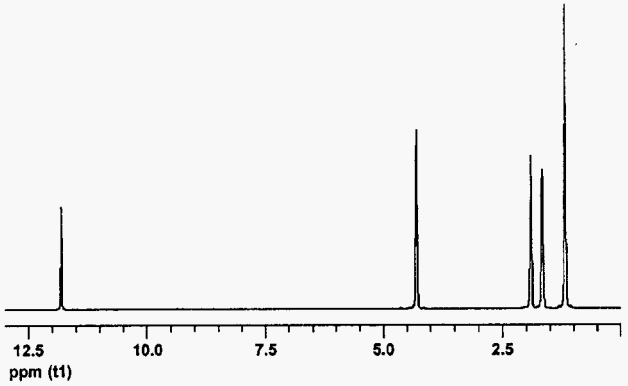

Figure 4. Typical PNMR spectrum of $TBP(HNO_3)_x(H_2O)_y$ with a D_2O insert. The sample was prepared by mixing 1.0 mL of 15.5 M HNO_3 with 4.0 mL of 98% TBP.

in an insert and fitted into an NMR tube containing a $TBP(HNO_3)_x(H_2O)_y$ solution. The purpose of the D_2O insert was to lock the NMR. A trace amount of HDO present in the deuterated water also allows calibration of the instrument. Other deuterated solvents can also be used for this insert technique. The objective of the NMR study is to investigate the chemical shift of the protons of HNO_3 and H_2O in the $TBP(HNO_3)_x(H_2O)_y$ complex as a probe for the chemical environment of the system.

A typical PNMR spectrum of $TBP(HNO_3)_x(H_2O)_y$ with a D_2O insert is shown in Figure 4. The singlet peak at 11.80 ppm corresponds to the protons of HNO_3 and water in the TBP phase. H_2O in a TBP–H_2O complex sample shows a singlet resonance peak at 3.85 ppm. In the $TBP(HNO_3)_x(H_2O)_y$ system, this singlet peak shifts upfield with increasing HNO_3 in the system. The NMR shift is attributed to a rapid exchange between the protons of H_2O and those of HNO_3 in the complex. A series of $TBP(HNO_3)_x(H_2O)_y$ samples prepared from a different volume ratio of TBP/HNO_3 (15.5 M) were studied. All NMR spectra in this series of samples showed a singlet peak for the protons corresponding to HNO_3 and H_2O. The PNMR shift of the HNO_3–H_2O singlet peak with respect to the molar ratio of HNO_3/TBP in the complex is shown in Figure 5. The chemical shift increases rapidly as the fraction of HNO_3 in the TBP phase increases in the region where the molar ratio of HNO_3/TBP is less than unity. The chemical shift of this peak approaches a constant when the HNO_3/TBP ratio in the complex is greater than 1. The two regions

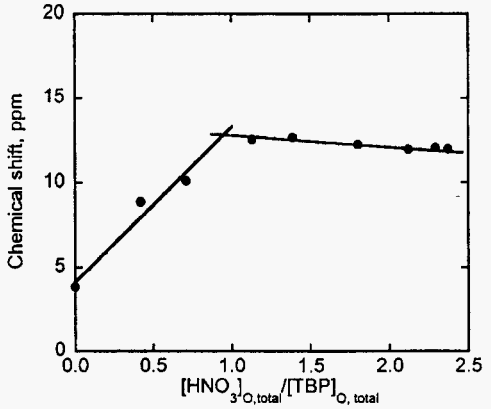

Figure 5. Chemical shift of the H_2O proton peak (in ppm) with respect to the molar ratio of HNO_3/TBP in $TBP(HNO_3)_x(H_2O)_y$.

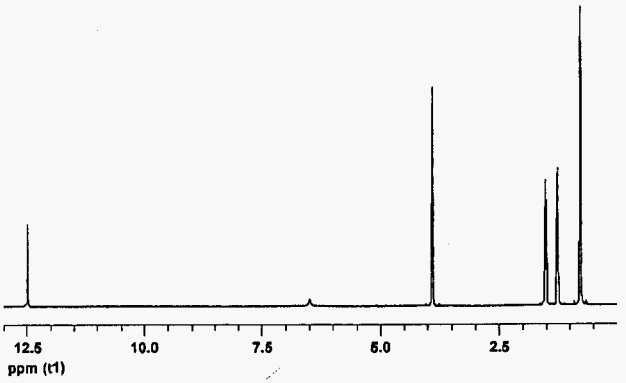

Figure 6. PNMR spectrum of $TBP(HNO_3)_x(H_2O)_y$ in $CDCl_3$. The complex was prepared by mixing 4 mL of TBP and 1 mL of 15.5 M HNO_3; volume ratio of $TBP(HNO_3)_x(H_2O)_y$ to $CDCl_3$ = 1:1.

of the chemical shift observed from the PNMR spectra support the titration results shown in Figure 3; i.e., there are probably two types of $TBP(HNO_3)_x(H_2O)_y$ depending on the HNO_3/TBP ratio in the complex.

NMR experiments to study the antisolvent effect of SF-CO_2 on the $TBP(HNO_3)_x(H_2O)_y$ complex are difficult to carry out at the present time because of the corrosive nature of the solute and the lack of a safe high-pressure NMR device in our laboratory. We chose to use chloroform ($CDCl_3$) to evaluate the antisolvent effect because chloroform has a small dielectric constant at room temperature ($\epsilon = 4.81$ at 20 °C). Two $TBP(HNO_3)_x(H_2O)_y$ complexes were prepared with the following mixtures: (i) 4 mL of TBP and 1 mL of 15.5 M HNO_3 and (ii) 2 mL of TBP and 2 mL of 15.5 M HNO_3. The PNMR spectra of these two $TBP(HNO_3)_x(H_2O)_y$ complexes in $CDCl_3$ are given in Figures 6 and 7. Both PNMR spectra show two peaks in addition to the protons in the butyl group of TBP. The peak at 6.49 ppm in Figure 6 and the peak at 8.13 ppm in Figure 7 are the peaks belonging to the nitric acid droplets formed in the system. The nitric acid droplets are not dissolved in the $CDCl_3$ solution. These peaks were identified by a separate NMR study using different concentrations of nitric acid mixed with $CDCl_3$. The nitric acid peak in $CDCl_3$ tends to shift upfield with increasing HNO_3 concentration in the acid solution. The peak at 12.49 ppm in Figure 6 and the peak at 12.09 ppm in Figure 7 are the peaks representing the averaged protons of HNO_3 and H_2O in the complex. The NMR results obtained from the $CDCl_3$–$TBP(HNO_3)_x(H_2O)_y$ system, though qualitative in nature, demonstrate the formation of nitric acid droplets from the

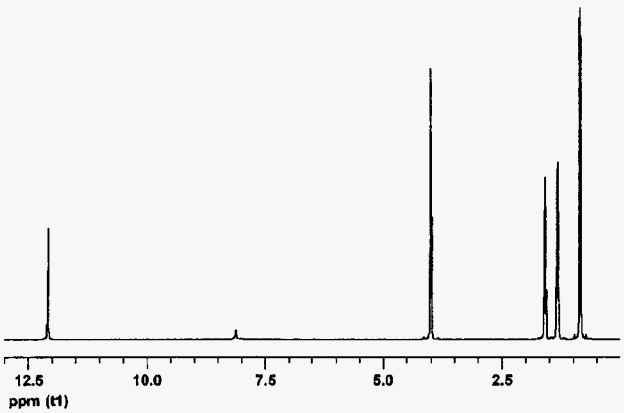

Figure 7. PNMR spectrum of $TBP(HNO_3)_x(H_2O)_y$ in $CDCl_3$. The complex was prepared by mixing 2 mL of TBP and 2 mL of 15.5 M HNO_3; volume ratio of $TBP(HNO_3)_x(H_2O)_y$ to $CDCl_3$ = 1:1.

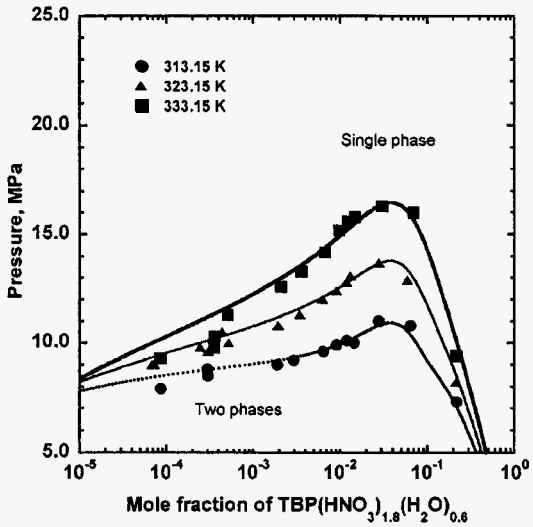

Figure 8. Phase diagram of $TBP(HNO_3)_{1.8}(H_2O)_{0.6}$ in SF-CO_2.

complex when dissolved in a low dielectric constant solvent as a result of an antisolvent effect. The acid droplets probably started with very small particles and aggregated to certain sizes that would make the solution cloudy. Future experiments to evaluate nitric acid formation from the complex due to the antisolvent effect of SF-CO_2 are currently in planning.

3. Phase Behavior of $TBP(HNO_3)_x(H_2O)_y$ in SF-CO_2. The phase behavior of a $TBP(HNO_3)_x(H_2O)_y$ complex in SF-CO_2 was also evaluated by visual observation of the solution using a high-pressure view cell. Figure 8 shows the phase boundaries of the $TBP(HNO_3)_{1.8}(H_2O)_{0.6}$ complex in SF-CO_2 at three different temperatures with respect to pressure and the mole fraction of the solute. The isothermal phase boundaries given in Figure 8 represent the transition pressures from a two-phase region into a single-phase solution for the complex with mole fractions greater than 10^{-4}. At each temperature investigated, there exists a maximum transition temperature above which the complex and CO_2 are miscible. For example, at 323.15 K the complex becomes miscible with SF-CO_2 at 14 MPa with any mole fractions. This implies that a large amount of the complex can be dissolved in SF-CO_2 above this specific pressure for the given temperature. The maximum phase transition temperature for the complex increases with the temperature of the system varying from 11 MPa at 313.15 K to 17 MPa at 333.15 K.

A similar phase behavior was reported for the TBP–CO_2 system.[11] The maximum transition pressure reported for the mixed TBP–CO_2 system at 323.15 K was 11 MPa, lower than that of the mixed $TBP(HNO_3)_{1.8}(H_2O)_{0.6}$–$CO_2$ system observed in this study. A critical opalescence was also observed in our system, suggesting the presence of a pseudocritical point for the mixture. The correlated curves plotted in Figure 8 were obtained by using the same approach as that described in the literature.[11]

Conclusions

Some properties of a CO_2-soluble Lewis acid–base complex composed of TBP and nitric acid are described in this paper. The complex with a general formula of $TBP(HNO_3)_x(H_2O)_y$ is miscible with SF-CO_2 above a certain pressure and allows dispersing of high concentrations of nitric acid in the supercritical fluid phase for chemical reactions. Chemical analysis and NMR spectroscopic data suggest that there are two types of this complex, one with a $[HNO_3]/[TBP]$ ratio of less than 1 and the other greater than 1. When the complex was dissolved in a low dielectric constant solvent (chloroform), nitric acid was observed in the solution according to PNMR measurements. Both types of the TBP–nitric acid complex are capable of dissolving uranium dioxide and lanthanide oxides in SF-CO_2. This method of dispersing inorganic acids in SF-CO_2 for dissolution of metal oxides may have a wide range of applications for chemical processing in SF-CO_2 with minimum liquid waste generation.

Acknowledgment

S.-C.L. and A.R. were supported by a DOE–EMSP grant at University of Idaho (DE-FG07-98ER14913). Support from Venture Business Laboratory and Nagoya University for C.M.W.'s sabbatical leave in the fall of 2002 is acknowledged.

Literature Cited

(1) Tomioka, O.; Enokida, Y.; Yamamoto, I. Solvent extraction of lanthanides from their oxides with TBP in supercritical CO_2. *J. Nucl. Sci. Technol.* **1998**, *35*, 515.

(2) Tomioka, O.; Enokida, Y.; Yamamoto, I. Selective recovery of neodymium from oxides by direct extraction method with supercritical CO_2 containing TBP–HNO_3 complex. *Sep. Sci. Technol.* **2002**, *37*, 1153.

(3) Tomioka, O.; Meguro, Y.; Enokida, Y.; Yoshida, Z.; Yamamoto, I. Dissolution behavior of uranium oxides with supercritical CO_2 using HNO_3–TBP complex as a reactant. *J. Nucl. Sci. Technol.* **2001**, *38*, 1097.

(4) Samsonov, M. D.; Wai, C. M.; Lee, S. C.; Kulyako, Y.; Smart, N. G. Dissolution of uranium dioxide in supercritical fluid carbon dioxide. *Chem. Commun.* **2001**, 1868.

(5) Enokida, Y.; El-Fatah, S. A.; Wai, C. M. Ultrasound enhanced dissolution of UO_2 in supercritical CO_2 containing a CO_2-philic TBP–HNO_3 complexant. *Ind. Eng. Chem. Res.* **2002**, *41*, 2282.

(6) Carrott, M. J.; Waller, B. E.; Smart, N. G.; Wai, C. M. High solubility of $UO_2(NO_3)_2$·2TBP complex in supercritical CO_2. *Chem. Commun.* **1998**, 373.

(7) Carrott, M. J.; Wai, C. M. UV–Vis spectroscopic measurement of solubilities in supercritical CO_2 using high-pressure fibre optic cells. *Anal. Chem.* **1998**, *70*, 2421.

(8) Wilson, P. D., Ed. *Nuclear Fuel Cycle, From Ore to Waste*; Oxford Science Publications: Oxford, U.K., 1996; p 381.

(9) Badden, M.; Schurhammer, R.; Wipff, G. Molecular dynamics study of the uranyl extraction by tri-*n*-butyl phosphate (TBP): Demixing of water/"oil"/TBP solutions with a comparison of supercritical CO_2 and chloroform. *J. Phys. Chem. B* **2002**, *106*, 434.

(10) Schurhammer, R.; Wipff, G. Interaction of trivalent lanthanide cations with nitrate anions: a quantum chemical investigation of monodentate/bidentate binding modes. *New J. Chem.* **2002**, *26*, 229−233.

(11) Joung, S. N.; Kim, S. J.; Yoo, K. P. Single-phase limit for mixtures of tri-*n*-butyl phosphate plus CO_2 and bis(2-ethylhexyl)-phosphoric acid plus CO_2. *J. Chem. Eng. Data* **1999**, *44*, 1034.

Received for review January 6, 2003
Revised manuscript received July 18, 2003
Accepted August 18, 2003

IE030010J

CHEMCOMM Communication
www.rsc.org/chemcomm

Dissolution of uranium dioxide in supercritical fluid carbon dioxide

M. D. Samsonov,[a] C. M. Wai,*[a] Su-Chen Lee,[a] Yuri Kulyako[b] and N. G. Smart[c]

[a] *Department of Chemistry, University of Idaho, Moscow, Idaho 83844, USA*
[b] *Laboratory of Radiochemistry, Vernadsky Institute of Geochemistry and Analytical Chemistry, Russian Academy of Sciences, 117975 Moscow, Russia*
[c] *Chemical Process Group, BNFL, Sellafield, Cumbria, UK CA20 1PG*

Received (in Cambridge, UK) 18th April 2001, Accepted 10th August 2001
First published as an Advance Article on the web 29th August 2001

Uranium dioxide can be dissolved in supercritical CO_2 with a CO_2-philic TBP–HNO_3 complexant to form a highly soluble $UO_2(NO_3)_2$·2TBP complex; this new method of dissolving UO_2 that requires no water or organic solvent may have important applications for reprocessing of spent nuclear fuels and for treatment of nuclear wastes.

A key chemical process in the nuclear industry is the extraction and purification of uranium in the initial production of fuel for nuclear reactors and in the reprocessing of spent nuclear fuel. The most commonly used commercial process to achieve this objective is the Purex (Plutonium Uranium Extraction) process, which involves the dissolution of spent nuclear fuel in strong nitric acid and the subsequent solvent extraction of uranium and plutonium from the acid solution using tri-*n*-butylphosphate (TBP) as an extractant.[1,2] The extracted uranium and plutonium nitrate TBP complexes are further separated by chemical steps to yield pure uranium and plutonium dioxide. The Purex process, though highly efficient, has the inherent drawbacks of liquid–liquid extraction including generation of aqueous and organic liquid wastes. The large volumes of high level wastes accumulated from the weapons build-up program during the Cold War period are one example of the nuclear waste problems facing the USA.[3] Spent fuels from commercial nuclear power plants are still reprocessed today using the Purex process to recover unused uranium for recycling by several countries excluding the USA. Developing techniques for effective treatment of the wastes generated in the past and for reprocessing of spent nuclear fuels in the future has been one of the most actively pursued research areas by nuclear scientists all over the world. In evaluating any acceptable new techniques for reprocessing of spent nuclear fuels in the future, reduction of waste generation is an important criterion for consideration.

The possibility of using supercritical fluid carbon dioxide as a solvent for reprocessing of spent nuclear fuels was suggested recently in the literature.[4] Supercritical CO_2 is considered a green solvent because it is non-toxic and environmentally benign. Carbon dioxide is also cheap, readily available in relatively pure form, and has moderate critical constants (T_c = 31.3 °C, P_c = 72.8 atm and ρ_c = 0.45 g cm^{-3}). A major advantage of using supercritical CO_2 for reprocessing spent nuclear fuels is the possibility of eliminating the acid and organic solvent required in the conventional Purex process. Since the solvation strength of a supercritical fluid depends on the density of the fluid phase, selective dissolution and separation of solutes may also be possible in supercritical CO_2. Rapid separation of the dissolved metal complexes can be easily achieved by reduction of the fluid pressure to cause precipitation of the solutes, and the gas can be recycled for repeated use. This approach does not directly contribute to global warming, as the CO_2 used in this process is generated as a by-product from other chemical processes. A major problem for developing this new process is to identify a complexing agent that will effectively dissolve the main component of the spent nuclear fuel, basically uranium dioxide, in supercritical fluid CO_2.

The hexavalent uranyl ion $(UO_2)^{2+}$ is known to form CO_2-soluble complexes with a number of complexing agents including TBP and β-diketones.[5] In an earlier report, we showed that uranyl ions in strong nitric acid solutions could be extracted by supercritical CO_2 containing TBP.[6] The extracted uranyl complex $UO_2(NO_3)_2$·2TBP has an unusually high solubility in supercritical CO_2, of the order of 4.2×10^{-1} mol L^{-1} at 40 °C and 200 atm.[7] In another report, we demonstrated that uranium trioxide UO_3 could be dissolved in supercritical CO_2 with a fluorinated β-diketone thenoyltrifluoroacetylacetone (Htta) and TBP forming the uranyl complex $UO_2(tta)_2$·2TBP which has a solubility of 7.5×10^{-3} mol L^{-1} at 40 °C and 200 atm in supercritical CO_2.[8] This reaction, however, is not effective for dissolution of tetravalent uranium dioxide UO_2. In our previous experiments regarding the extraction of uranyl ions from nitric acid solutions, we noticed that HNO_3 could also be extracted by TBP forming a highly soluble complex in the supercritical CO_2 phase.[9] Our recent experiments show that this CO_2-philic TBP–HNO_3 complexant can oxidize UO_2 to the hexavalent state leading to the formation of the highly soluble $UO_2(NO_3)_2$·2TBP in supercritical CO_2. This paper describes the initial results obtained from our laboratory regarding the direct dissolution of uranium dioxide in supercritical CO_2 using the TBP–HNO_3 complexant as an extracting agent.

TBP is known to form complexes with aqueous HNO_3, and the 1:1 and 2:1 (TBP:HNO_3 mole ratio) complexes are the predominating species when formed with 3 M or lower molarity nitric acid solutions.[10] The TBP–HNO_3 complexes also contain water with different hydration numbers.[10] In this study, the TBP–HNO_3 reagent was prepared by adding 5.0 mL of TBP to 0.82 mL concentrated nitric acid (69.5%, ρ = 1.42 g cm^{-3}) in a glass tube with a stopper. This mixture of TBP and HNO_3 (about 1:0.7 mole ratio) was shaken vigorously for 5 min followed by centrifuging for 20 min. After centrifugation, 3 mL of the TBP phase was removed for supercritical fluid experiments. The density of the TBP phase was measured to be 1.035 g cm^{-3}. The remaining aqueous phase was found to have a pH about 1 after 20 times dilution in water, indicating most of the HNO_3 had reacted with TBP to form the TBP–HNO_3 complex. Upon addition of the TBP–HNO_3 complex to $CDCl_3$, small water droplets were formed in the solution indicating the water in the complex would precipitate in the organic solution. A 300 MHz proton NMR spectrum of the TBP–HNO_3 complex was taken by placing D_2O in an insert separated from the complex sample in a regular NMR tube. The D_2O in this case was used to lock the NMR spectrum. The NMR spectrum showed a resonance peak at 10.28 ppm which is attributed to HNO_3 and other peaks at 4.26 ppm (dt), 1.86 ppm (qnt), 1.61 ppm (sext) and 1.14 (t) ppm for TBP. The peak areas of TBP and HNO_3 indicated a proton ratio close to 27:2 for the TBP–HNO_3 complex. The HNO_3 proton NMR peak suggests a hydrated HNO_3 species complexed with TBP. The solubility of this TBP–HNO_3 complex in liquid CO_2 at room temperature and 80 atm is about 0.38 mL/mL CO_2. The TBP–HNO_3 complex (about 3 mL) was placed in a 10.4 mL stainless steel cell which was connected upstream to a 3.47 mL extraction cell containing about 40–60 mg of a uranium oxide. Liquid CO_2 was added to the cells using an ISCO model 260D syringe pump and the system was heated in an oven at a desired temperature. Uranium

 DOI: 10.1039/b103468p

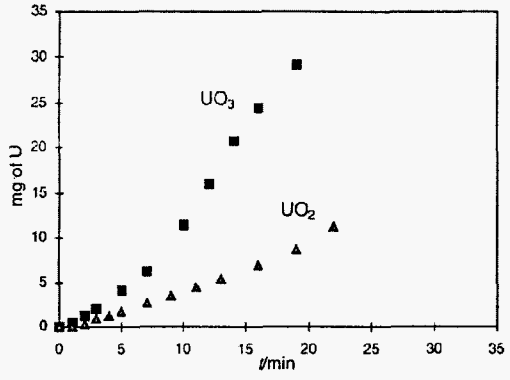

Fig. 1 Cumulative mass of uranium extracted from UO_3 and UO_2 with time by supercritical CO_2 containing the TBP–HNO_3 extractant (60 °C, 150 atm, flow rate = 0.4 mL min^{-1}).

dioxide in a powder form with size < 0.15 mm in diameter was obtained from Alfa Aesar (Ward Hill, MA). Uranium trioxide was also obtained from Alfa Aesar with a size of about 0.15–0.25 mm.

The uranium oxide dissolution experiments were performed with supercritical CO_2 containing TBP–HNO_3 flowing through the system at a rate of 0.4 mL min^{-1} measured at the pump. The dissolved uranium complex was collected in chloroform followed by back extraction with 8 M HNO_3 and washed by deionized water twice. The combined acid-water solution was analyzed by spectrophotometric method[11] and by ICP-AES for uranium determination. UV–VIS spectroscopy showed that the trapped uranium complex had an identical absorption spectrum to that reported for $UO_2(NO_3)_2{\cdot}2TBP$.[7] Fig. 1 shows the dissolution of UO_2 and UO_3 in supercritical CO_2 with the TBP–HNO_3 complexant at 60 °C and 150 atm (ρ = 0.613 g cm^{-3}). The results are expressed as the cumulative mass of uranium (in mg) found in the collection solution with time. The amount of the TBP–HNO_3 complexant dissolved in the CO_2 phase during the dynamic extraction process was determined by measuring the volume change of the complexant before and after the experiment. The amount of the TBP–HNO_3 complexant in the supercritical CO_2 stream was determined to be about 0.08 mL/mL of CO_2 at 60 °C and 150 atm. The amount of the TBP–HNO_3 complexant was in excess with respect to UO_2 in our dynamic extraction experiments. Direct dissolution of UO_2 in supercritical CO_2 under the specified conditions apparently occurred rapidly. Dissolution of UO_3 in supercritical CO_2 under the same conditions was more effective than that of UO_2. This is expected because UO_3 is in the hexavalent oxidation state which is ready to form the CO_2 soluble $UO_2(NO_3)_2{\cdot}2TBP$ complex. The dissolution of UO_2 may be represented by eqn. (1) assuming the TBP–HNO_3 complex has a 1:1 stoichiometry:

$$UO_2(\text{solid}) + 8/3\ \text{TBP–HNO}_3 \rightarrow UO_2(NO_3)_2{\cdot}2TBP + 2/3\ NO + 4/3\ H_2O + 2/3\ TBP \quad (1)$$

Similar equations can be written for the 2:1 and other TBP–HNO_3 complexes with different stoichiometry.

Dissolution of UO_2 in liquid CO_2 was slow relative to that observed in the supercritical CO_2 experiments (Fig. 2). Because oxidation of UO_2 was required in the dissolution process, diffusion of the oxidized products in the liquid phase could be a factor limiting the dissolution rate. The diffusion coefficient of supercritical CO_2 is typically an order of magnitude higher than that of the liquid. Under the same liquid CO_2 conditions, dissolution of UO_3 was about the same as that in the supercritical phase perhaps because oxidation was not required in this case.

The density of supercritical CO_2 is known to influence the solvation strength and hence solubility of solutes in the supercritical fluid phases. The dissolution of UO_2 in supercritical CO_2 increased rapidly with the density of the fluid phase as shown in Fig. 3. The amount of UO_2 dissolved in the supercritical CO_2 phase at density 0.7662 g cm^{-3} was about an

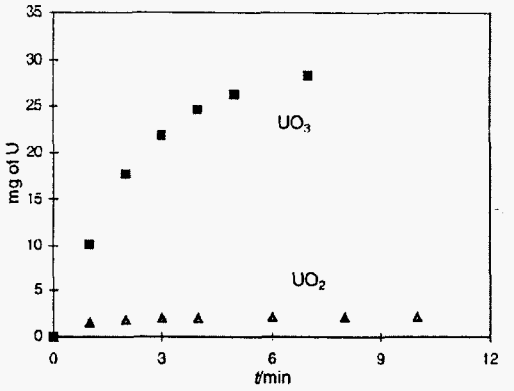

Fig. 2 Cumulative mass of uranium extracted from UO_3 and UO_2 in liquid CO_2 containing the TBP–HNO_3 extractant (21 °C, 80 atm, flow rate = 0.4 mL min^{-1}).

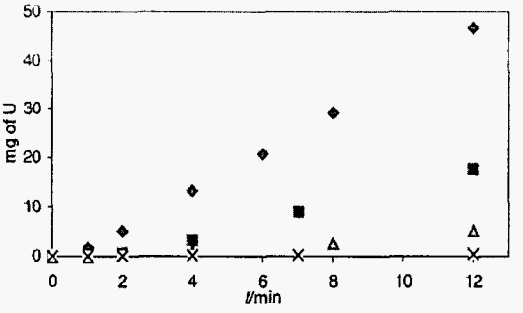

Fig. 3 Cumulative mass of uranium extracted from UO_2 by supercritical CO_2 with the aid of the TBP–HNO_3 complexant at different densities (g cm^{-3}). (◆) 0.766 (65 °C, 250 atm), (■) 0.732 (60 °C, 200 atm), (△) 0.613 (60 °C, 150 atm), (×) 0.378 (60 °C, 110 atm).

order of magnitude higher than that at density 0.6125 g cm^{-3} after 12 minutes of dynamic extraction. The density effect could be partly due to the increased amount of the TBP–HNO_3 complex in the supercritical CO_2 stream caused by the increase in density of the fluid phase. This strong dependence of UO_2 dissolution on supercritical CO_2 density may be used as a parameter for selective dissolution and separation of UO_2 in supercritical CO_2. The direct dissolution of uranium dioxide demonstrated in this study suggests a possibility of dissolving spent nuclear fuels in supercritical CO_2 without the use of conventional acid and organic solvents. This new technique could offer many benefits for the 21st century nuclear industry including reduction in waste generation and improved efficiency of chemical processing.

This work was partially supported by DOE Office of Environmental Management, EMSP Program (grant number DE-FG07-98ER14913) and by BNFL.

Notes and references

1 G. T. Seaborg, *The Actinide Elements*, McGraw-Hill, Inc., New York, 1954, pp. 273–284.
2 A. Schneider and B. G. Wahling, *Actinide Separations*, ACS Symposium Series 117, ACS, Washington, D.C., 1980, pp. 279–290.
3 U.S. Office of the Assistant Secretary for Nuclear Energy, Washington D.C., Dept. of Energy, 1979 (DOE/EIS-0023).
4 N. G. Smart, C. L. Phelps and C. M. Wai, *Chem. Br.*, 1998, **34(8)**, 34.
5 C. M. Wai and S. Wang, *J. Chromatogr. A.*, 1997, **785**, 369.
6 Y. Lin, N. G. Smart and C. M. Wai, *Environ. Sci. Technol.*, 1995, **29**, 2706.
7 M. J. Carrott, B. E. Waller, N. G. Smart and C. M. Wai, *Chem. Commun.*, 1998, 373.
8 M. J. Carrott and C. M. Wai, *Anal. Chem.*, 1998, **70**, 2421.
9 C. M. Wai, Y. Lin, M. Ji, K. L. Toews and N. G. Smart, *Progress in Metal Ion Separation and Preconcentration*, ACS Symposium Series 716, ACS, Washington, D.C., 1999, ch. 23, p. 390.
10 H. Naganawa and S. Tachimori, *Bull. Chem. Soc. Jpn.*, 1997, **70**, 809.
11 J. S. Fritz and M. Jonson-Richard, *Anal. Chim. Acta.*, 1959, **20**, 164.